Heavy ion physics: how high energy experiments are carried out

Alexey Aparin, LHEP JINR

LHEP
ЛФВЭ

NICA
NUCLOTRON BASED ION COLLIDER FACILITY

Introduction

What do we know
Is there something else we want to know
How can we do it

Problems of our experience bias

If we try to describe something completely new to us we are limited in our capabilities

How six blind scientists investigate what an elephant is

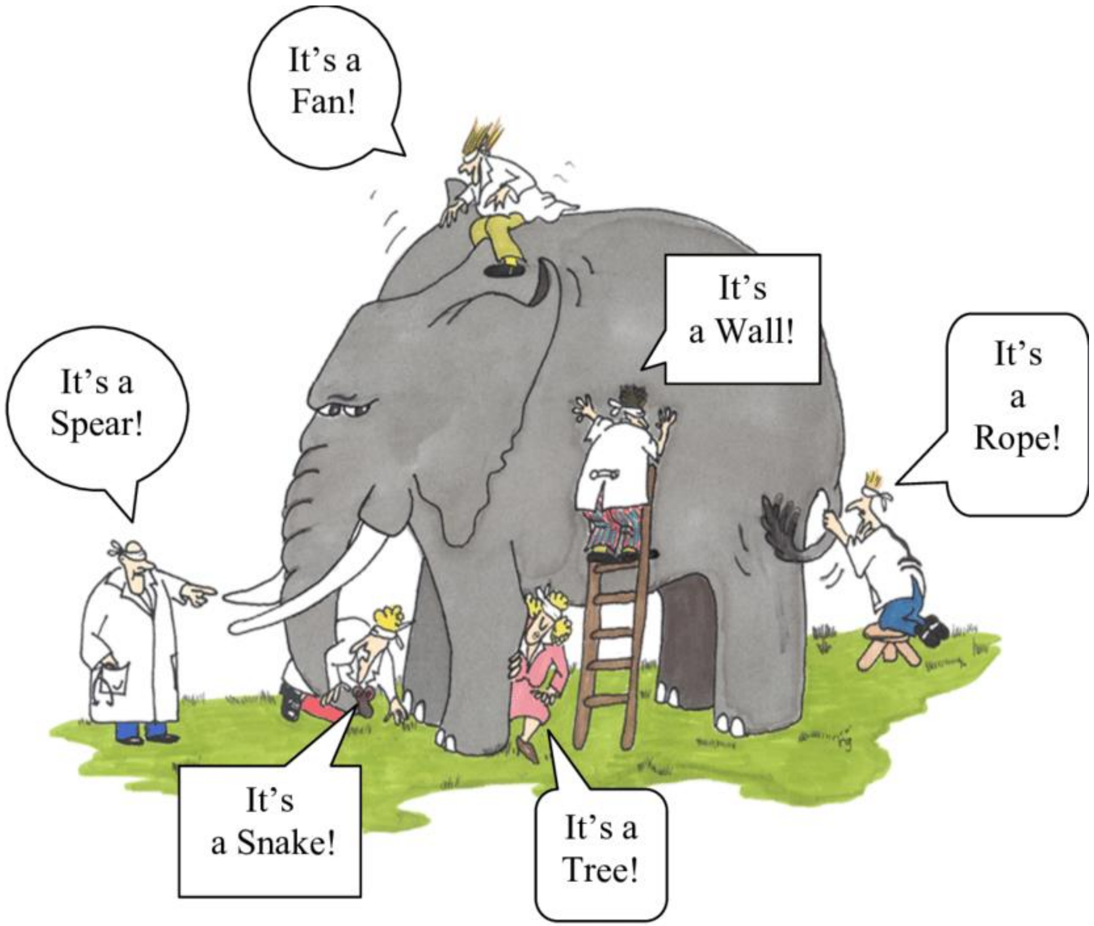

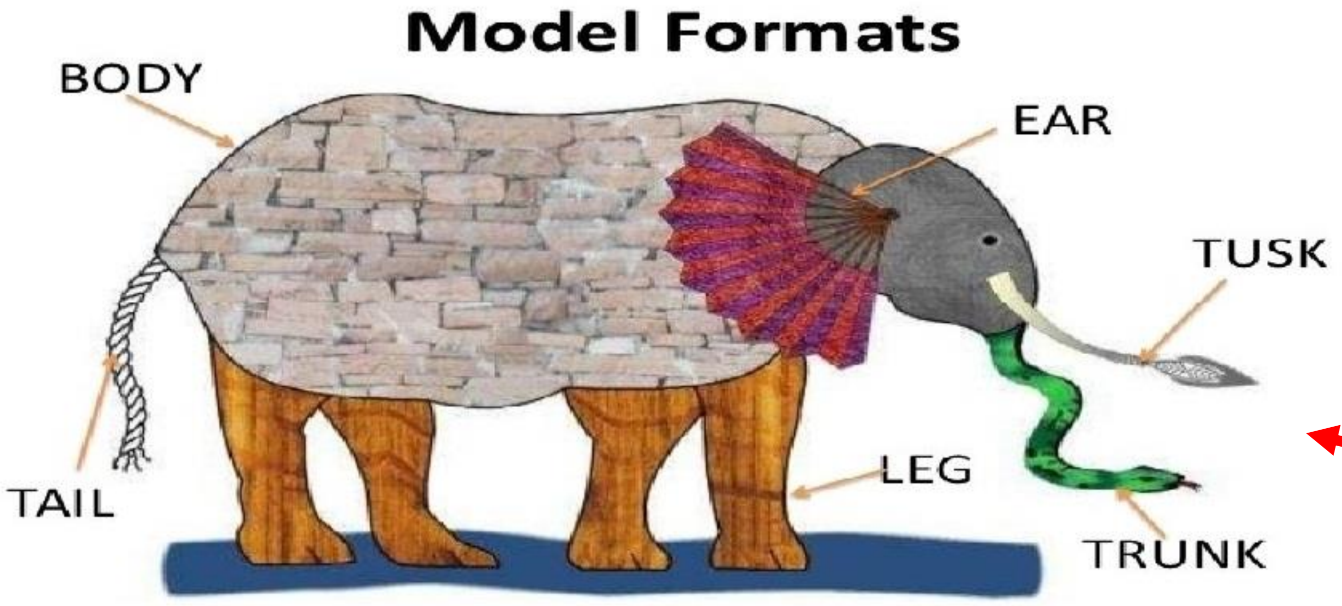

Their working model of an elephant
Best description of the data so far

How it is then transferred to public

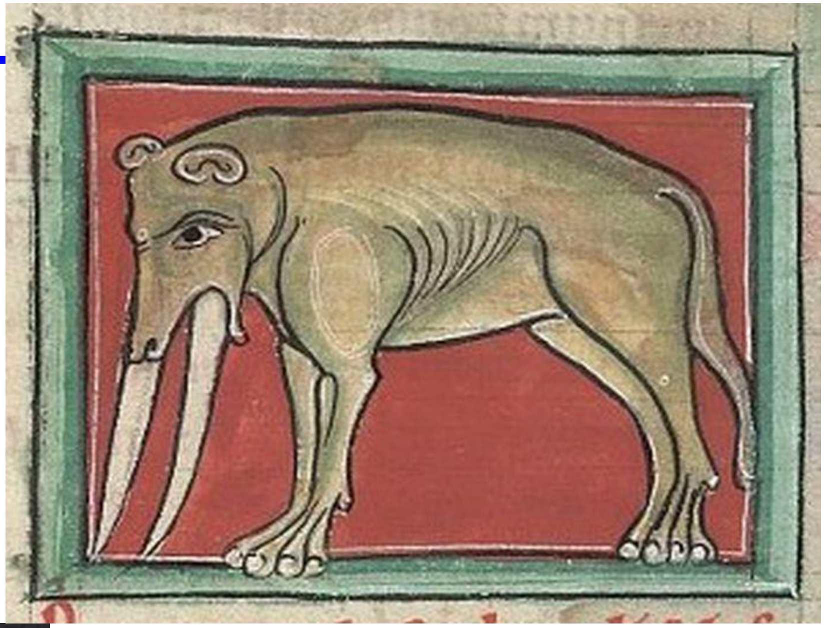

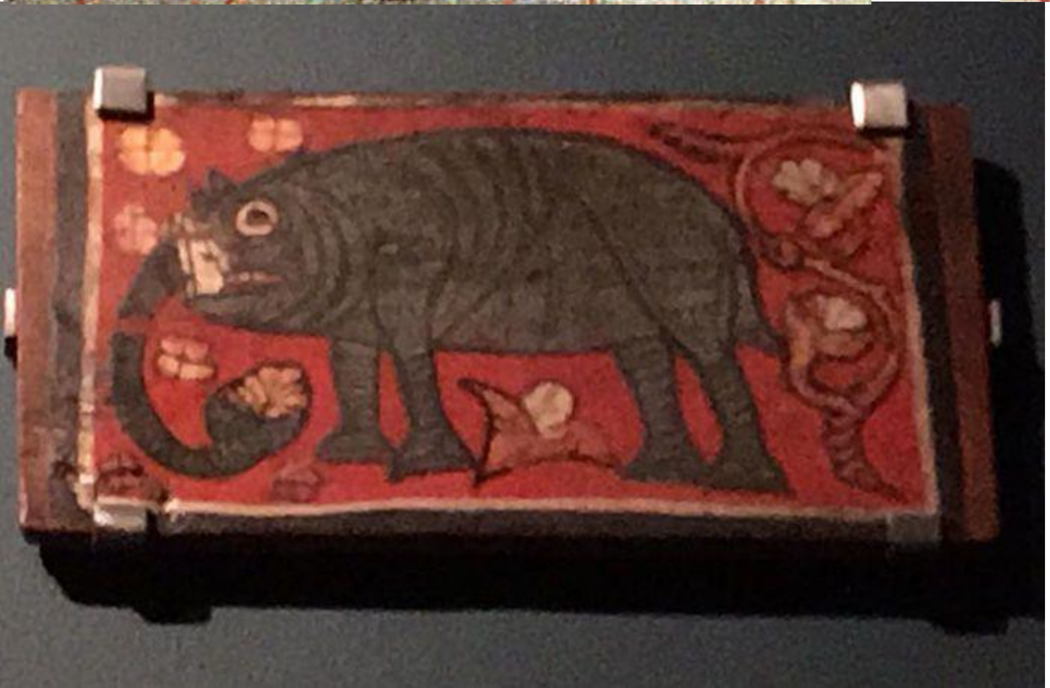

Standard Model

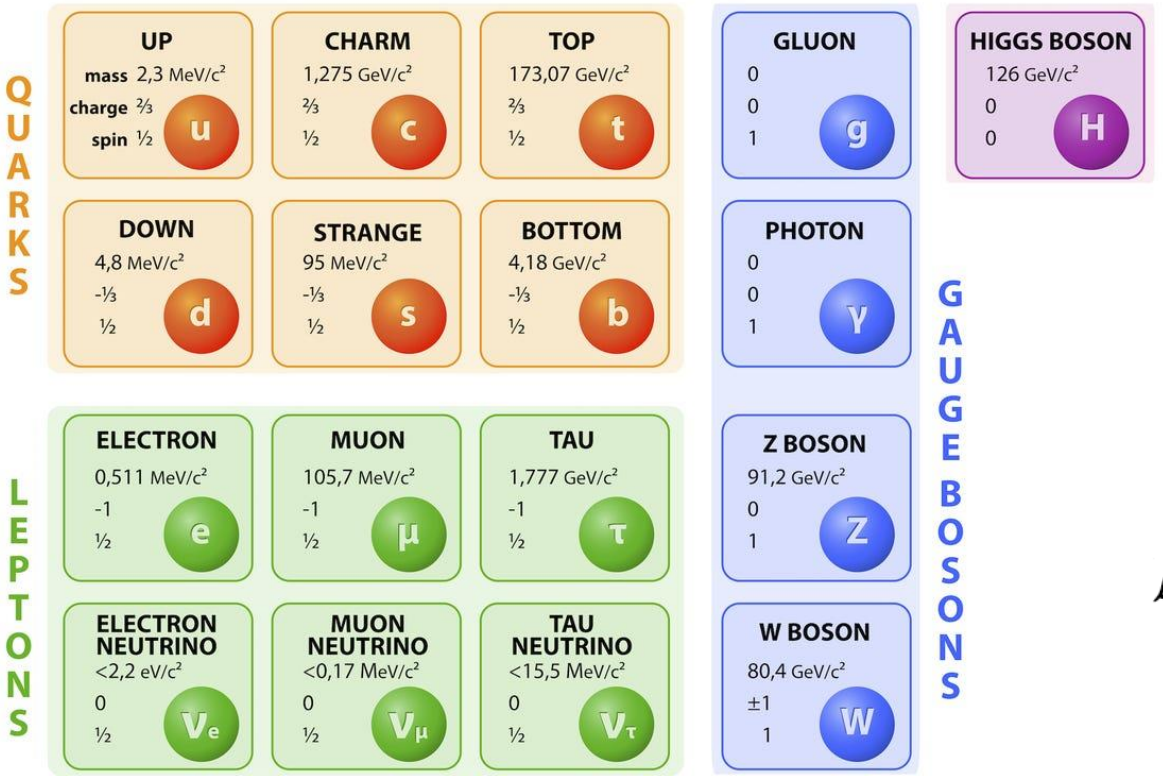

General theory of matter and fundamental interactions.

But what do we learn from it and what else is there unattended?

$$\mathcal{L} = -\frac{1}{4}F_{\mu\nu}F^{\mu\nu} + |D_\mu\phi|^2 - V(\phi) + i\bar{\psi}\hat{D}\psi + (\bar{\psi}_i Y_{ij}\psi_j\phi + \mathrm{h.c.})$$

Standard Model

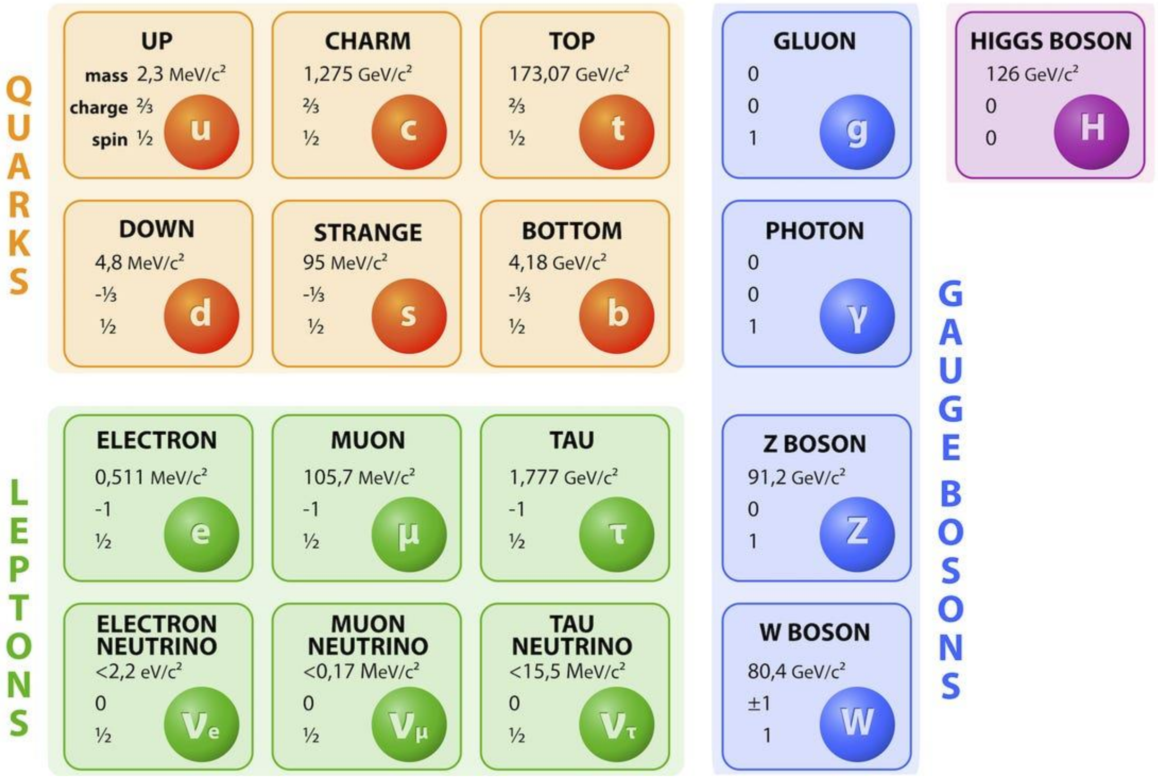

*

1 $-\frac{1}{2}\partial_\nu g^a_\mu \partial_\nu g^a_\mu - g_s f^{abc}\partial_\mu g^a_\nu g^b_\mu g^c_\nu - \frac{1}{4}g_s^2 f^{abc}f^{ade}g^b_\mu g^c_\nu g^d_\mu g^e_\nu +$

$\frac{1}{2}ig_s^2(\bar{q}^\sigma_i\gamma^\mu q^\sigma_j)g^a_\mu + \bar{G}^a\partial^2G^a + g_s f^{abc}\partial_\mu\bar{G}^a G^b g^c_\mu - \partial_\nu W^+_\mu\partial_\nu W^-_\mu -$

2 $M^2W^+_\mu W^-_\mu - \frac12\partial_\nu Z^0_\mu\partial_\nu Z^0_\mu - \frac{1}{2c_w^2}M^2Z^0_\mu Z^0_\mu - \frac12\partial_\mu A_\nu\partial_\mu A_\nu - \frac12\partial_\mu H\partial_\mu H -$

$\frac12 m_h^2H^2 - \partial_\mu\phi^+\partial_\mu\phi^- - M^2\phi^+\phi^- - \frac12\partial_\mu\phi^0\partial_\mu\phi^0 - \frac{1}{2c_w^2}M\phi^0\phi^0 - \beta_h[\frac{2M^2}{g^2} +$

$\frac{2M}{g}H + \frac12(H^2+\phi^0\phi^0+2\phi^+\phi^-)] + \frac{2M^4}{g^2}\alpha_h - igc_w[\partial_\nu Z^0_\mu(W^+_\mu W^-_\nu -$

$W^+_\nu W^-_\mu) - Z^0_\nu(W^+_\mu\partial_\nu W^-_\mu - W^-_\mu\partial_\nu W^+_\mu) + Z^0_\mu(W^+_\nu\partial_\nu W^-_\mu -$

$W^-_\nu\partial_\nu W^+_\mu)] - igs_w[\partial_\nu A_\mu(W^+_\mu W^-_\nu - W^+_\nu W^-_\mu) - A_\nu(W^+_\mu\partial_\nu W^-_\mu -$

$W^-_\mu\partial_\nu W^+_\mu) + A_\mu(W^+_\nu\partial_\nu W^-_\mu - W^-_\nu\partial_\nu W^+_\mu)] - \frac12 g^2W^+_\mu W^-_\mu W^+_\nu W^-_\nu +$

$\frac12 g^2W^+_\mu W^-_\nu W^+_\mu W^-_\nu + g^2c_w^2(Z^0_\mu W^+_\mu Z^0_\nu W^-_\nu - Z^0_\mu Z^0_\mu W^+_\nu W^-_\nu) +$

$g^2s_w^2(A_\mu W^+_\mu A_\nu W^-_\nu - A_\mu A_\mu W^+_\nu W^-_\nu) + g^2s_wc_w[A_\mu Z^0_\nu(W^+_\mu W^-_\nu -$

$W^+_\nu W^-_\mu) - 2A_\mu Z^0_\mu W^+_\nu W^-_\nu] - g\alpha[H^3 + H\phi^0\phi^0 + 2H\phi^+\phi^-] -$

$\frac18 g^2\alpha_h[H^4+(\phi^0)^4+4(\phi^+\phi^-)^2+4(\phi^0)^2\phi^+\phi^-+4H^2\phi^+\phi^-+2(\phi^0)^2H^2] -$

$gMW^+_\mu W^-_\mu H - \frac12 g\frac{M}{c_w^2}Z^0_\mu Z^0_\mu H - \frac12 ig[W^+_\mu(\phi^0\partial_\mu\phi^- - \phi^-\partial_\mu\phi^0) -$

$W^-_\mu(\phi^0\partial_\mu\phi^+ - \phi^+\partial_\mu\phi^0)] + \frac12 g[W^+_\mu(H\partial_\mu\phi^- - \phi^-\partial_\mu H) - W^-_\mu(H\partial_\mu\phi^+ -$

$\phi^+\partial_\mu H)] + \frac12 g\frac{1}{c_w}(Z^0_\mu(H\partial_\mu\phi^0 - \phi^0\partial_\mu H) - ig\frac{s_w^2}{c_w}MZ^0_\mu(W^+_\mu\phi^- - W^-_\mu\phi^+) +$

$igs_wMA_\mu(W^+_\mu\phi^- - W^-_\mu\phi^+) - ig\frac{1-2c_w^2}{2c_w}Z^0_\mu(\phi^+\partial_\mu\phi^- - \phi^-\partial_\mu\phi^+) +$

$igs_wA_\mu(\phi^+\partial_\mu\phi^- - \phi^-\partial_\mu\phi^+) - \frac14 g^2W^+_\mu W^-_\mu[H^2+(\phi^0)^2+2\phi^+\phi^-] -$

$\frac14 g^2\frac{1}{c_w^2}Z^0_\mu Z^0_\mu[H^2+(\phi^0)^2+2(2s_w^2-1)^2\phi^+\phi^-] - \frac12 g^2\frac{s_w^2}{c_w}Z^0_\mu\phi^0(W^+_\mu\phi^- +$

$W^-_\mu\phi^+) - \frac12 ig^2\frac{s_w^2}{c_w}Z^0_\mu H(W^+_\mu\phi^- - W^-_\mu\phi^+) + \frac12 g^2s_wA_\mu\phi^0(W^+_\mu\phi^- +$

$W^-_\mu\phi^+) + \frac12 ig^2s_wA_\mu H(W^+_\mu\phi^- - W^-_\mu\phi^+) - g^2\frac{s_w}{c_w}(2c_w^2-1)Z^0_\mu A_\mu\phi^+\phi^- -$

$g^1 s_w^2A_\mu A_\mu\phi^+\phi^- - \bar{e}^\lambda(\gamma\partial+m_e^\lambda)e^\lambda - \bar\nu^\lambda\gamma\partial\nu^\lambda - \bar{u}^\lambda_j(\gamma\partial+m_u^\lambda)u^\lambda_j -$

3 $\bar d^\lambda_j(\gamma\partial+m_d^\lambda)d^\lambda_j + igs_wA_\mu[-(\bar e^\lambda\gamma^\mu e^\lambda) + \frac23(\bar u^\lambda_j\gamma^\mu u^\lambda_j) - \frac13(\bar d^\lambda_j\gamma^\mu d^\lambda_j)] +$

$\frac{ig}{4c_w}Z^0_\mu[(\bar\nu^\lambda\gamma^\mu(1+\gamma^5)\nu^\lambda) + (\bar e^\lambda\gamma^\mu(4s_w^2-1-\gamma^5)e^\lambda) + (\bar u^\lambda_j\gamma^\mu(\frac43 s_w^2 -$

$1-\gamma^5)u^\lambda_j) + (\bar d^\lambda_j\gamma^\mu(1-\frac83 s_w^2-\gamma^5)d^\lambda_j)] + \frac{ig}{2\sqrt2}W^+_\mu[(\bar\nu^\lambda\gamma^\mu(1+\gamma^5)e^\lambda) +$

$(\bar u^\lambda_j\gamma^\mu(1+\gamma^5)C_{\lambda\kappa}d^\kappa_j)] + \frac{ig}{2\sqrt2}W^-_\mu[(\bar e^\lambda\gamma^\mu(1+\gamma^5)\nu^\lambda) + (\bar d^\kappa_j C^\dagger_{\lambda\kappa}\gamma^\mu(1+$

$\gamma^5)u^\lambda_j)] + \frac{ig}{2\sqrt2}\frac{m_e^\lambda}{M}[-\phi^+(\bar\nu^\lambda(1-\gamma^5)e^\lambda) + \phi^-(\bar e^\lambda(1+\gamma^5)\nu^\lambda)] -$

4 $\frac{g}{2}\frac{m_e^\lambda}{M}[H(\bar e^\lambda e^\lambda) + i\phi^0(\bar e^\lambda\gamma^5e^\lambda)] + \frac{ig}{2M\sqrt2}\phi^+[-m_d^\kappa(\bar u^\lambda_jC_{\lambda\kappa}(1-\gamma^5)d^\kappa_j) +$

$m_u^\lambda(\bar u^\lambda_jC_{\lambda\kappa}(1+\gamma^5)d^\kappa_j] + \frac{ig}{2M\sqrt2}\phi^-[m_d^\lambda(\bar d^\lambda_jC^\dagger_{\lambda\kappa}(1+\gamma^5)u^\kappa_j) - m_u^\kappa(\bar d^\lambda_jC^\dagger_{\lambda\kappa}(1-$

$\gamma^5)u^\kappa_j] - \frac g2\frac{m_u^\lambda}{M}H(\bar u^\lambda_ju^\lambda_j) - \frac g2\frac{m_d^\lambda}{M}H(\bar d^\lambda_jd^\lambda_j) + \frac{ig}{2}\frac{m_u^\lambda}{M}\phi^0(\bar u^\lambda_j\gamma^5u^\lambda_j) -$

$\frac{ig}{2}\frac{m_d^\lambda}{M}\phi^0(\bar d^\lambda_j\gamma^5d^\lambda_j) + \bar X^+(\partial^2-M^2)X^+ + \bar X^-(\partial^2-M^2)X^- + \bar X^0(\partial^2 -$

5 $\frac{M^2}{c_w^2})X^0 + \bar Y\partial^2Y + igc_wW^+_\mu(\partial_\mu\bar X^0X^- - \partial_\mu\bar X^+X^0) + igs_wW^+_\mu(\partial_\mu\bar YX^- -$

$\partial_\mu\bar X^+Y) + igc_wW^-_\mu(\partial_\mu\bar X^-X^0 - \partial_\mu\bar X^0X^+) + igs_wW^-_\mu(\partial_\mu\bar X^-Y -$

$\partial_\mu\bar YX^+) + igc_wZ^0_\mu(\partial_\mu\bar X^+X^+ - \partial_\mu\bar X^-X^-) + igs_wA_\mu(\partial_\mu\bar X^+X^+ -$

$\partial_\mu\bar X^-X^-) - \frac12 gM[\bar X^+X^+H + \bar X^-X^-H + \frac{1}{c_w^2}\bar X^0X^0H] +$

$\frac{1-2c_w^2}{2c_w}igM[\bar X^+X^0\phi^+ - \bar X^-X^0\phi^-] + \frac{1}{2c_w}igM[\bar X^0X^-\phi^+ - \bar X^0X^+\phi^-] +$

$igMs_w[\bar X^0X^-\phi^+ - \bar X^0X^+\phi^-] + \frac12 igM[\bar X^+X^+\phi^0 - \bar X^-X^-\phi^0]$

*Note: Thomas Gutierrez, an assistant professor of Physics at California Polytechnic State University, transcribed the Standard Model Lagrangian for the web. He derived it from Diagrammatica, a theoretical physics reference written by Nobel Laureate Martinus Veltman. In Gutierrez's dissemination of the transcript, he noted a sign error he made somewhere in the equation. Good luck finding it!

How do we study nuclear matter?

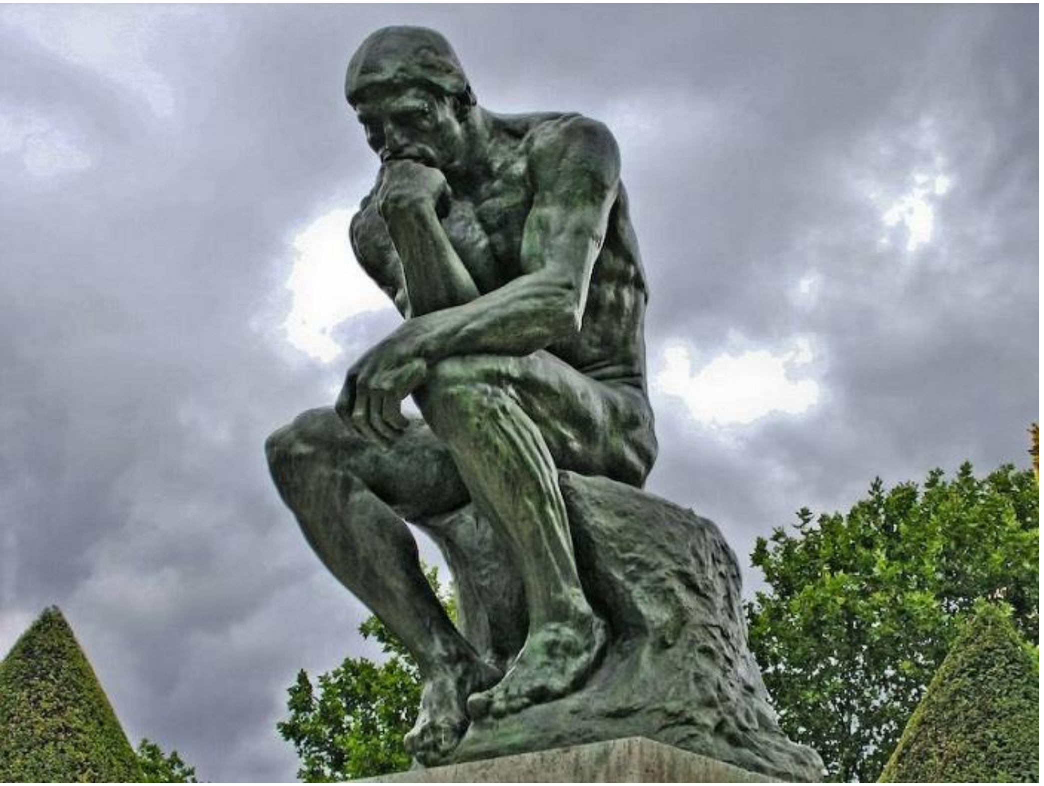

How do we study nuclear matter?

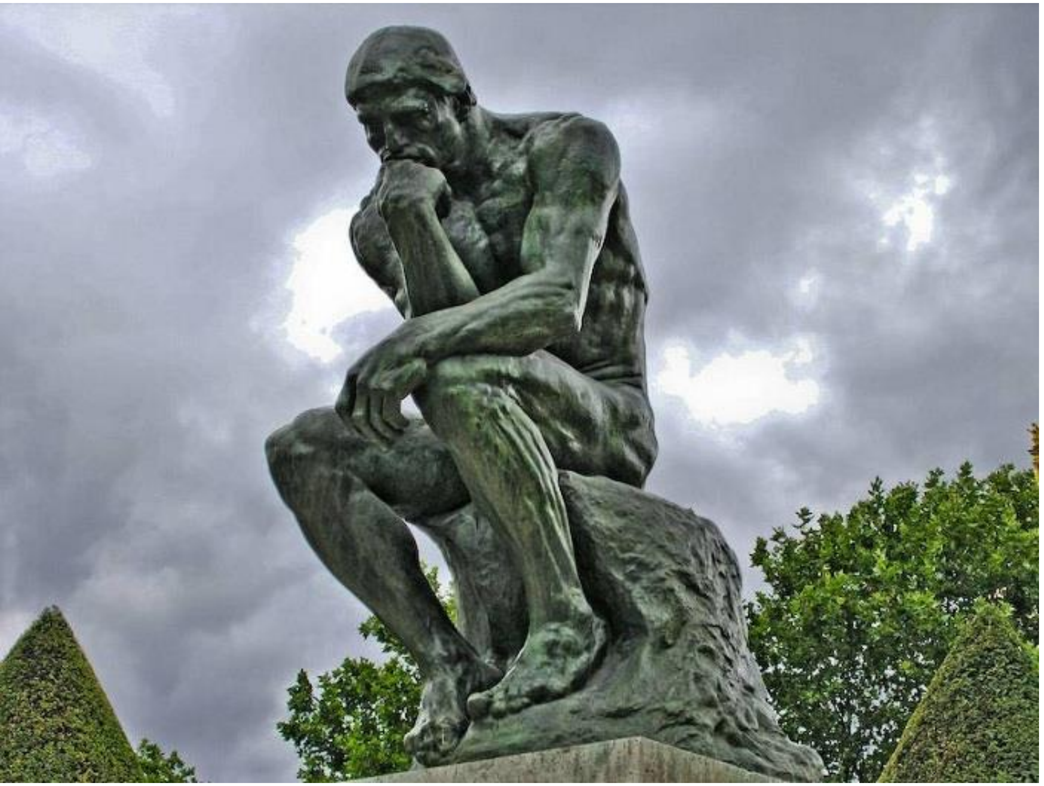

Typical scale of high energy experiment 1 fm = 10^{-15} sm
Typical timeframe ~ 1 – 100 fm/c = 0.3 – 30 * 10^{-25} sec

We need to use some beam of test particles to collide it into the sample we want to investigate

How do we study nuclear matter?

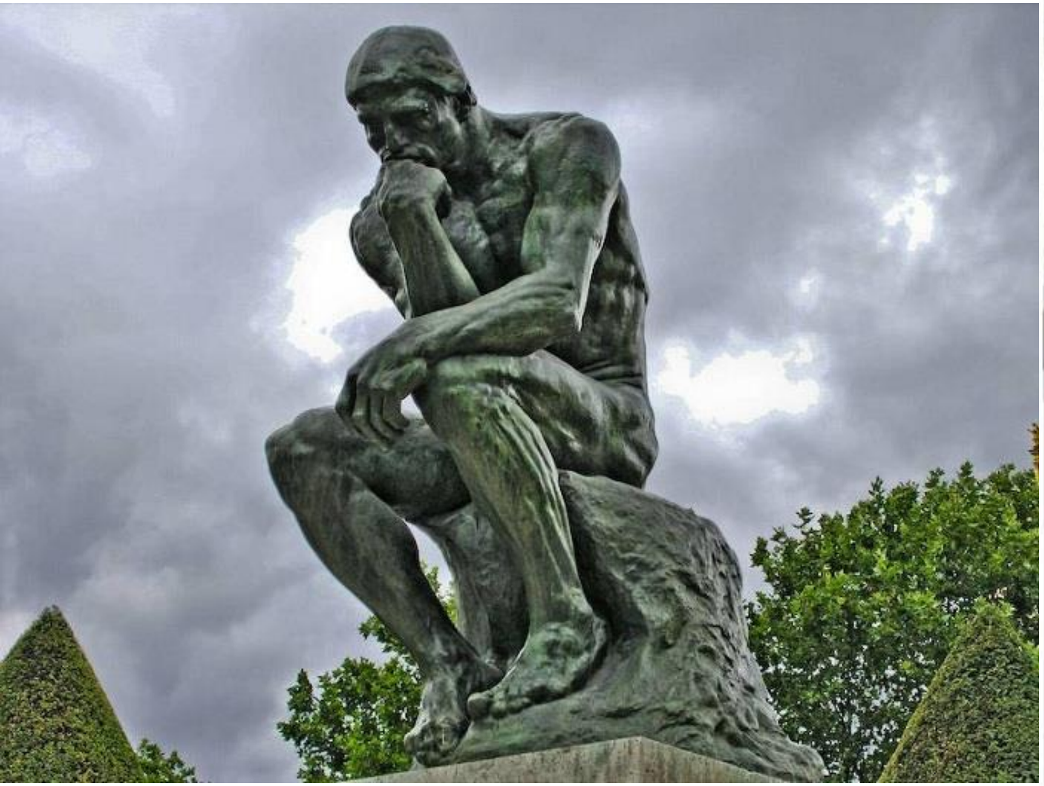

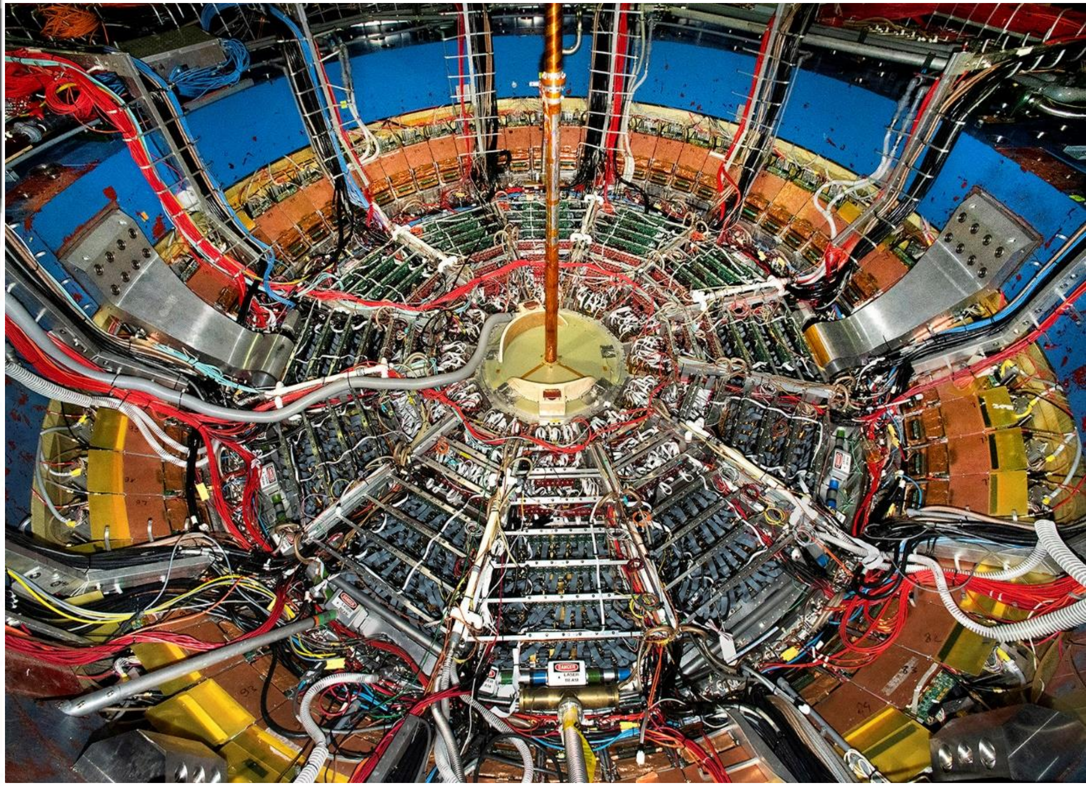

We need to understand well what we are going to collide!

How does the nucleus look like?

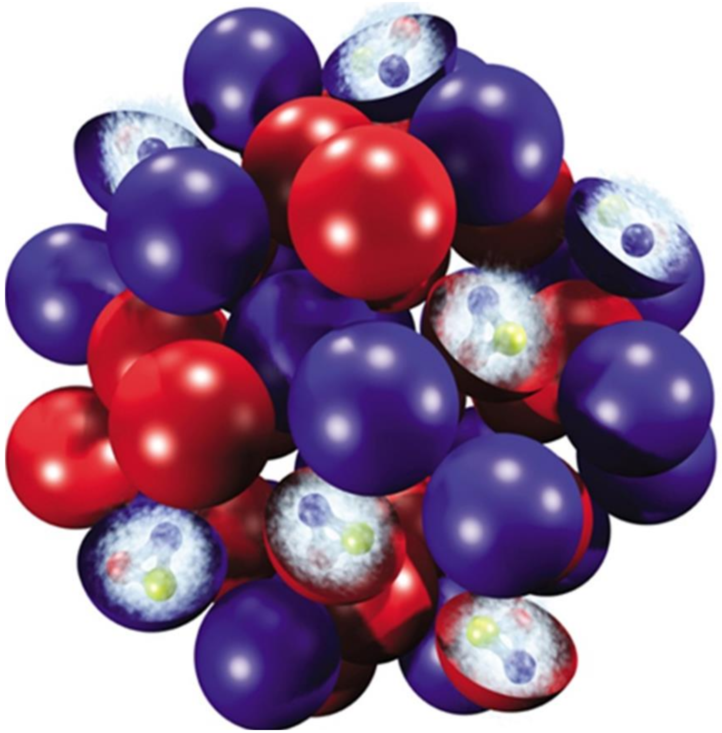

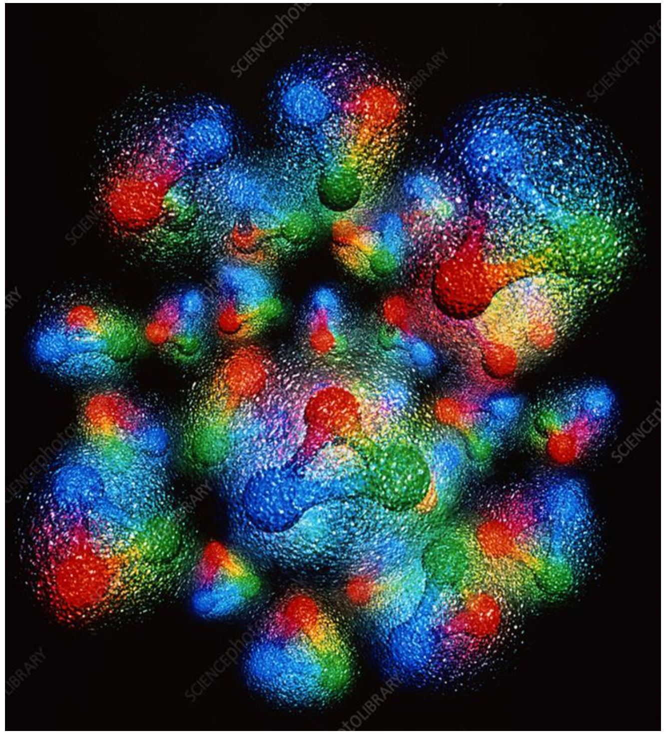

Which of the Si nucleus models is more realistic and why?

How does the nucleus look like – it depends!

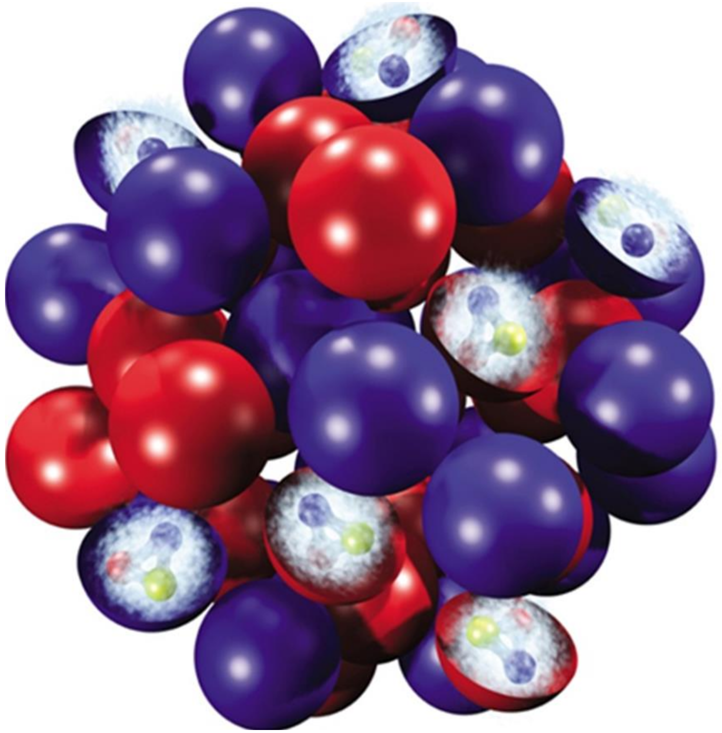

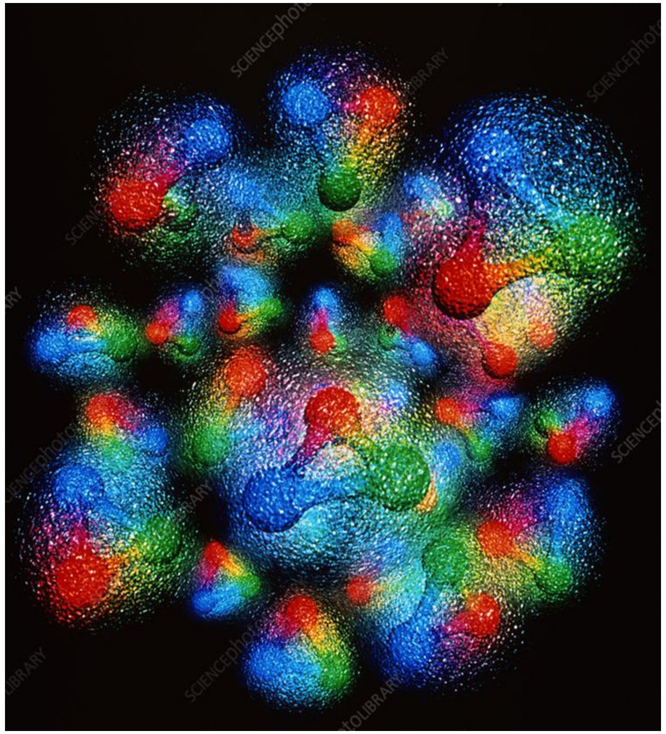

• deBroglie wavelength of constituent partons is effected by the beam energy.

$$\lambda = h/p \quad E = h\nu$$

At lower energy, nucleons are opaque, and the valence quarks are stopped in the fireball.
Excess quarks ➔ higher μ_B

At higher energy, nucleons are transparent, and the valence quarks are pass through and exit the fireball.
Equal quarks and anti-quarks ➔ lower μ_B

Two regimes of the strong force

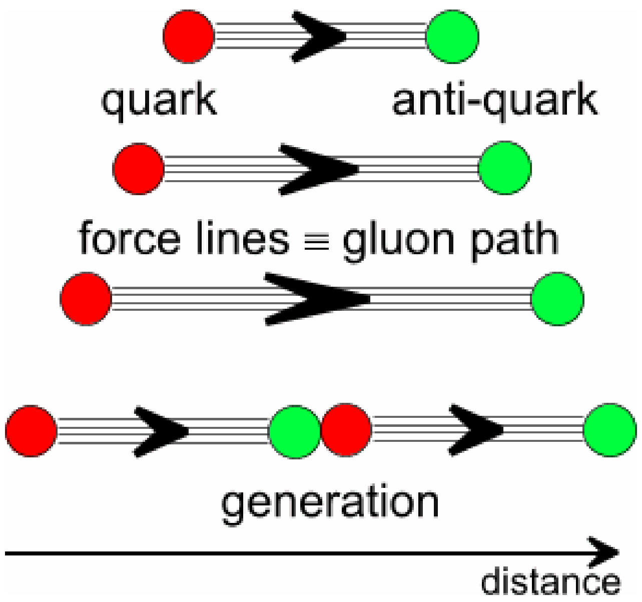

Confinement for color objects
Attraction force can create new quark – antiquark pair from vacuum to remain color neutral

Asymptotic freedom at very small scales/large energies

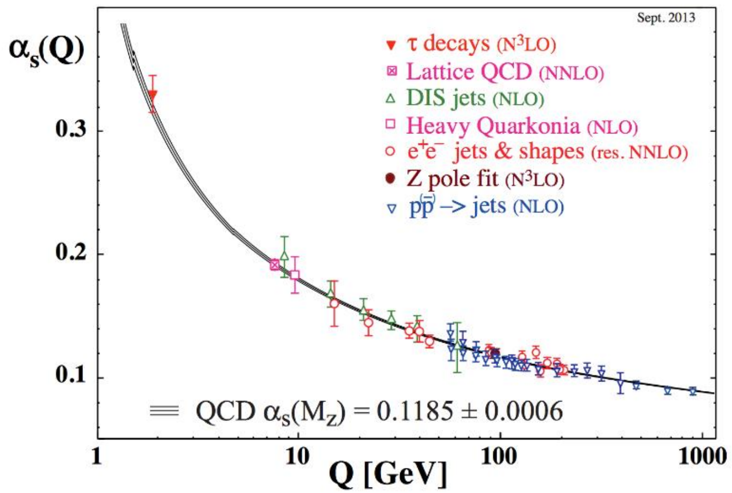

$$\alpha_s(k^2) \stackrel{\text{def}}{=} \frac{g_s^2(k^2)}{4\pi} \approx \frac{1}{\beta_0 \ln\left(\frac{k^2}{\Lambda^2}\right)}$$

(Wilczek, Gross and Politzer)
Nobel prize 2004

$\Lambda_{QCD} \simeq 1\ \text{fm}^{-1}$ – sets scale most important parameter in QCD

Strong interaction potentials

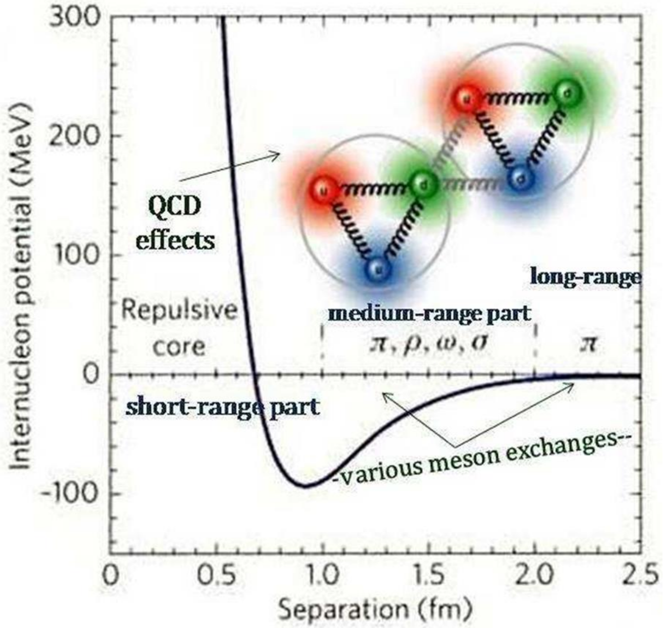

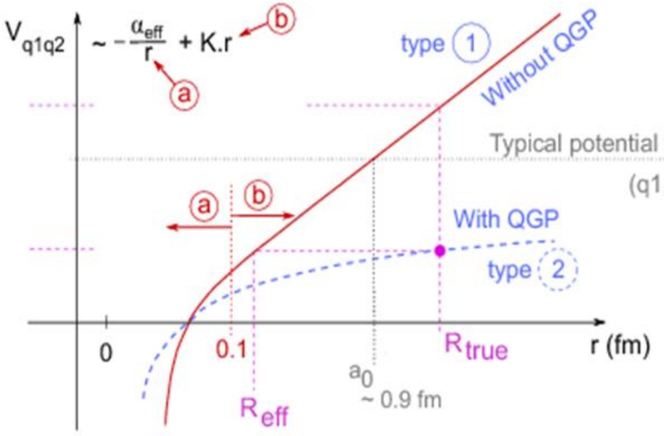

Gold nucleus

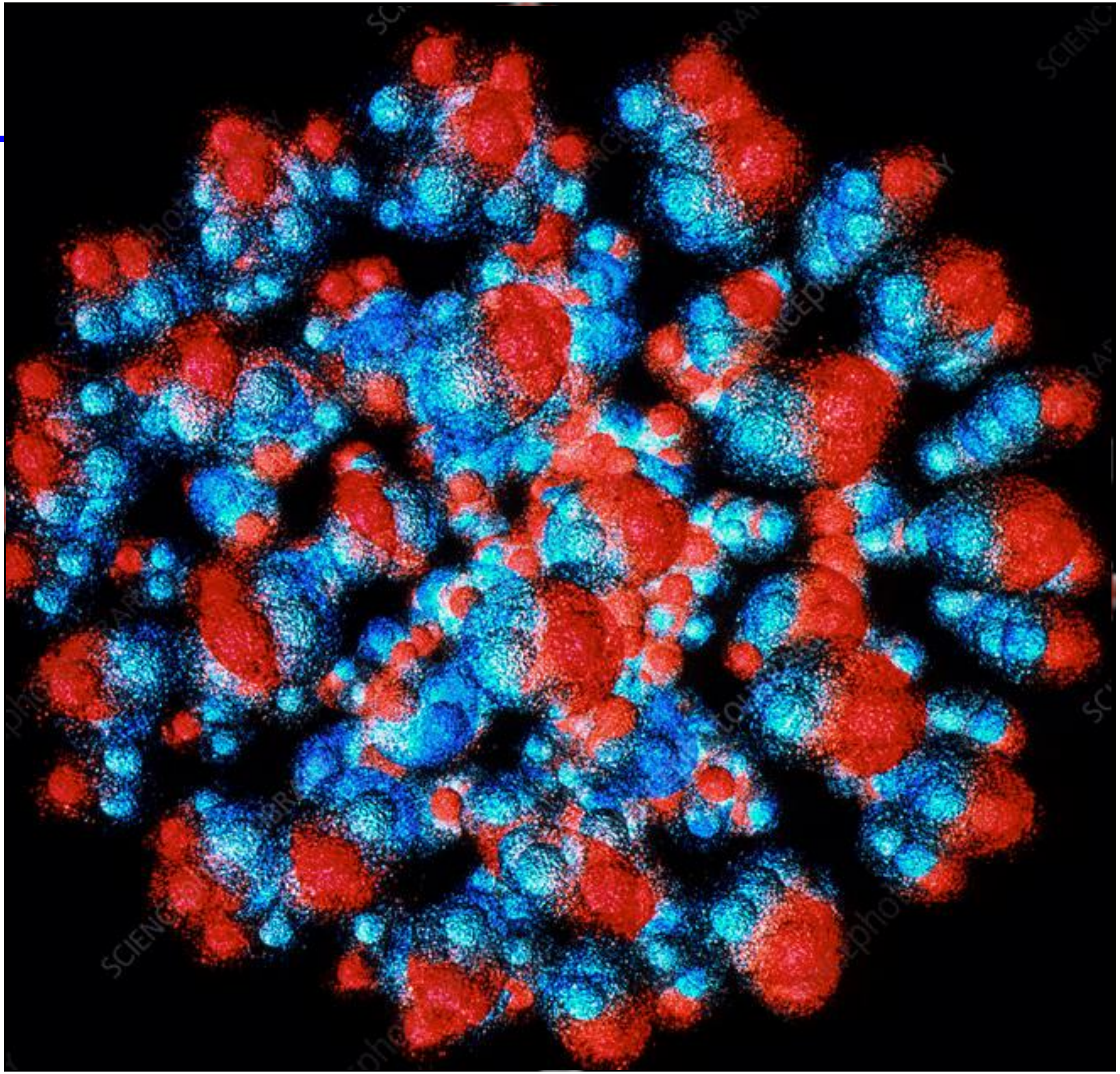

Part 1 Setting the scene

Model description of HIC
Equation of State
History lessons

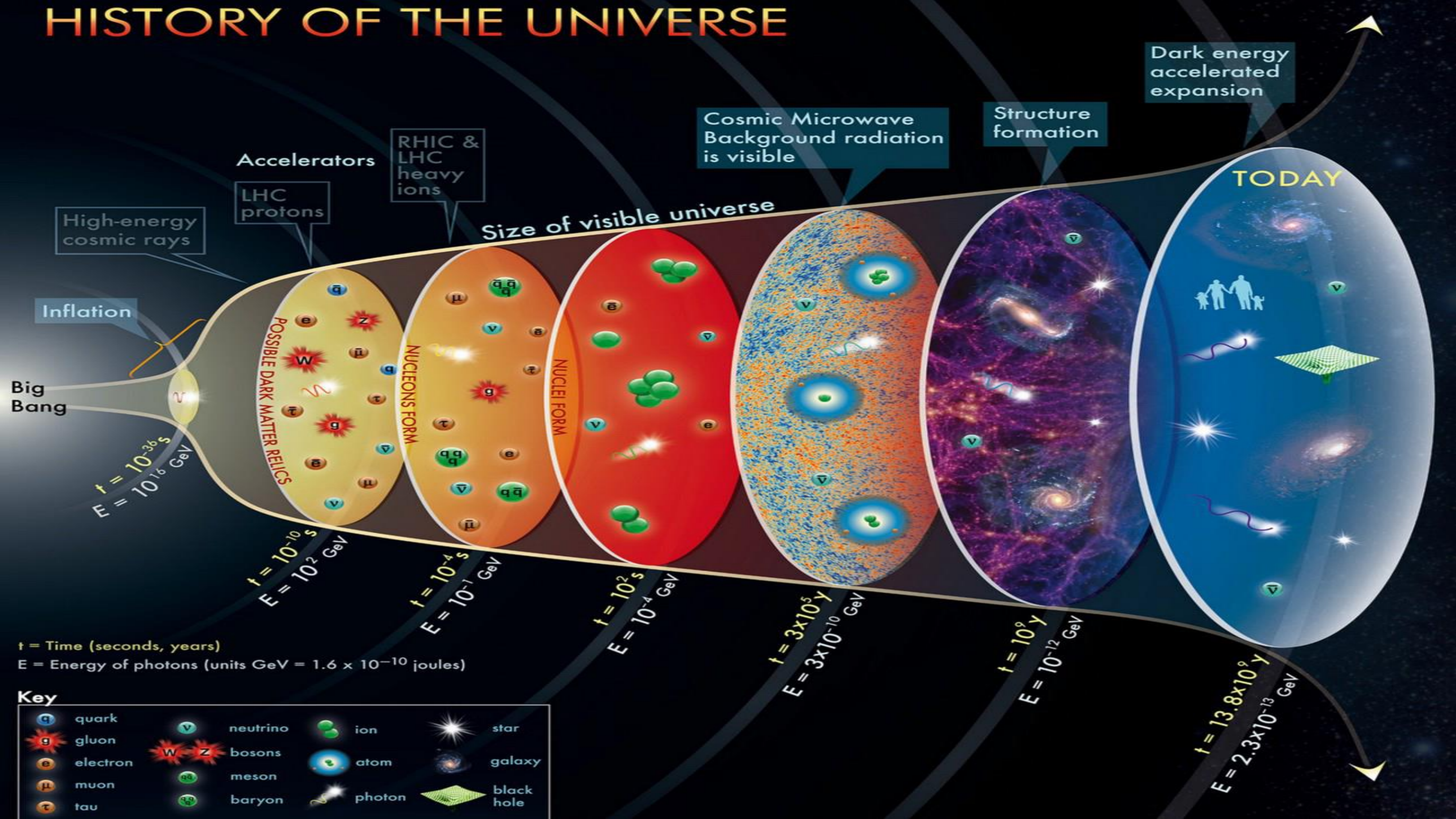
HISTORY OF THE UNIVERSE
Dark energy accelerated expansion
Structure formation
Cosmic Microwave Background radiation is visible
RHIC & LHC heavy ions
Accelerators
LHC protons
High-energy cosmic rays
Size of visible universe
TODAY
Inflation
Big Bang
POSSIBLE DARK MATTER RELICS
NUCLEONS FORM
NUCLEI FORM
t = 10^-36 s
E = 10^16 GeV
t = 10^-10 s
E = 10^2 GeV
t = 10^-4 s
E = 10^-1 GeV
t = 10^2 s
E = 10^-4 GeV
t = 3x10^5 y
E = 3x10^-10 GeV
t = 10^9 y
E = 10^-12 GeV
t = 13.8x10^9 y
E = 2.3x10^-13 GeV
t = Time (seconds, years)
E = Energy of photons (units GeV = 1.6 x 10^-10 joules)
Key
quark
gluon
electron
muon
tau
neutrino
bosons
meson
baryon
ion
atom
photon
star
galaxy
black hole

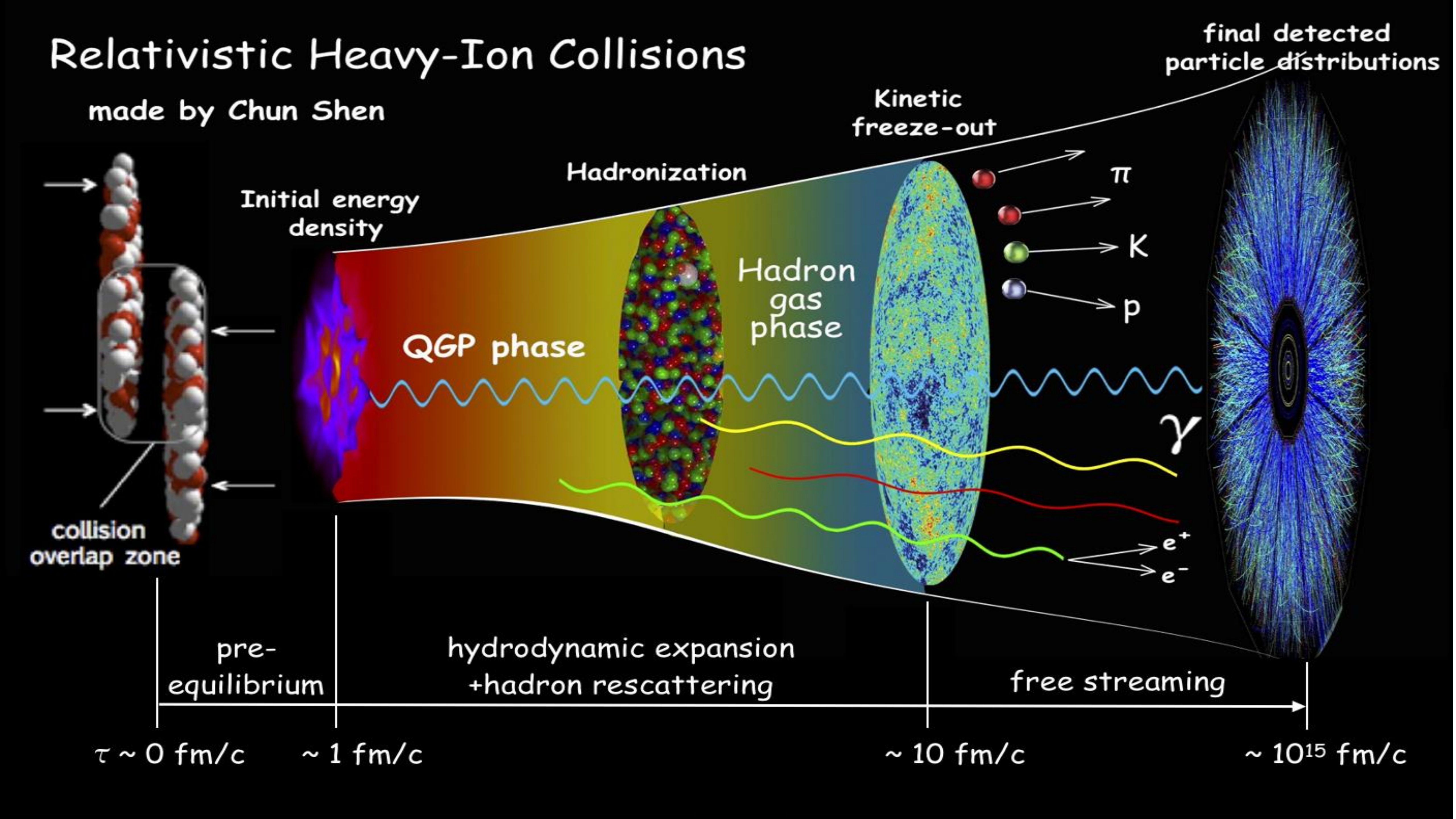

Relativistic Heavy-Ion Collisions
made by Chun Shen
final detected particle distributions
Kinetic freeze-out
Hadronization
Initial energy density
Hadron gas phase
QGP phase
π
K
p
γ
e+
e−
collision overlap zone
pre-equilibrium
hydrodynamic expansion +hadron rescattering
free streaming
τ ~ 0 fm/c
~ 1 fm/c
~ 10 fm/c
~ 10^15 fm/c

Equation of State. Ideal gas

- In simple Bag model QGP is described as an ideal gas of massless quarks (zero chemical potential) and gluons
- Equations of State (Bag model):

$$\varepsilon = k\frac{\pi^2}{30}\frac{T^4}{(\hbar c)^3} + B \rightarrow energy \quad density$$

$$p = k\frac{\pi^2}{90}\frac{T^4}{(\hbar c)^3} - B \rightarrow pressure$$

$$s = \frac{\varepsilon + p}{T} = \frac{4}{3}k\frac{\pi^2}{30}T^3 \rightarrow entropy$$

T – gas temperature

B – pressure in the bag ~ 0.4 GeV/fm^3

κ – number of degrees of freedom

Equation of State. Ideal liquid

Relativistic hydrodynamic equation set for ideal liquid

$$\partial_\mu T^{\mu\nu} = 0$$

$$\partial_\mu N^\mu = 0$$

$$T^{\mu\nu} = (\varepsilon + \overline{p})u^\mu u^\nu - pg^{\mu\nu}$$

$$N^\mu = nu^\mu$$

$T^{\mu\nu}$ – energy-momenta tensor
N^μ – number of particles flow through the liquid cell μ,
u^μ – local 4-speed of liquid cell μ,
ε – energy density
n – particle number density
p – pressure

If we know EoS p=p(ε) and initial conditions this system can be resolved (analytically or numerically)

5 equations for 5 independent variables

$$\varepsilon, n, u^\mu$$

Equation of State. Viscous liquid

Relativistic hydrodynamic equation set for a viscous liquid

$$\partial_\mu T^{\mu\nu} = 0$$

$$\partial_\mu N^\mu = 0$$

$$T^{\mu\nu} = \varepsilon u^\mu u^\nu - pP^{\mu\nu}(p + \Pi) - P^{\mu\nu\alpha\beta}\pi_{\alpha\beta}$$

$$N^\mu = nu^\mu - P^{\mu\nu}v_\nu$$

$$P^{\mu\nu} = \overline{p} - g^{\mu\nu}$$

9 additional variables, now it's not guaranteed to have a solution

$$\varepsilon, n, u^\mu, \Pi, \pi^{\mu\nu}, v^\mu$$

QGP – was it really discovered?

The press conference at BNL on 24 April 2005

Evidence for a **new type of nuclear matter**:

At the Relativistic Heavy Ion Collider (RHIC) at Brookhaven National Lab (BNL), two beams of gold atoms are smashed together, the goal being to recreate the conditions thought to have prevailed in the universe only a few microseconds after the big bang, so that novel forms of nuclear matter can be studied. At this press conference, RHIC scientists will sum up all they have learned from several years of observing the world's most energetic collisions of atomic nuclei. The four experimental groups operating at RHIC will present a consolidated, surprising, exciting new interpretation of their data…

QGP – was it really discovered?

At the RHIC Users' Meeting June 9-12, 2015 a 10 year anniversary session “The Perfect Liquid at RHIC: 10 Years of Discovery" was held, the press release of June 26, 2015 says:

“RHIC lets us look back at matter as it existed throughout our universe at the dawn of time, before QGP cooled and formed matter as we know it,” said Berndt Mueller, Brookhaven's Associate Laboratory Director for Nuclear and Particle Physics. “*The discovery of the perfect liquid was a turning point in physics, and now, 10 years later, RHIC has revealed a wealth of information about this remarkable substance, which we now know to be a QGP, and is more capable than ever of measuring its most subtle and fundamental properties.”*

QGP – was it really discovered?

CERN special seminar 10 February 2000

At the seminar spokespersons from the experiments on CERN's Heavy Ion programm presented compelling evidence for the existence of a new state of matter in which quarks, instead of being bound up into more complex particles such as protons and neutrons, are liberated to roam freely.

Professor Luciano Maiani, CERN Director General, said:
"The combined data coming from the seven experiments on CERN's Heavy Ion program have given a clear picture of a new state of matter. This result verifies an important prediction of the present theory of fundamental forces between quarks. It is also an important step forward in the understanding of the early evolution of the universe. We now have evidence of a new state of matter where quarks and gluons are not confined. There is still an entirely new territory to be explored concerning the physical properties of quark-gluon matter. The challenge now passes to the Relativistic Heavy Ion Collider at the Brookhaven National Laboratory and later to CERN's Large Hadron Collider."

In an interview in January 2017 with Luciano Maiani, Director General of CERN from 1999 to 2003 we read:

Luciano Maiani: *I think that the announcement was quite clear. I have the text of it with me, it reads: "The data provide evidence for color deconfinement in the early collision stage and for a collective explosion of the collision fireball in its late stages. The new state of matter exhibits many of the characteristic features of the theoretically predicted Quark-Gluon Plasma." The key word is "evidence", not discovery, and the evidence was there, indeed*

QGP – was it really discovered?

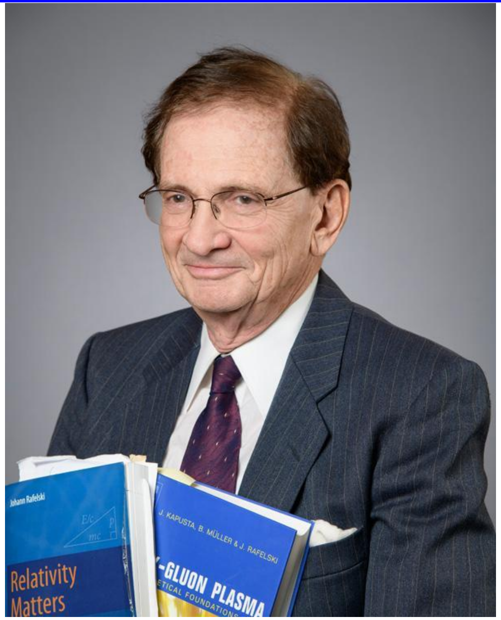

In the book "**Quark-Gluon Plasma: Theoretical Foundations An Annotated Reprint Collection**" prepared in 2002 by Berndt Muller, Joseph Kapusta and Johann Rafelski.

This book introduces the theoretical roots of QGP with a time cut off in 1992. The rationale of the authors was to look more than 10 years back in 2002/3, since in 1992 QGP was already discovered but recognized only by a small subset of researchers.

Looking back at the Universe the Size of a Melon

Already in the mid-90s there was some indication for quark-gluon plasma in heavy ion experiments at CERN and at Brookhaven National Laboratory. However, I was at that time due to fragmentary data very cautious. In hindsight I know my position was too cautious…

Actually, I hoped that this procedure would switch off the quark-gluon plasma in a controlled manner, but this attempt failed. Also at SPS energies there are in the now much more extensive data records unmistakable signatures.

 Eur. Phys. J. Special Topics 229, 1-140 (2020)

Time evolution of the collision

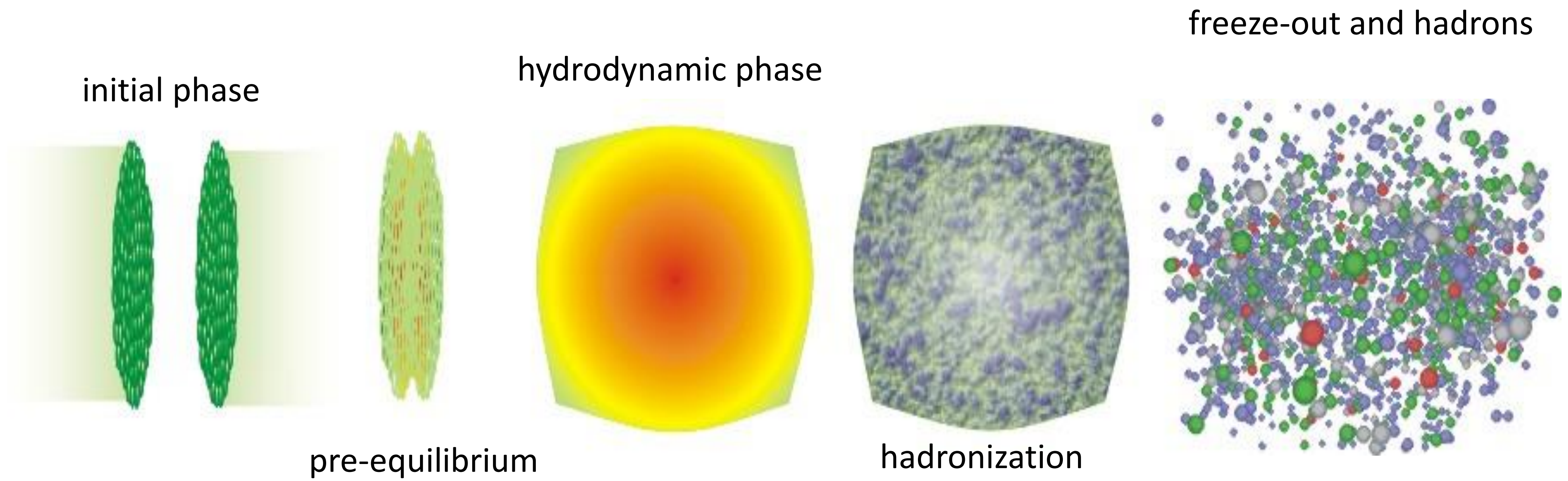

«Soft» probes ($p_T \sim T_{kin} = 150$ MeV)

- particle spectra at small transverse momenta p_T and momentum correlations
- flow effect
- thermal photons and dileptons
- strange particle yields

"Hard" probes ($p_T >> T_{kin} = 150$ MeV)

- particle spectra at large transverse momenta p_T and angle correlations
- hadron jets
- quarkonia
- heavy quark probes

Thermodynamic systems

Van-der-Waals Equation of State

$$\left(p + \frac{a \cdot n^2}{V^2}\right)(V - n \cdot b) = n \cdot R \cdot T$$

p	-	pressure
V	-	volume
T	-	temperature
R	-	gas constant
a, b	-	specific constants for each gas

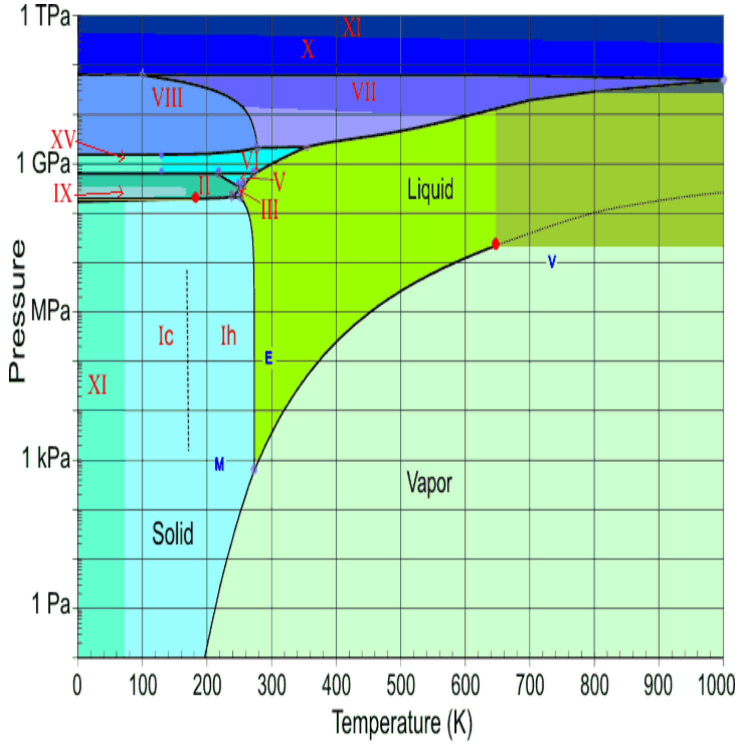

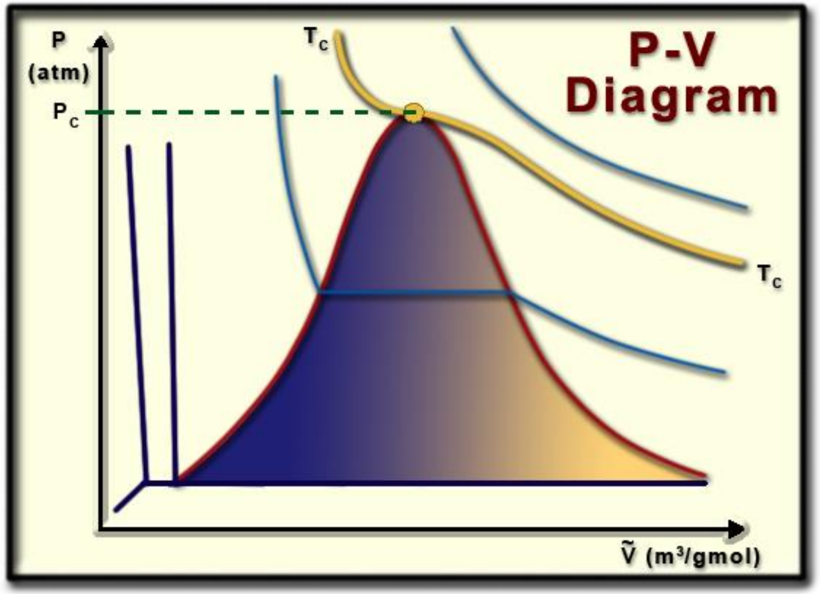

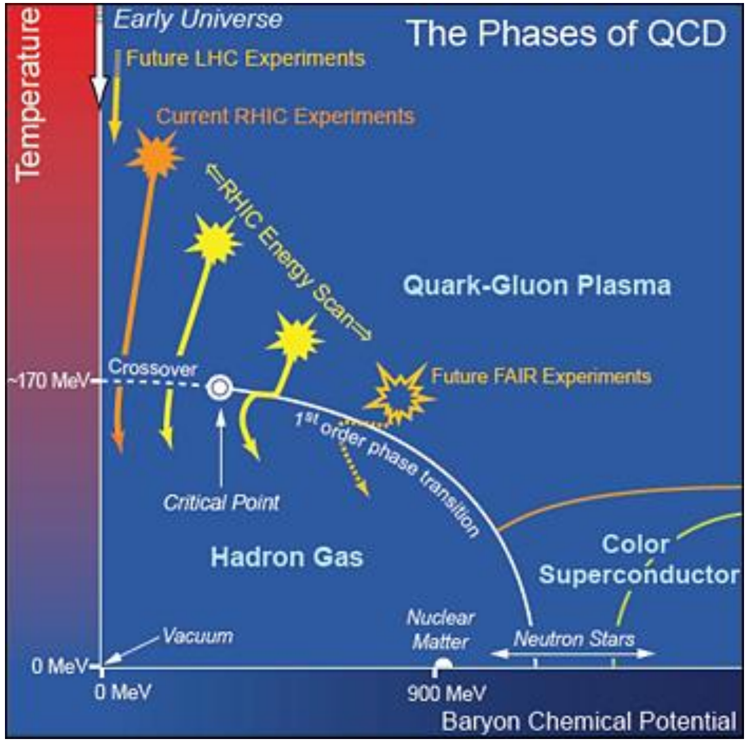

well studied

- Phases
- Phase boundaries
- Transition types
- Critical Point

under investigation

Phase diagram of QCD matter

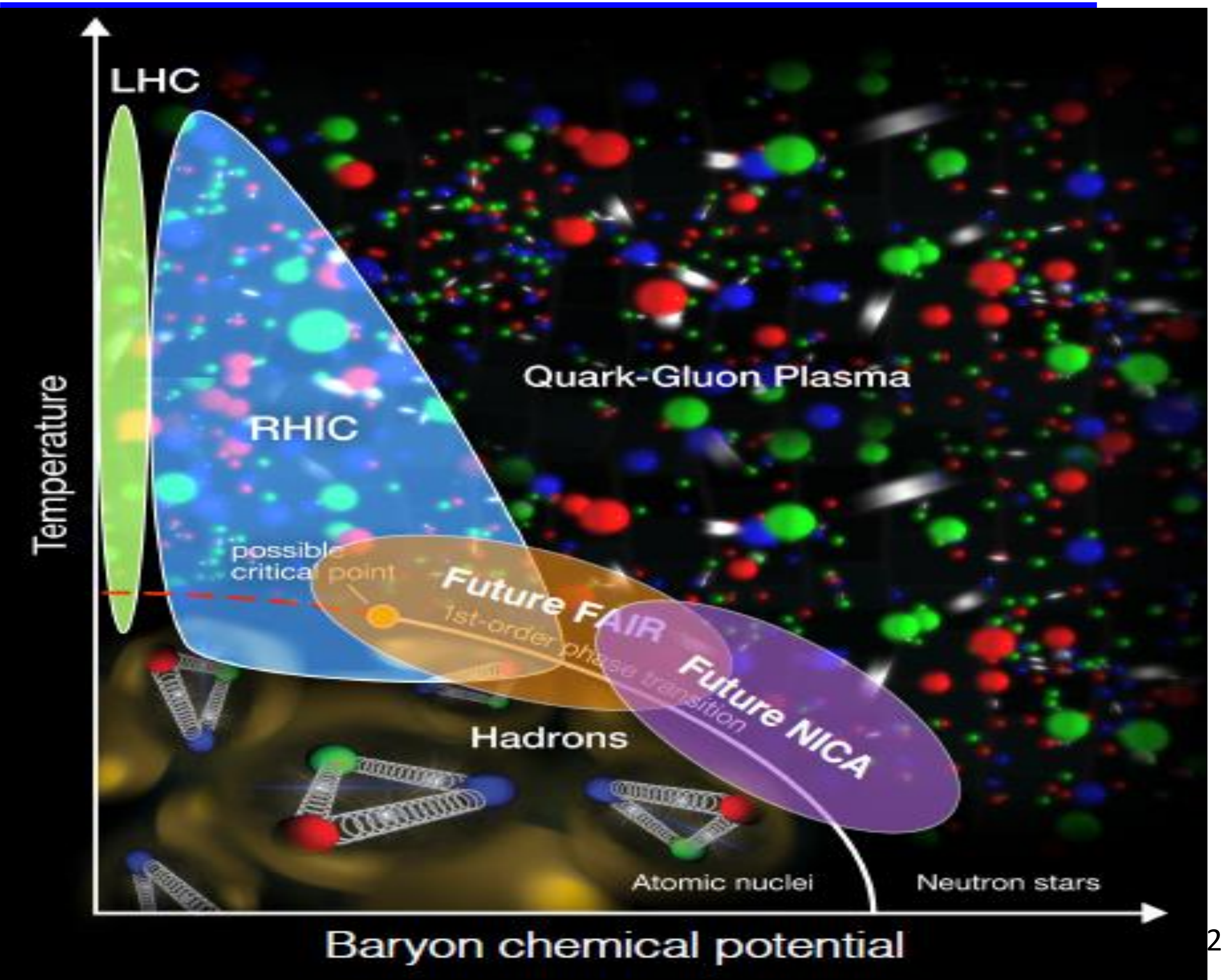

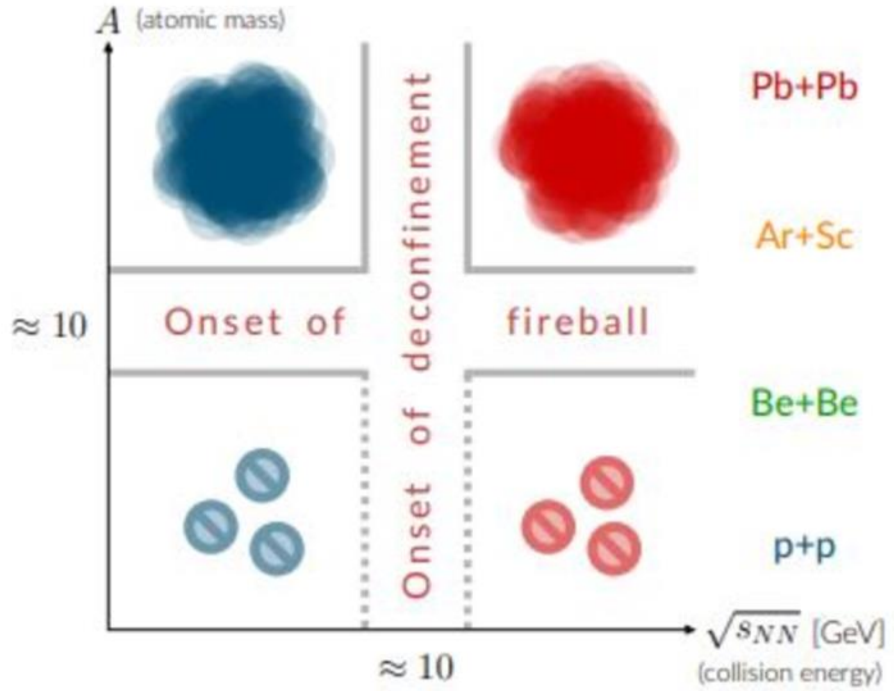

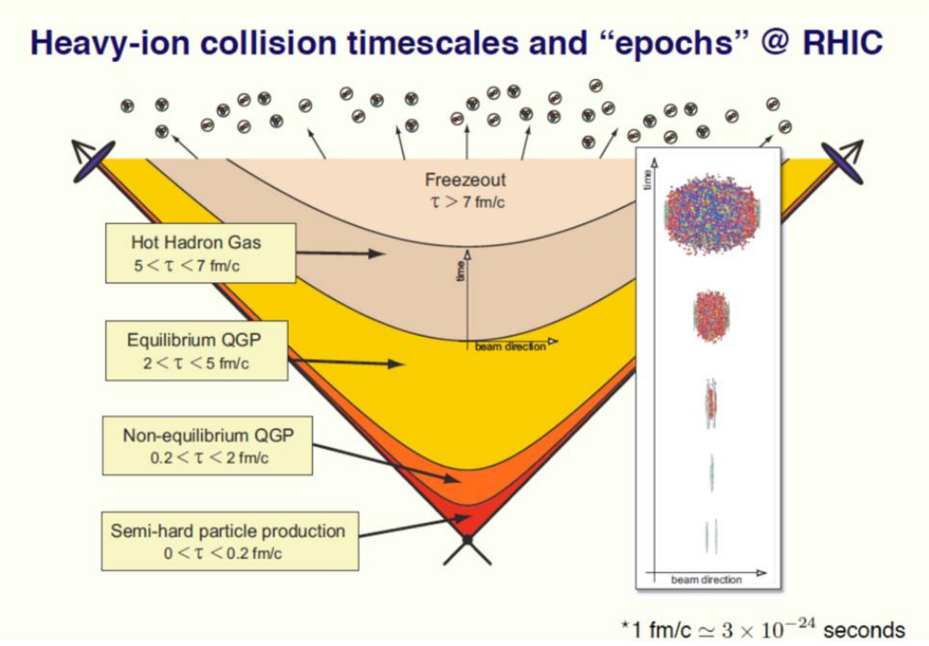

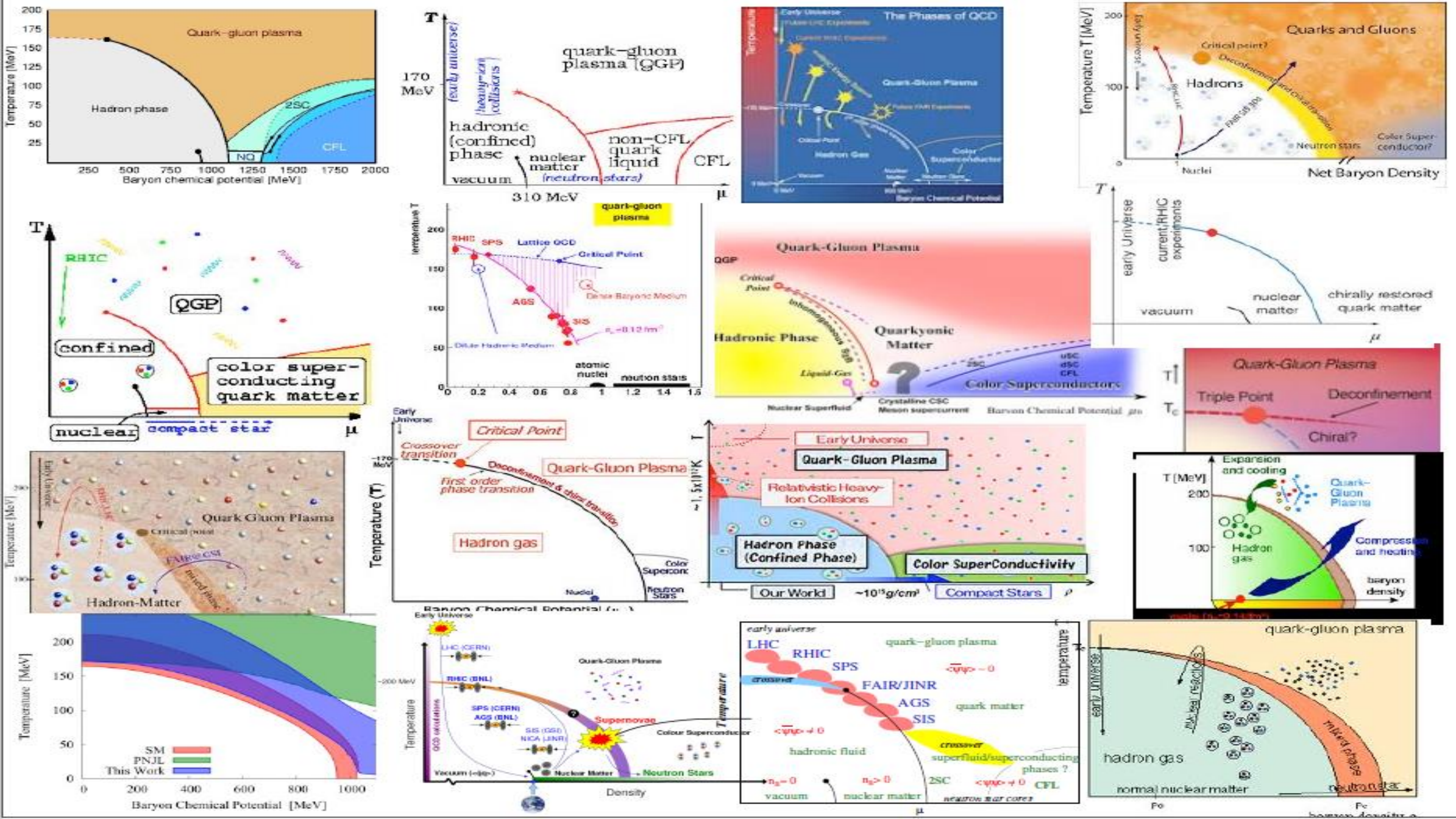

Quark–gluon plasma
Hadron phase
2SC
NQ
CFL
Temperature [MeV]
Baryon chemical potential [MeV]
quark–gluon plasma (QGP)
170 MeV
hadronic (confined) phase
nuclear matter
vacuum
non–CFL quark liquid
CFL
(neutron stars)
310 MeV
μ
The Phases of QCD
Early Universe
Quark-Gluon Plasma
Hadron Gas
Color Superconductor
Baryon Chemical Potential
Quarks and Gluons
Critical point?
Hadrons
Nuclei
Neutron stars
Color Super conductor?
Net Baryon Density
RHIC
QGP
confined
color super-conducting quark matter
nuclear
compact star
quark-gluon plasma
RHIC
SPS
Lattice QCD
Critical Point
AGS
SIS
Dense Baryonic Medium
Dilute Hadronic Medium
atomic nuclei
neutron stars
Quark-Gluon Plasma
Critical Point
Hadronic Phase
Quarkyonic Matter
Liquid-Gas
Color Superconductors
Nuclear Superfluid
Crystalline CSC
Meson supercurrent
Baryon Chemical Potential
early Universe
current RHIC experiments
vacuum
nuclear matter
chirally restored quark matter
Quark-Gluon Plasma
Triple Point
Deconfinement
Chiral?
Early Universe
Critical Point
Crossover transition
First order phase transition
Quark-Gluon Plasma
Hadron gas
Temperature (T)
Early Universe
Quark-Gluon Plasma
Relativistic Heavy-Ion Collisions
Hadron Phase (Confined Phase)
Color SuperConductivity
Our World
Compact Stars
Expansion and cooling
Quark-Gluon Plasma
T [MeV]
Hadron gas
Compression and heating
baryon density
Quark Gluon Plasma
Critical point
Hadron-Matter
Temperature [MeV]
SM
PNJL
This Work
Baryon Chemical Potential [MeV]
Early Universe
LHC (CERN)
RHIC (BNL)
SPS (CERN)
AGS (BNL)
Quark-Gluon Plasma
Supernovae
Colour Superconductor
Nuclear Matter
Neutron Stars
Temperature
Density
early universe
LHC
RHIC
SPS
FAIR/JINR
AGS
SIS
quark–gluon plasma
crossover
quark matter
hadronic fluid
superfluid/superconducting phases ?
2SC
CFL
vacuum
nuclear matter
quark-gluon plasma
early universe
hadron gas
mixed phase
normal nuclear matter
neutron star
temperature

Accelerator complexes for HIC

Relativistic Heavy Ion Collider (RHIC)

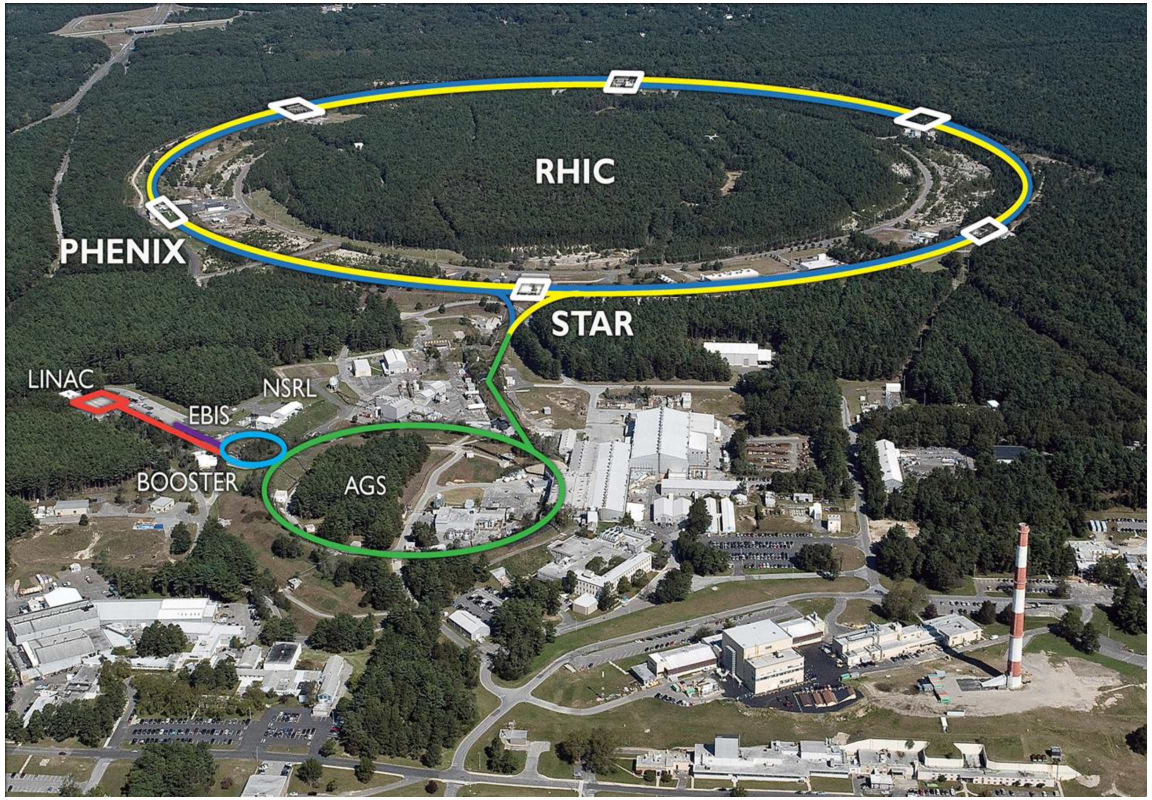

Brookhaven National Laboratory
In operation since 1999 Collider length 3,83 km
200 GeV Au+Au
510 GeV p+p

Large Hadron Collider (LHC)

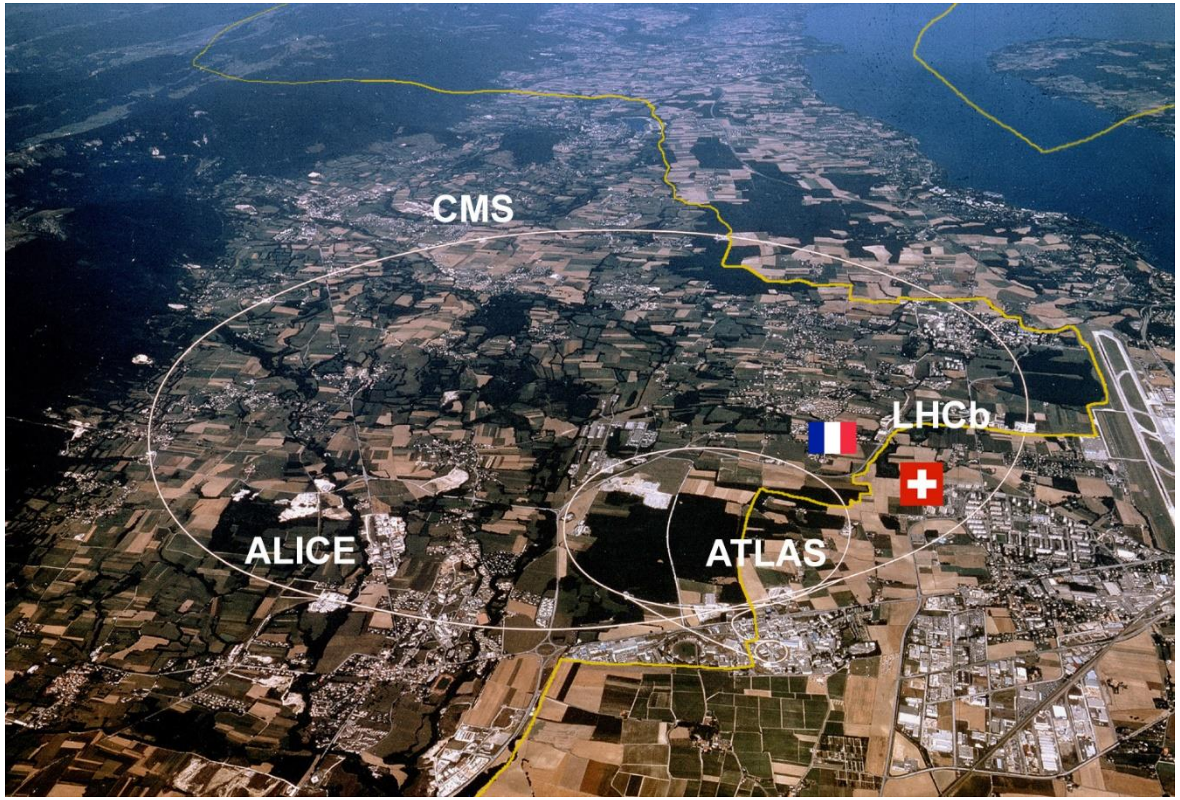

European Organization for Nuclear Research (CERN)
In operation since 2008 Collider length 27 km
5,02 TeV Pb+Pb
13 TeV p+p

Data systems available atHIC experiments

NA61/SHINE

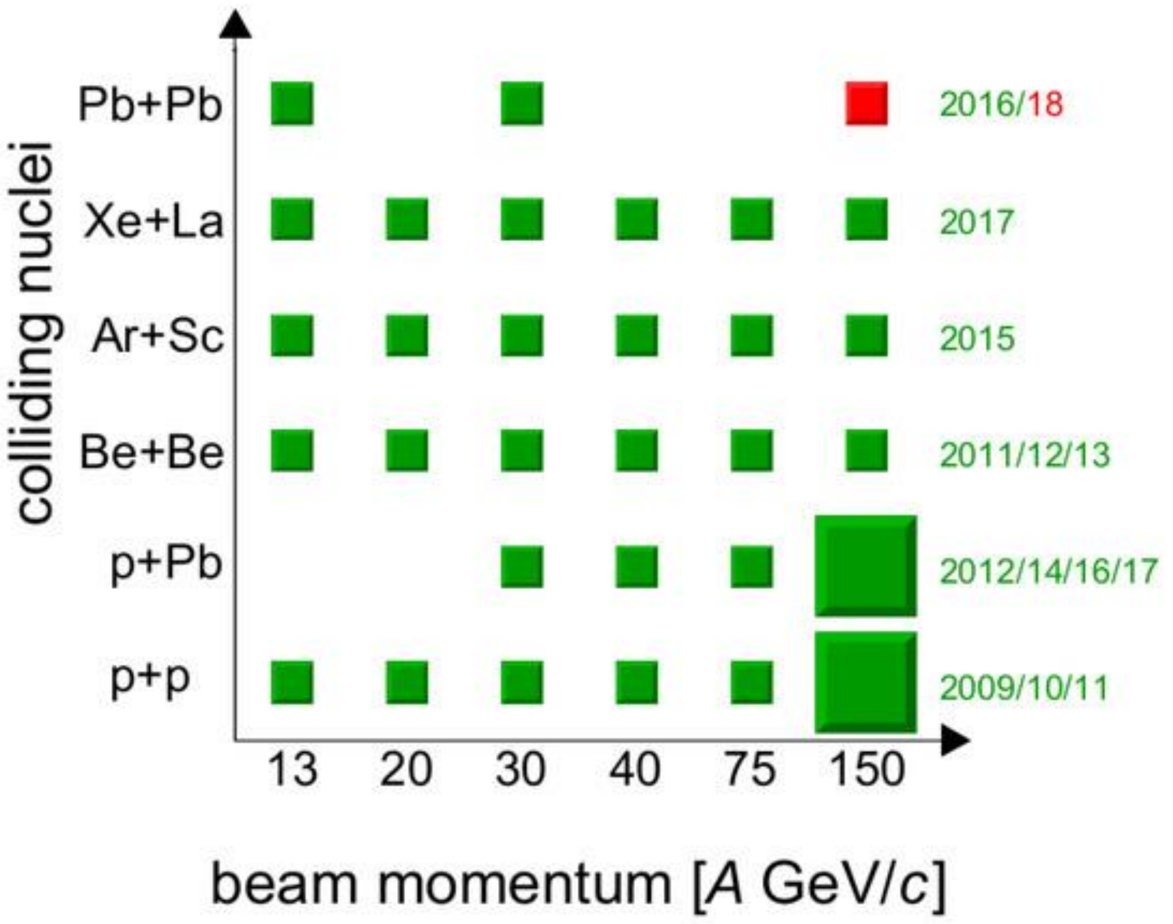

STAR

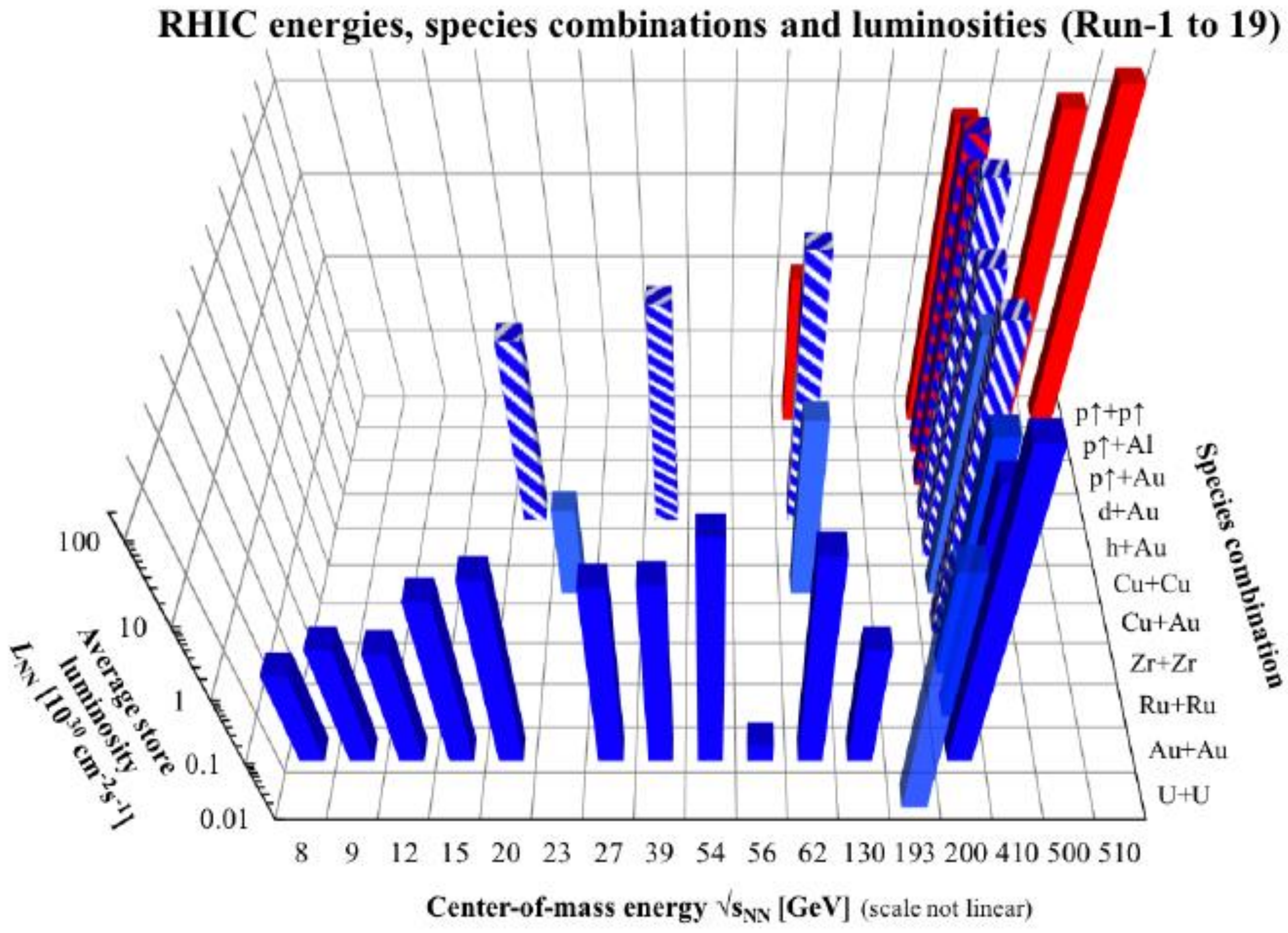

How do we see the ion collisions

https://online.star.bnl.gov/aggregator/livedisplay/

Au+Au @ STAR 200 GeV

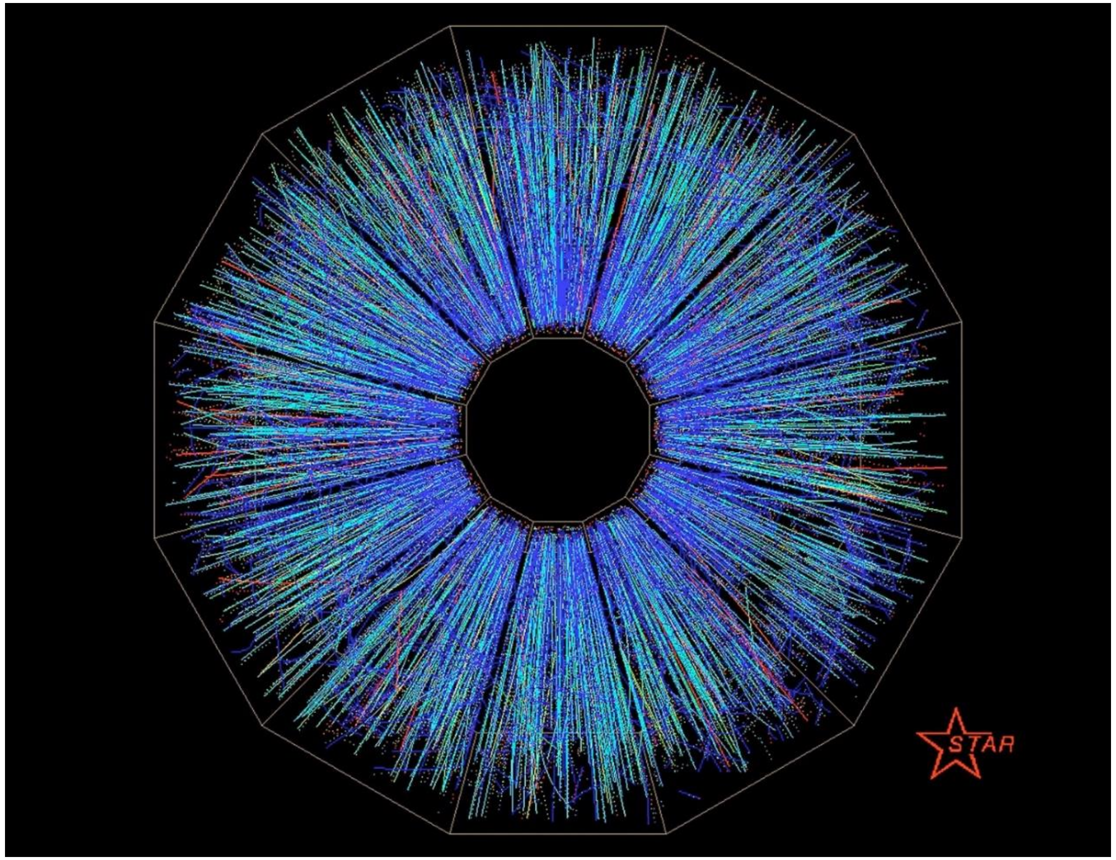

Pb+Pb @ ALICE 2,76 TeV

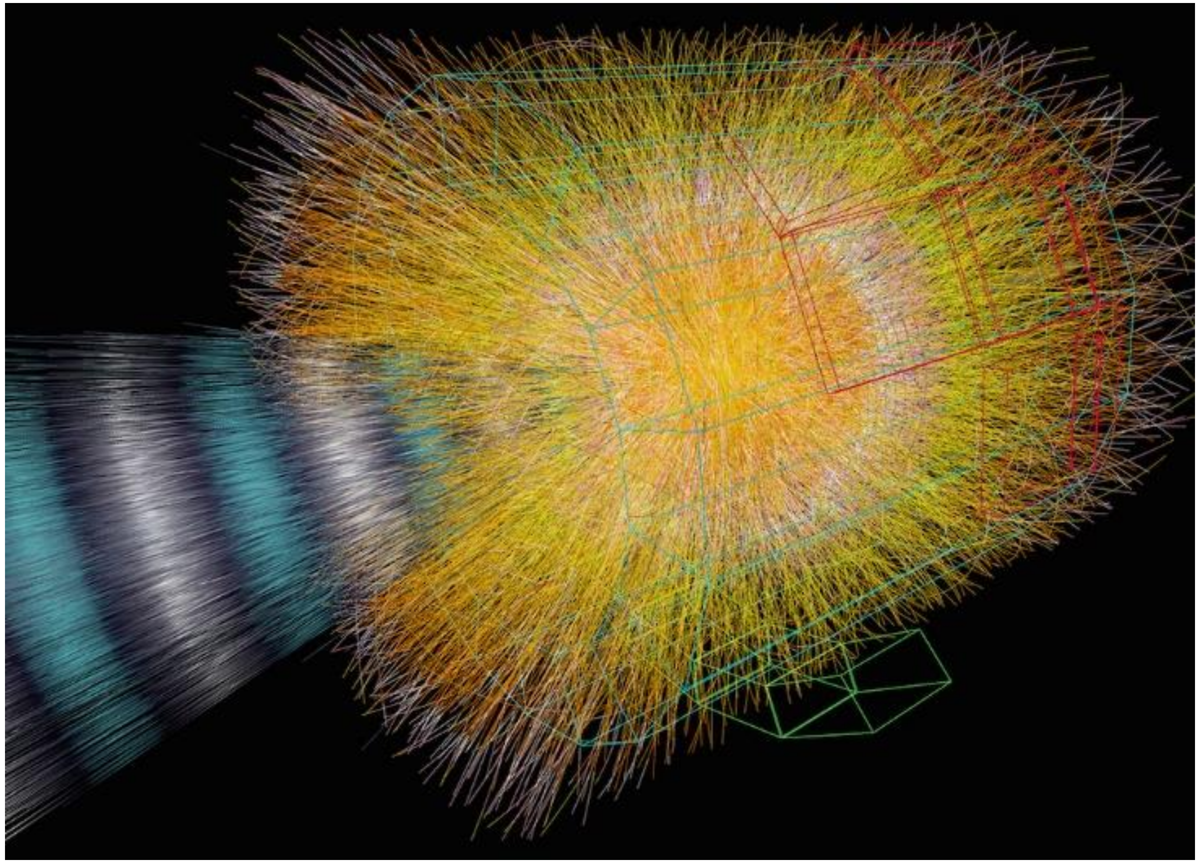

Heavy ion collisions provide a huge number of produced particles. We detect hundreds and thousands charged particles after each collision.

At 200 GeV ~ 1 000 charged particles are produced and at 2,76 GeV ~ 8 000 to 10k

Overview of HIC experiments

Experimental programs at SPS, ALICE, RHIC, NICA, SIS, J-PARC

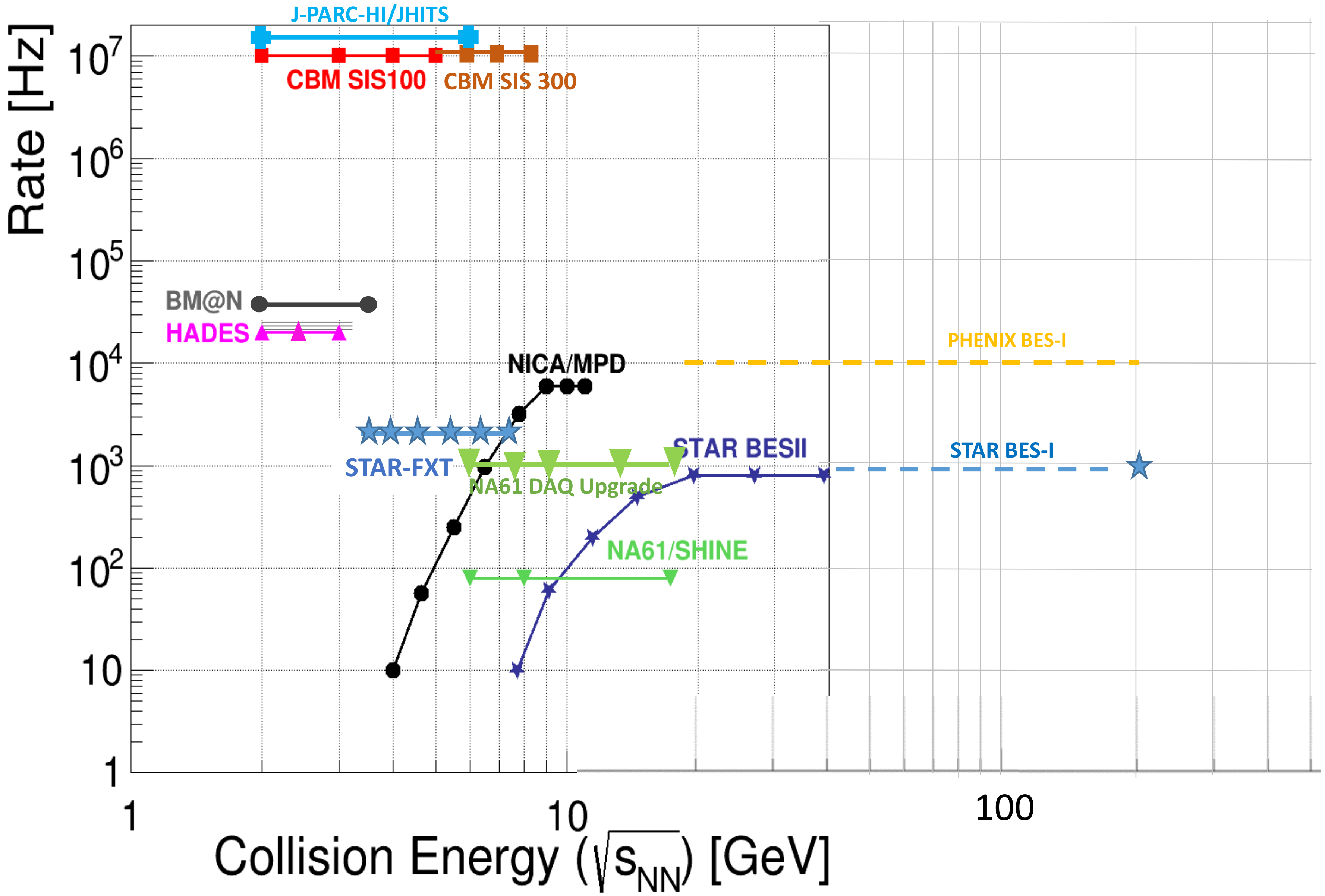

Part 2 Signatures of QGP

Particle spectra and Yields
Collective flow
Femtoscopy
Global polarization
Other probes

How to extract properties of the medium

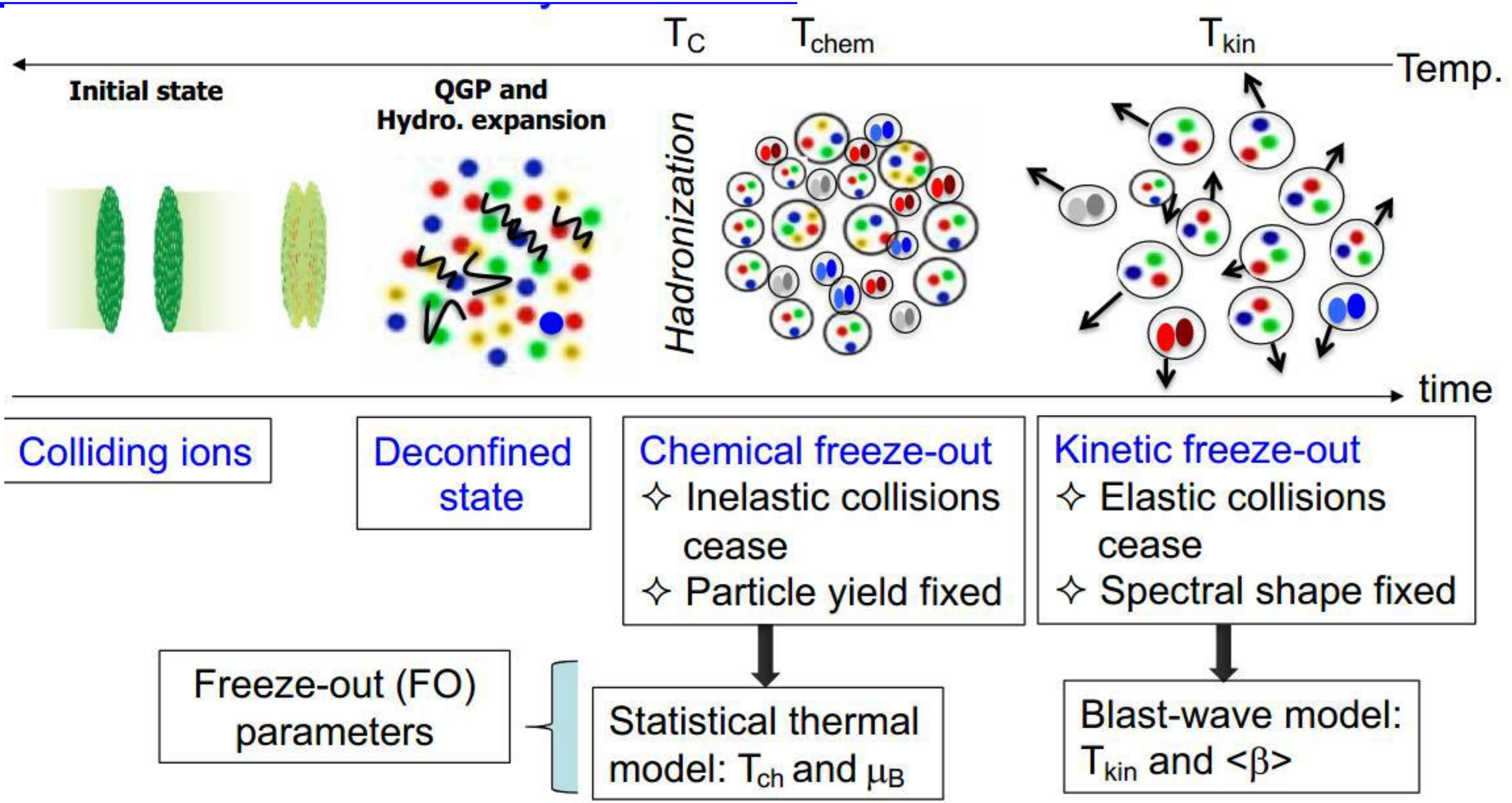

Particle Yields and **Ratios:** provide Information about QCD phase diagram

What we knew from early experiments

- Summary of AGS, SPS, and early RHIC Results
- Inclusive observables ➔ *onset of deconfinement* at 7-8 GeV.
- The observables suggest a change in the nature of the system.
- More discriminating studies were needed to understand the nature of the phase transition and to search for critical behavior.
- It is best to study regions above and below the possible onset energy.

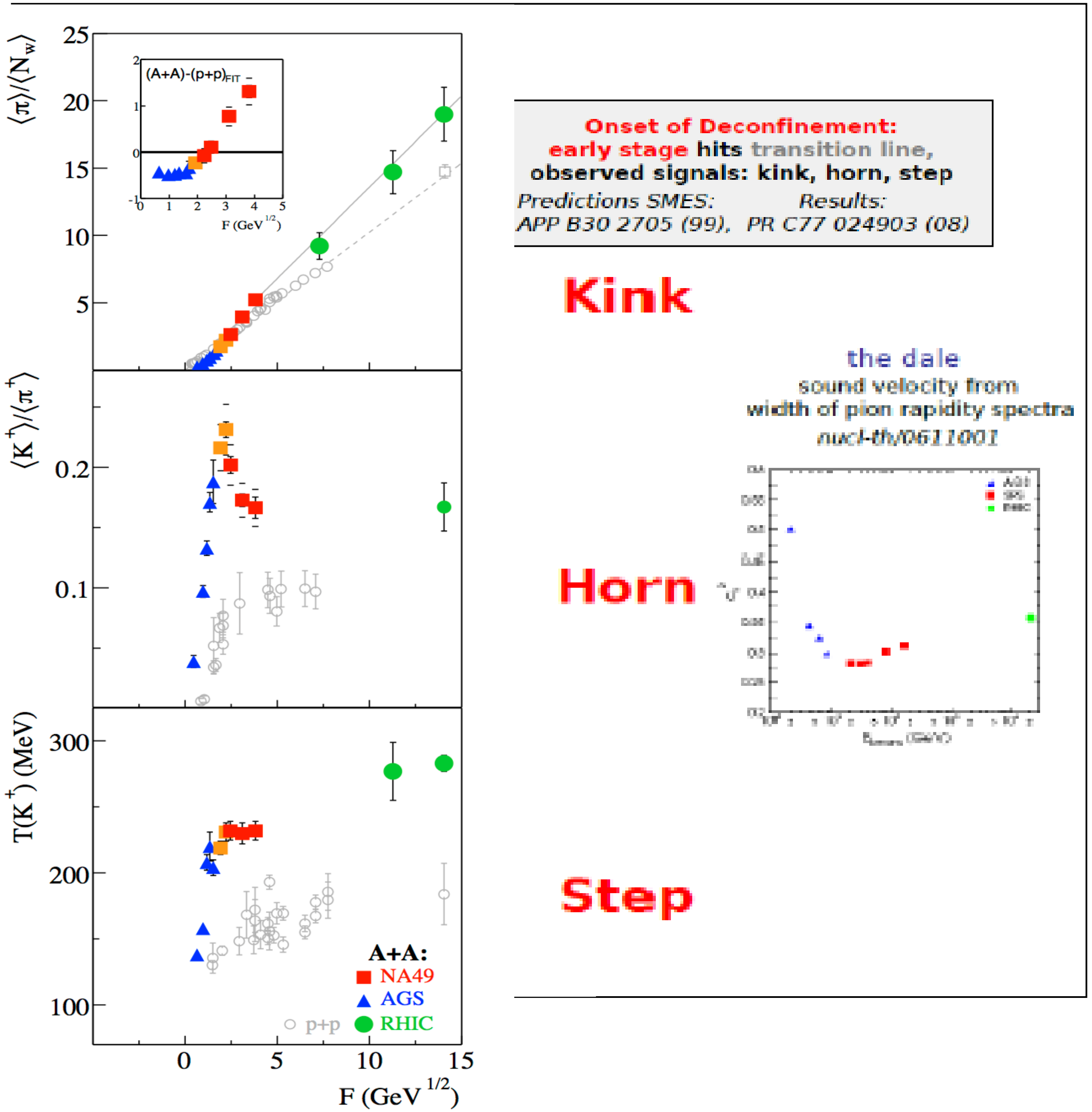

Particle production differential and integral

$$y = \frac{1}{2}\ln\frac{E+p_z}{E-p_z}$$

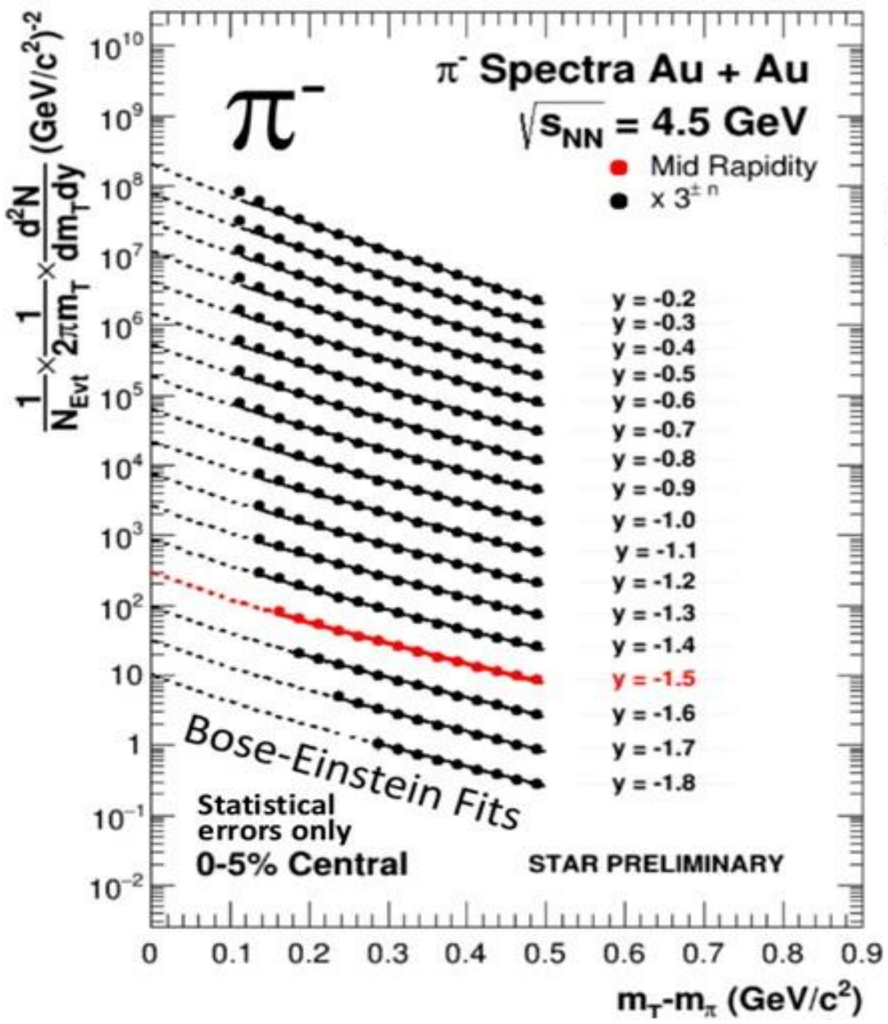

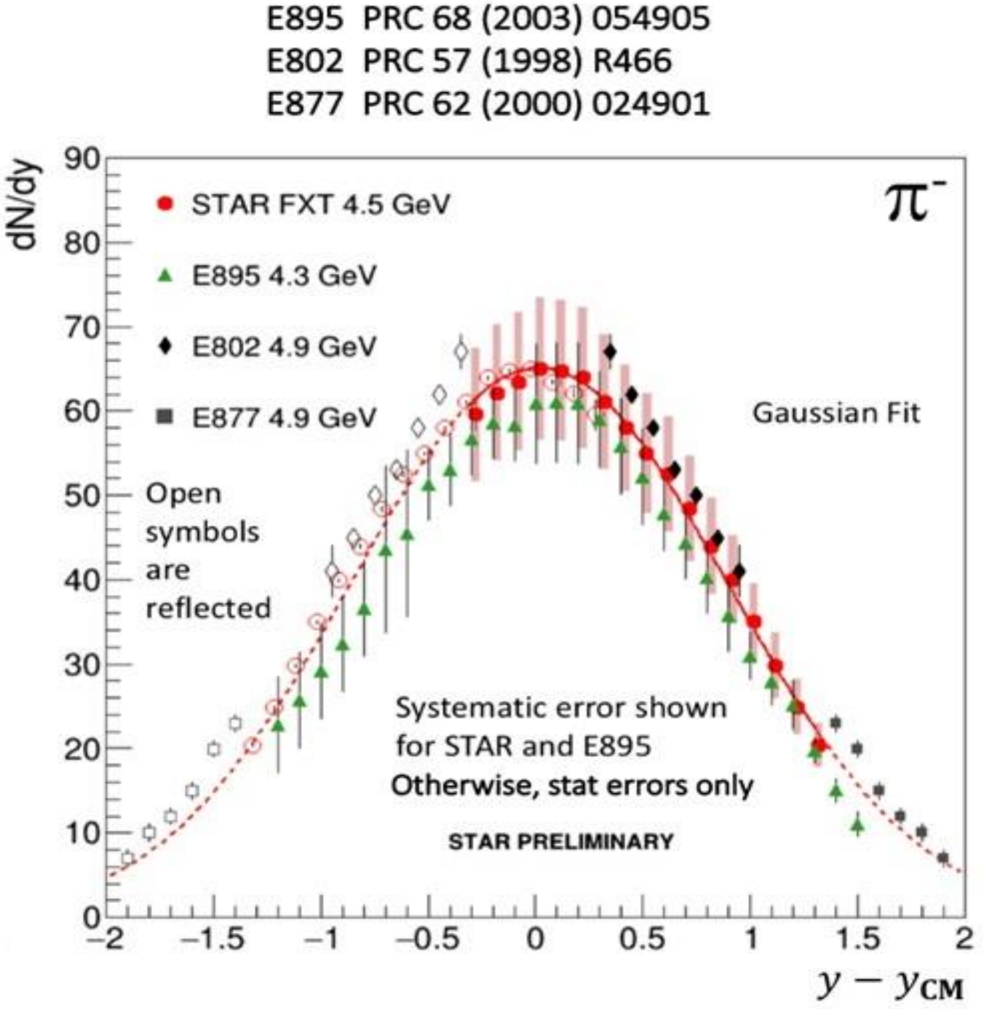

Thermal model and kinematic freeze-out

Inelastic collisions among the particles cease; the particle yields and ratios gets fixed

Statistical thermal model: J. Cleymans et al., Comp. Phys. Comm. **180**, 84 (2009)

$$n = \frac{1}{V}\frac{\partial(T\ln Z)}{\partial\mu} = \frac{VTm_i^2 g_i}{2\pi^2}\sum_{k=1}^{\infty}\frac{(\pm1)^{k+1}}{k}\left(e^{\beta k\mu_i}\right)K_2\left(\frac{km_i}{T}\right)$$

(Grand canonical ensemble)

$\beta \cong 1/T$; -1(+1) for fermions (bosons),
Z - partition function;
m_i - mass of hadron species i;

V - volume; T - Temperature;
K_2 - 2nd-order Bessel function;
g_i - degeneracy; μ_i - chemical potential

Model Features: Assumes
- ❑ Non-interacting hadrons and resonances
- ❑ Thermodynamically equilibrium system

Energy dependence of yields

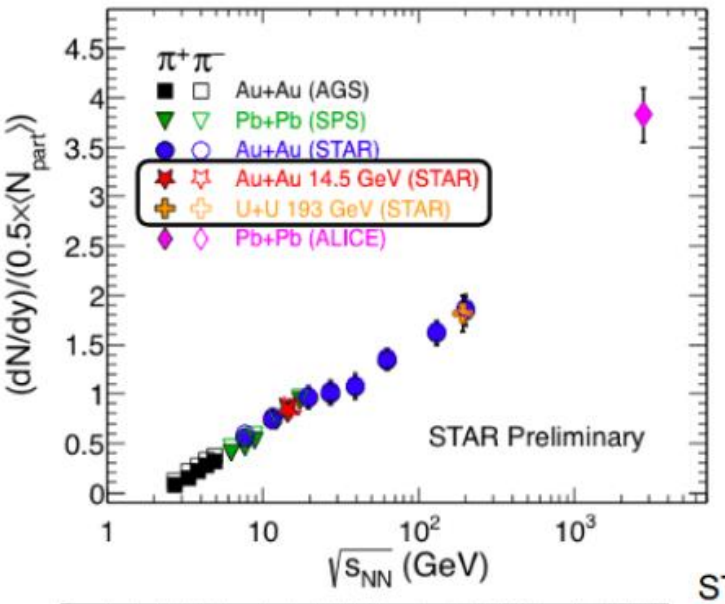

STAR: PRC **96**, 044904 (2017)

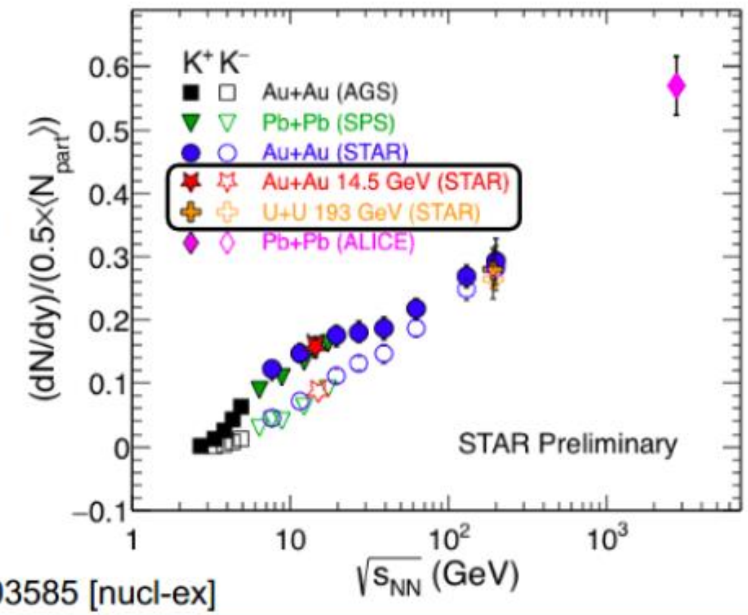

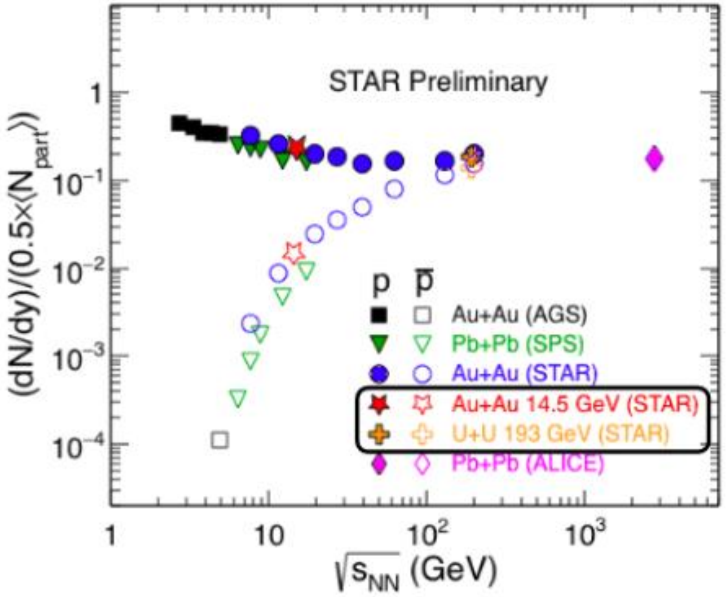

STAR: arXiv:1908.03585 [nucl-ex]

- Yields increase as a function of collision energy except for protons
- *Au+Au 14.5 GeV and U+U 193 GeV fit well in the trend*
- **Higher energies:** Similar (pair) production of particle and anti-particle

Lower energies: $\pi^- > \pi^+$, $K^+ > K^-$, $p > \bar{p}$

Energy dependence of particle ratios

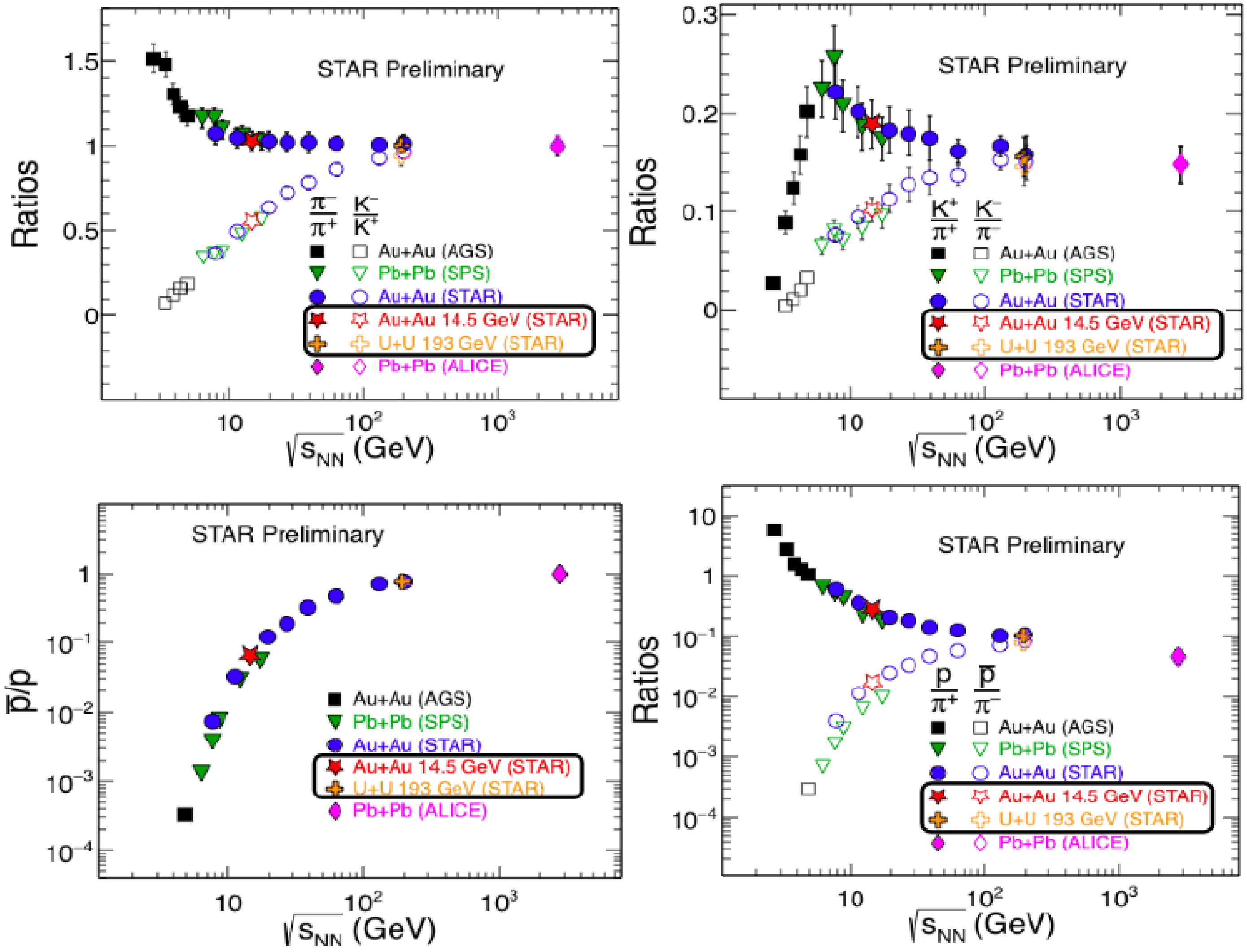

STAR: PRC **96**, 044904 (2017)   STAR: arXiv: 1908.03585 [nucl-ex]

Ratios shows interesting trends for energy dependence

Au+Au 14.5 and U+U 193 fit well in established trend

Almost no barion asymmetry at high energies

At lower energies

$$\pi^- > \pi^+, K^+ > K^-, p > \bar{p}$$

Thermal model particle production

$$\frac{p}{T^4} = \frac{1}{T^3}\frac{\partial \ln Z(V,T,\mu)}{\partial V}$$

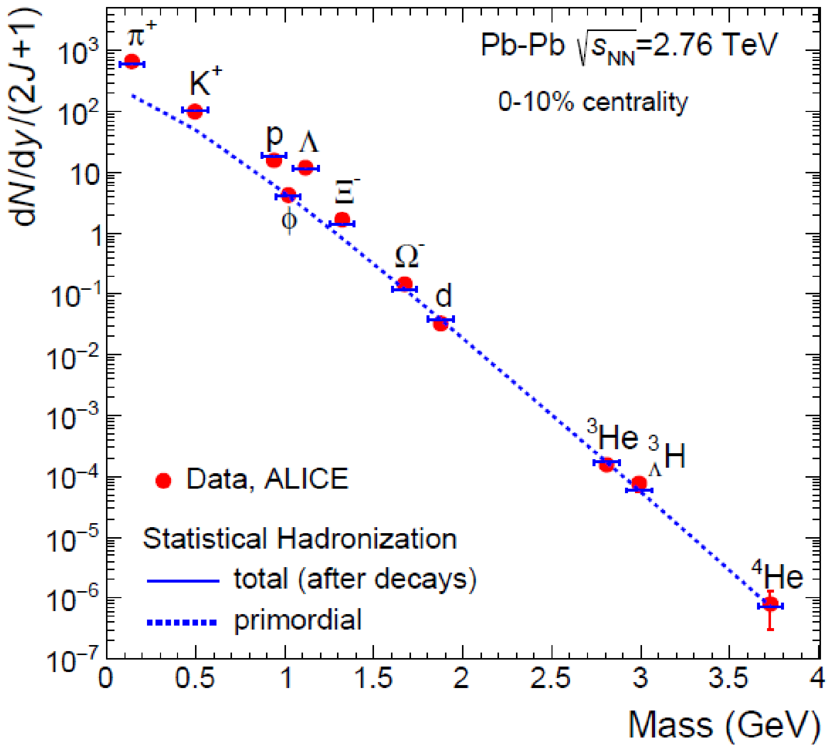

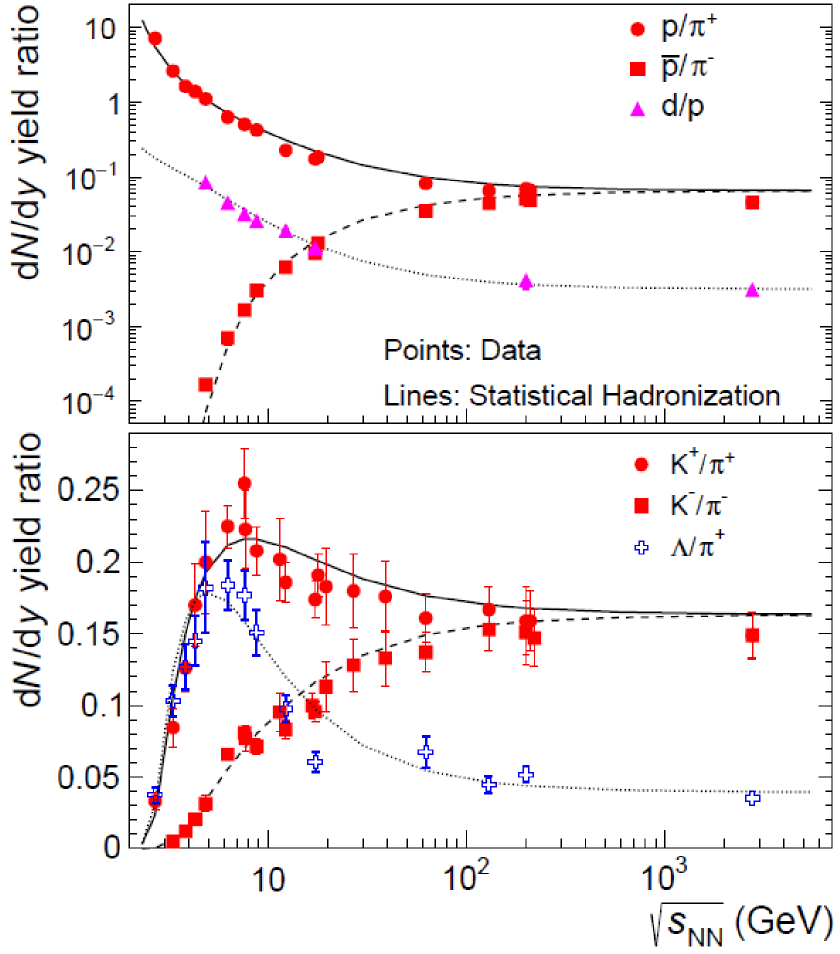

Blast-Wave model and chemical freeze-out

Elastic collisions among the particles cease and the momentum distribution gets fixed

Blast-Wave (BW) Model:

$$\frac{dN}{p_T dp_T} \propto \int_0^R r dr m_T I_0\left(\frac{p_T \sinh \rho(r)}{T_{kin}}\right) \times K_1\left(\frac{m_T \cosh \rho(r)}{T_{kin}}\right)$$

E. Schnedermann, J. Sollfrank, and U. W. Heinz, Phys. Rev. C **48**, 2462 (1993).

I_0, K_1: Modified Bessel functions
$\rho(r) = \tanh^{-1}\beta$, r/R: relative radial position; R: radius of fireball
β: transverse radial flow velocity, T_{kin}: Kinetic freeze-out temperature

Model Features:

- Hydrodynamic based model
- Assumes particles are locally thermal at a kinetic freeze-out temperature and moving with a common radial flow velocity

Phys. Rev. C **102** (2020) 34909

Momentum spectra of strange particles at BES-I

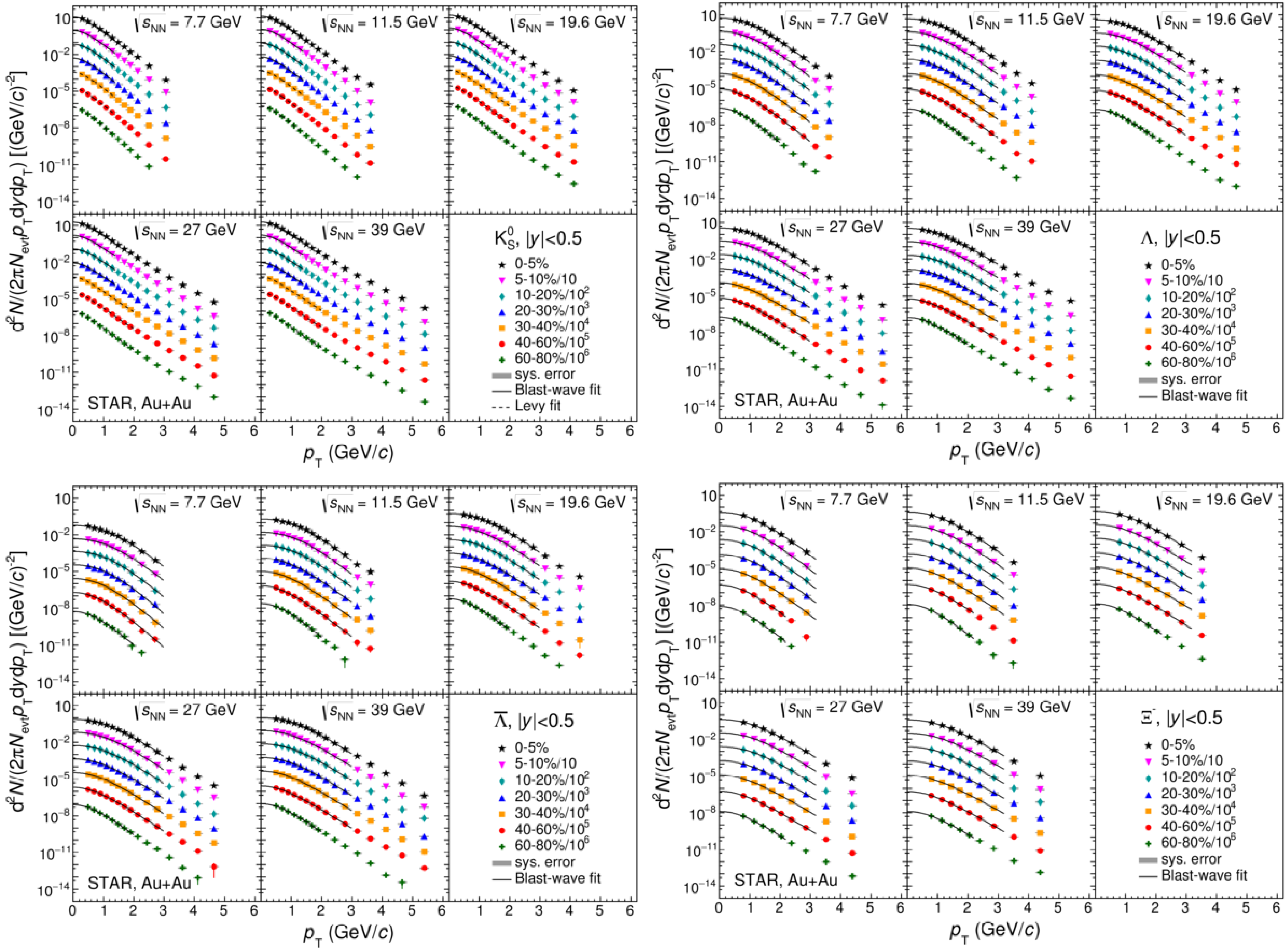

K^0_s, Λ, anti-Λ, Ξ^- transverse momentum spectra at midrapidity |y| < 0.5

Levy fit

$$\frac{d^2N}{2\pi p_T dp_T dy} \propto \left(1+\frac{m_T - m_0}{nT}\right)^{-n}$$

Blast-wave fit

$$\frac{d^2N}{2\pi p_T dp_T dy} \propto \int_0^R r dr m_T I_0\left(\frac{p_T \sinh\rho(r)}{T}\right) \times K_1\left(\frac{m_T \cosh\rho(r)}{T}\right)$$

Phase diagram scan

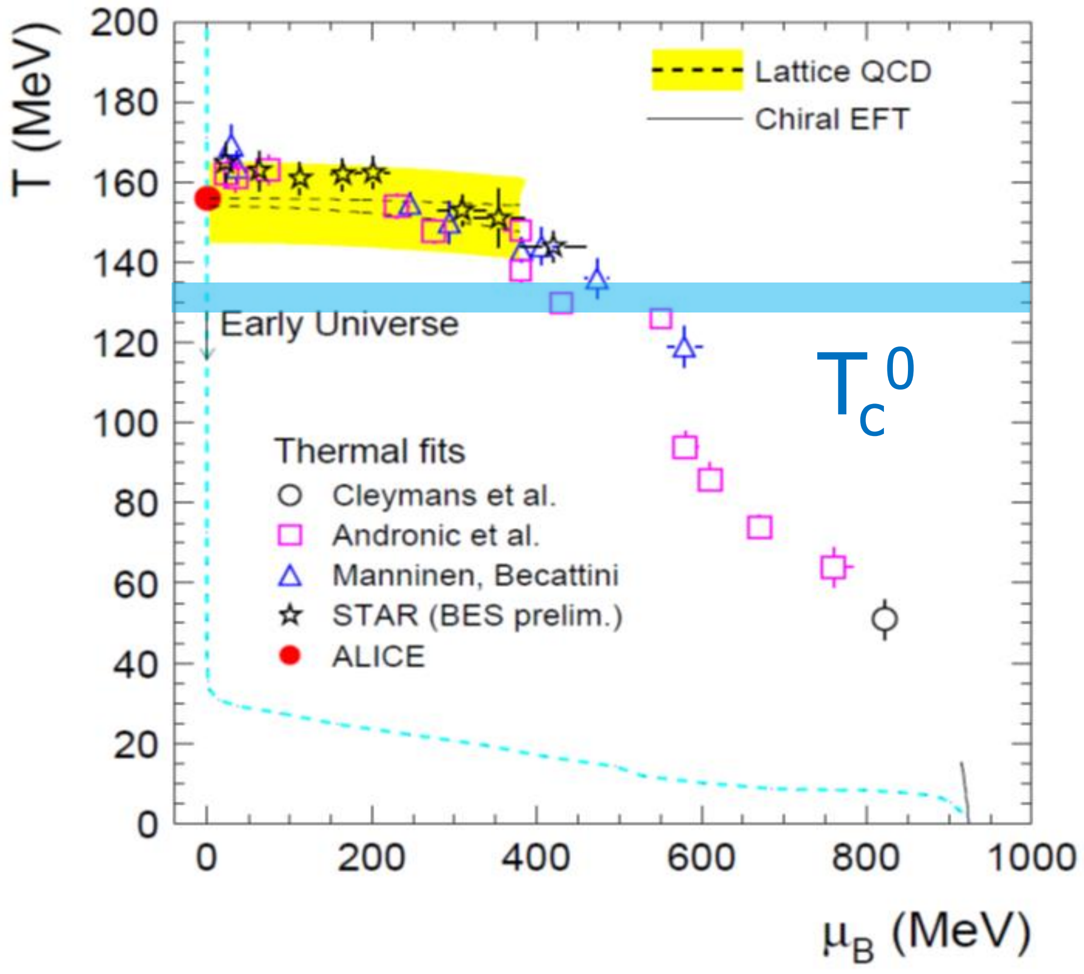

A. Andronic et al., Jour. Phys. G38 (2011)

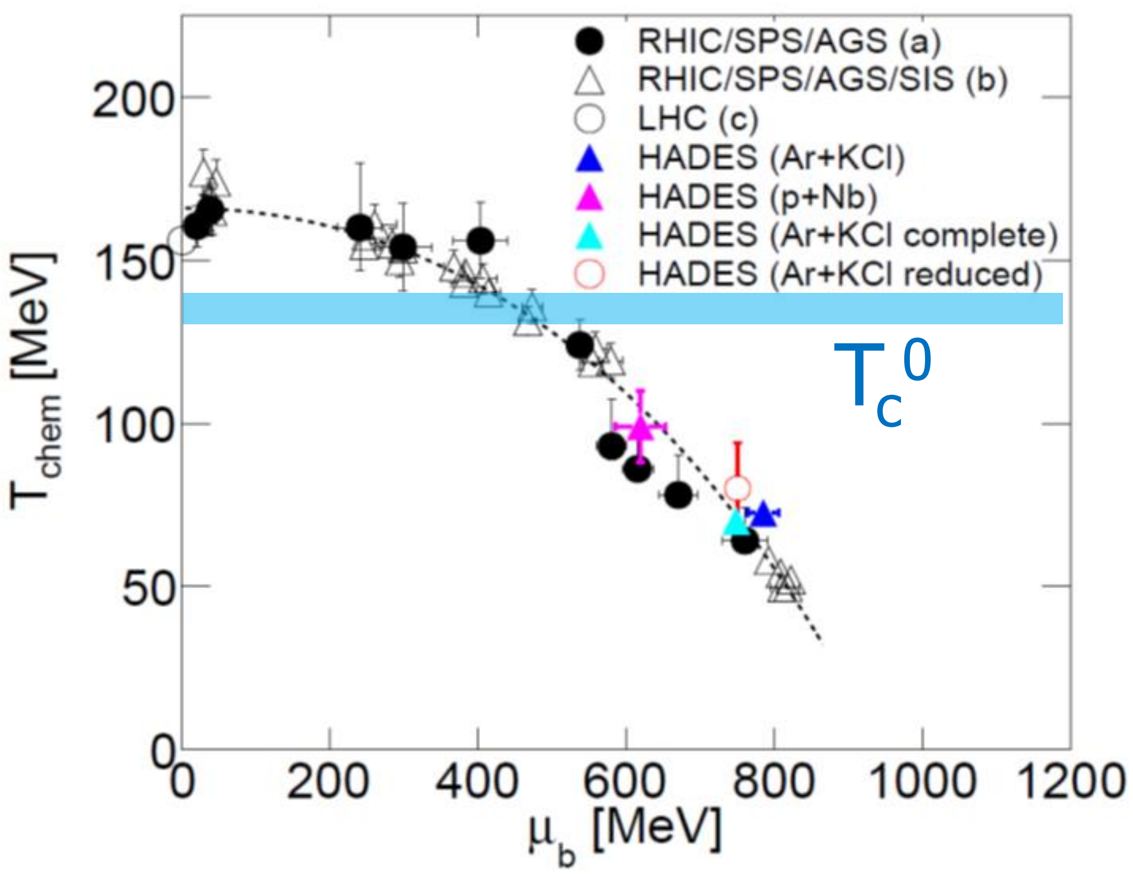

G. Agakishiev et al., arXiv:1512.07070

Phase diagram scan

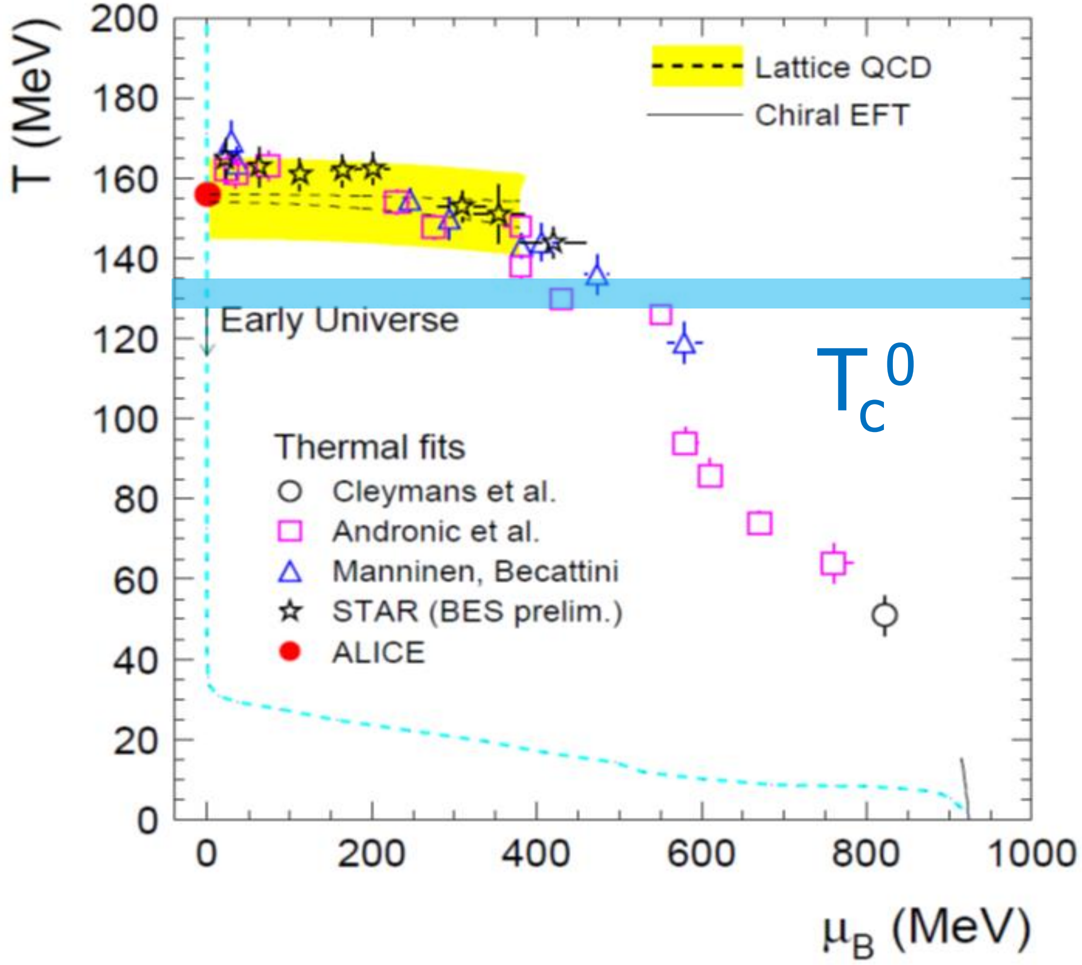

T_c^0

T_{chem} and T_{kin} diverge at around 7 GeV.

T_{kin} and <β> flatten

Softening of the EoS?

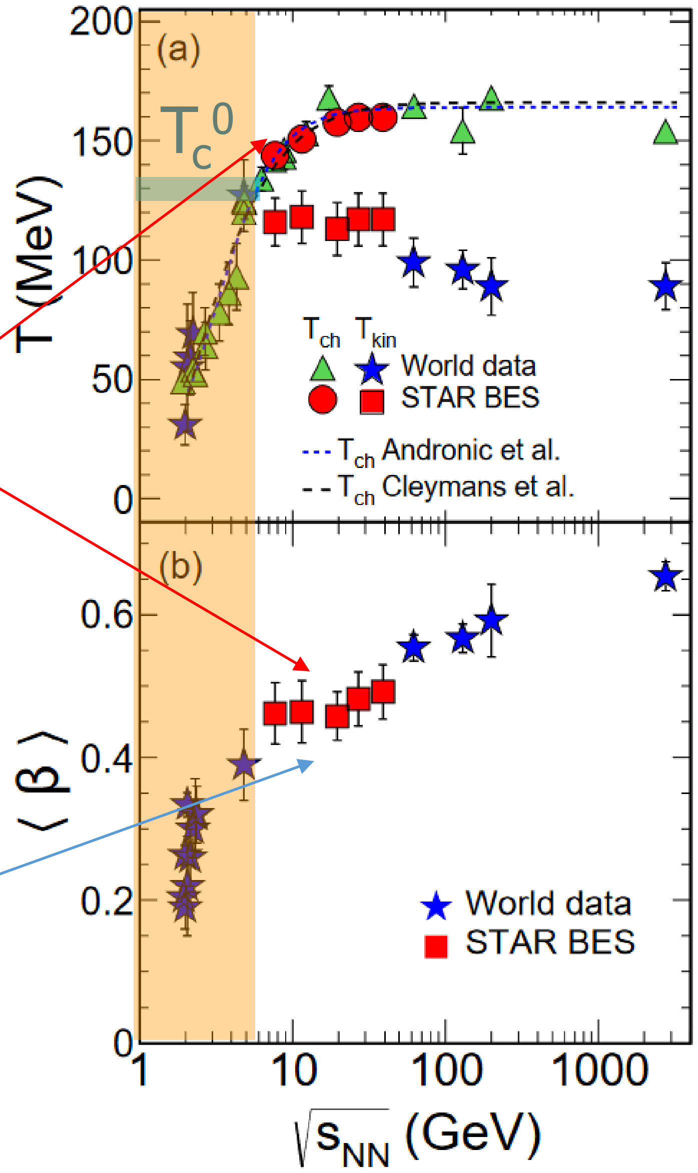

T_{ch}

T_{kin}

L. Adamczyk, et al. STAR Collaboration Phys. Rev. C96 (2017) 044904

Strange particle production

Pike is observed in particle ratios for strange/non-strange particles for HIC and not observed for light collision systems

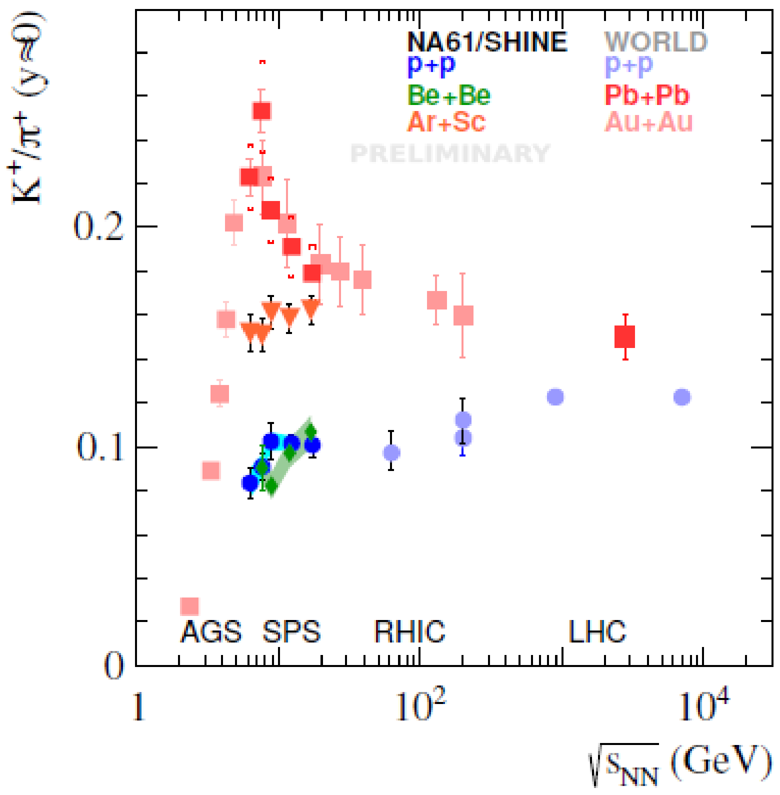

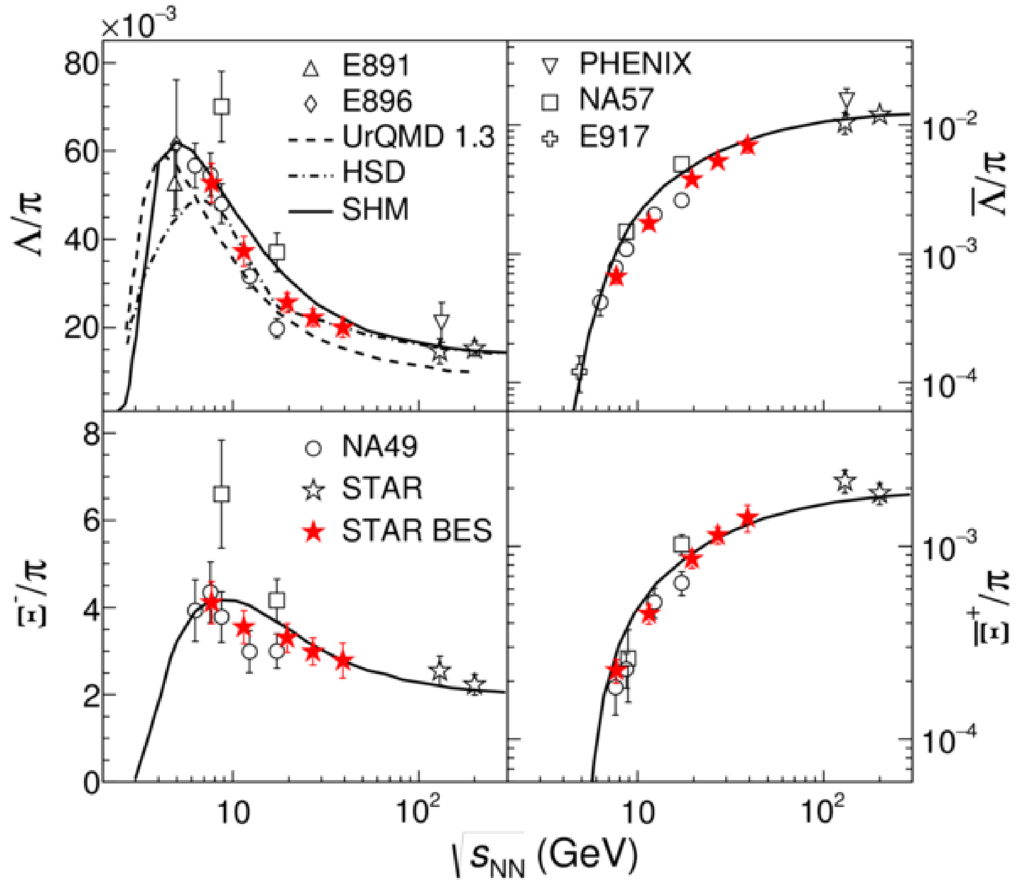

Collective flow

$$\frac{dN}{d(\phi-\psi_n)} = \frac{1}{2\pi}\left(1 + 2\sum_{n=1}^{+\infty} v_n cos\ [n(\phi-\psi_n)]\right)$$

Initial spatial asymmetry is transferred to the final momentum asymmetry

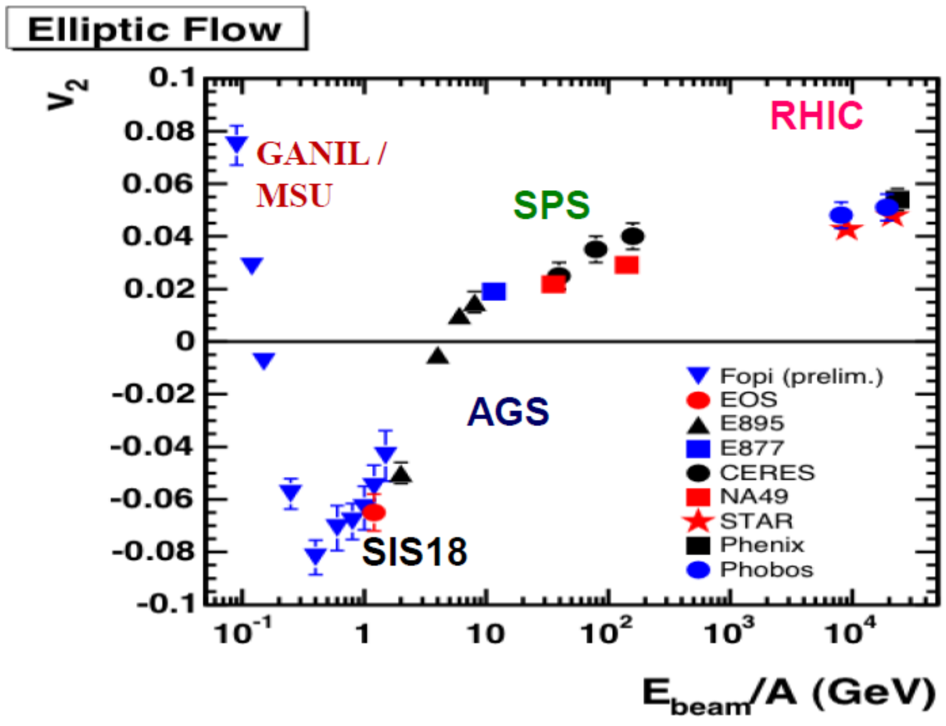

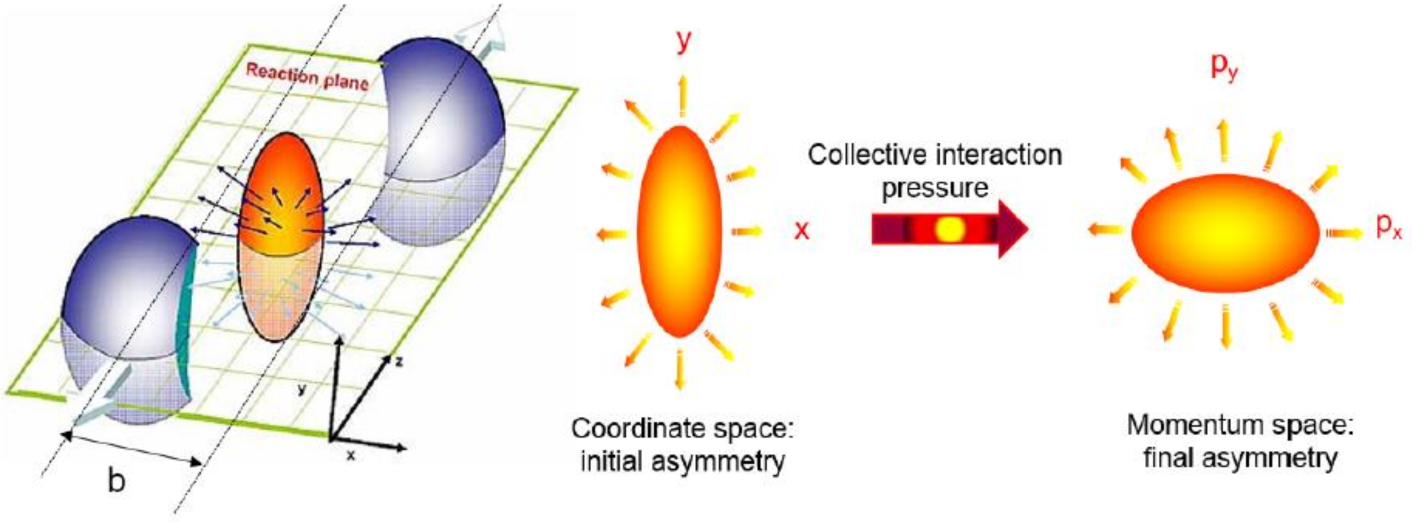

$$E\frac{d^3N}{dp^3} = \frac{1}{2\pi}\frac{d^2N}{p_t dp_t dy}\left(1+\sum_{n=1}^{\infty} 2v_n \cos[n(\varphi-\Psi_r)]\right)$$

Elliptic flow, NCQ-scaling

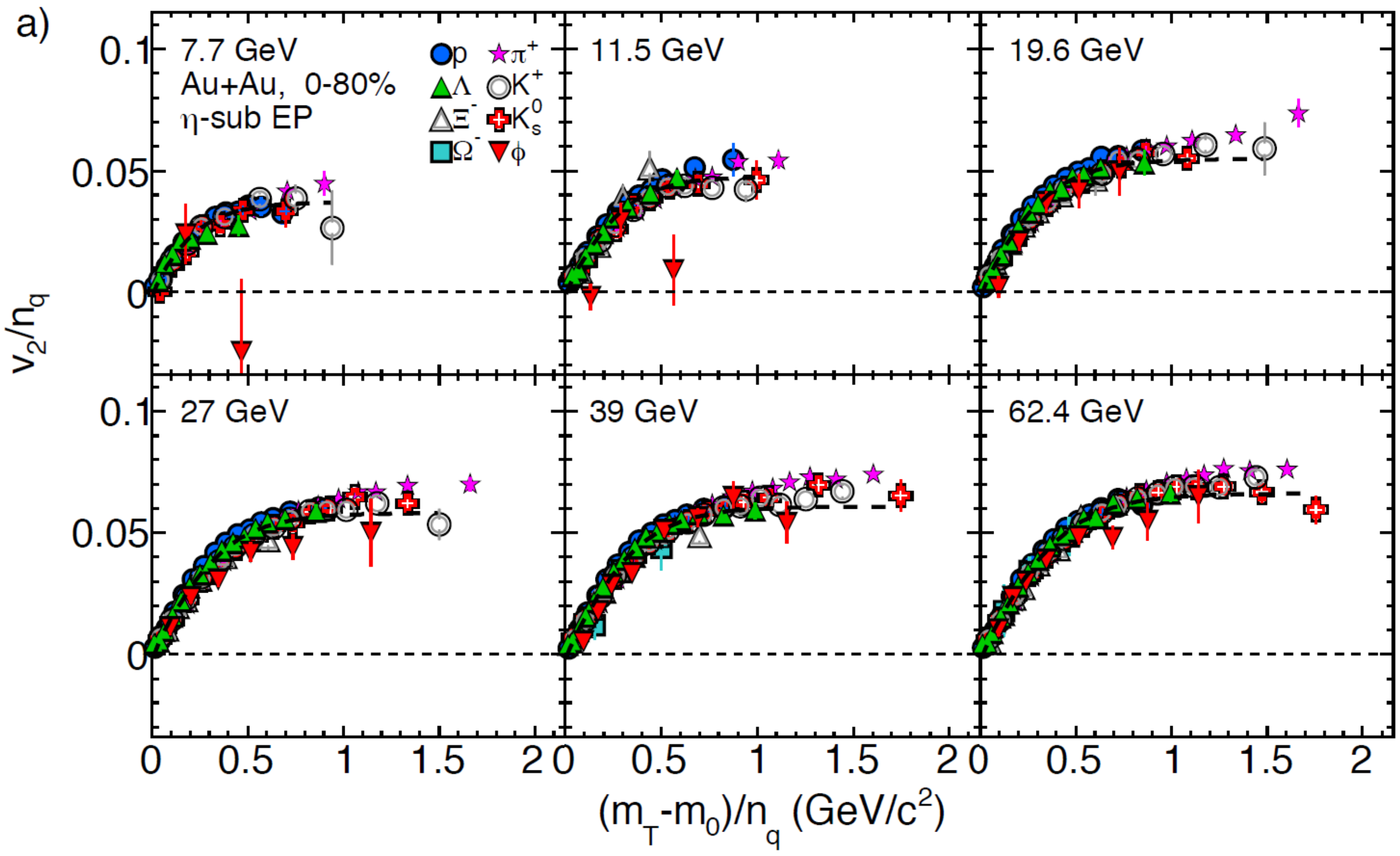

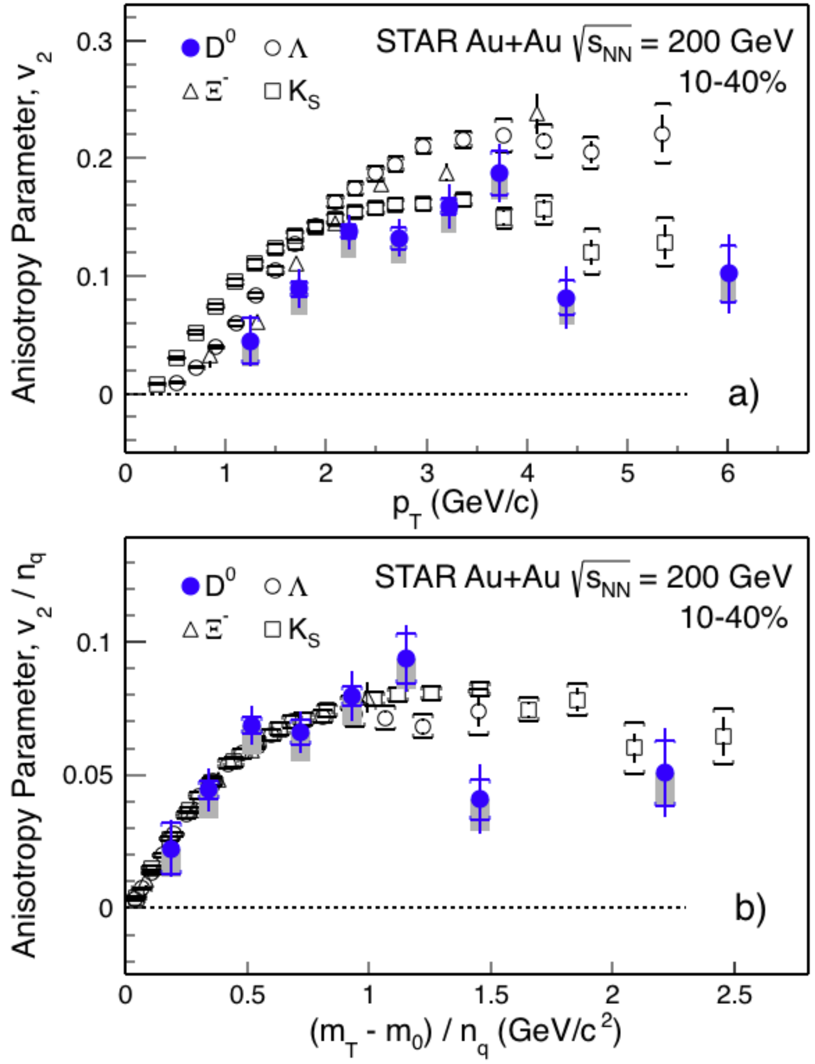

Elliptic flow, NCQ-scaling

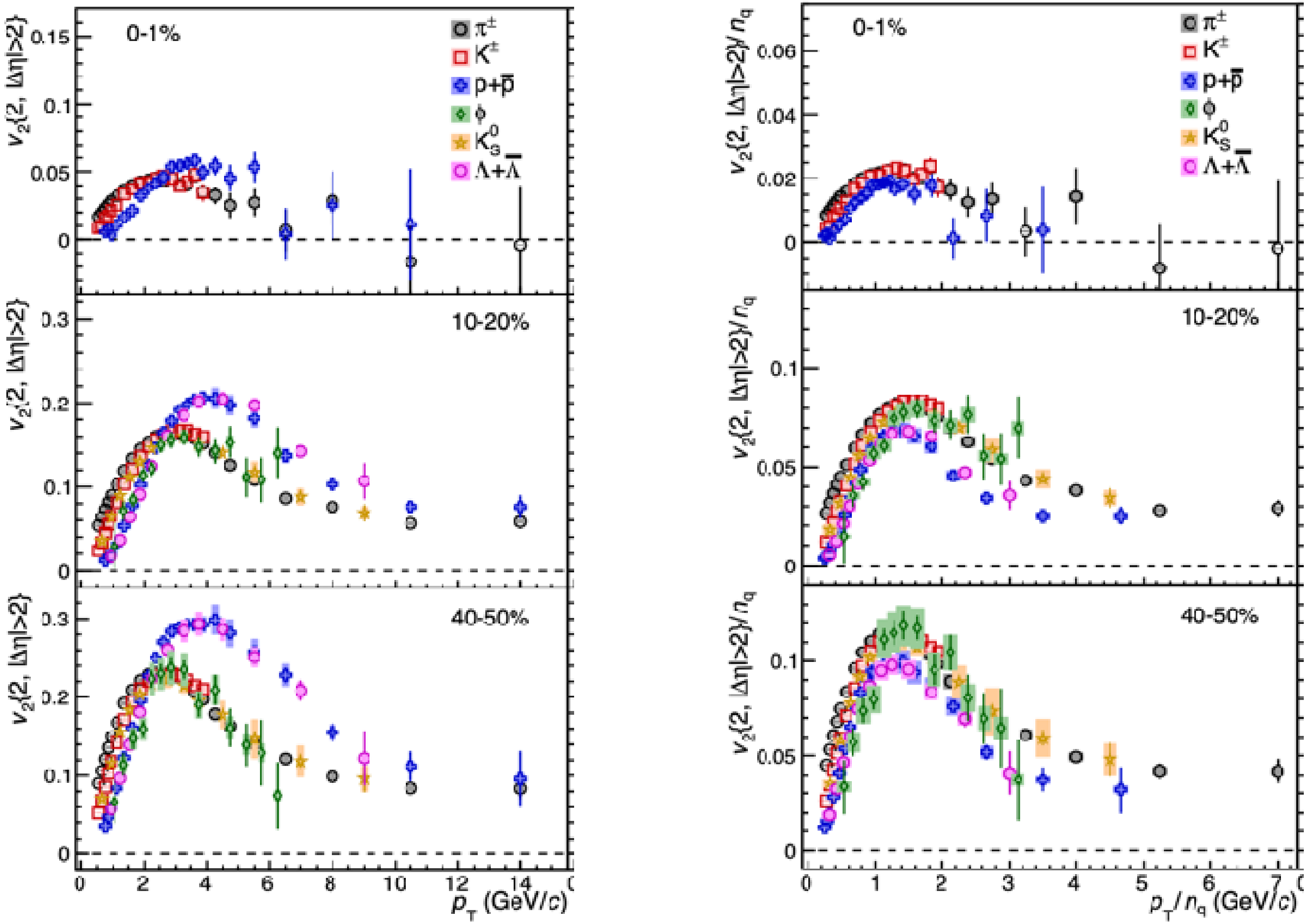

All data from RHIC and LHC are consistent with the interpretation that collective flow is established at the quark level and imprinted on the flow pattern of hadrons.

Valence quark scaling laws of flow observables are our most direct evidence that light quarks are unconfined in the QGP

HBT and femtoscopy

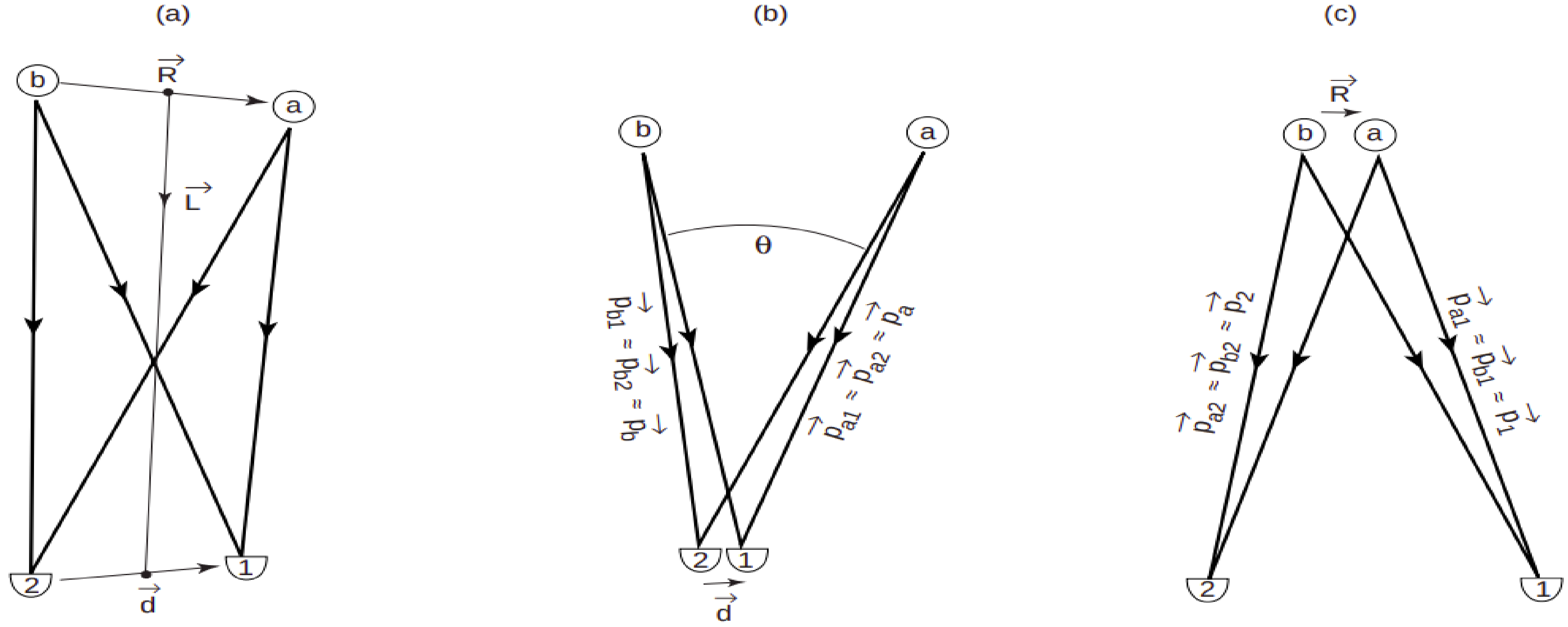

1,2 — detectors; a,b — sources
(a) — general idea
(b) — astronomy R>>d
(c) — nuclear physics R<<d

Similar to the astrophysics, HBT correlations

Sov.J.Nucl.Phys. 35 (1982) 770
Phys.Lett.B 373 (1996) 30-34

Correlation function effects

$$C(\vec{k}^*) = \int S(\vec{r}^*)\,|\psi(\vec{k}^*,\vec{r}^*)|^2\,d^3r^*$$

➡ Relative wave function sensitive to interaction potential

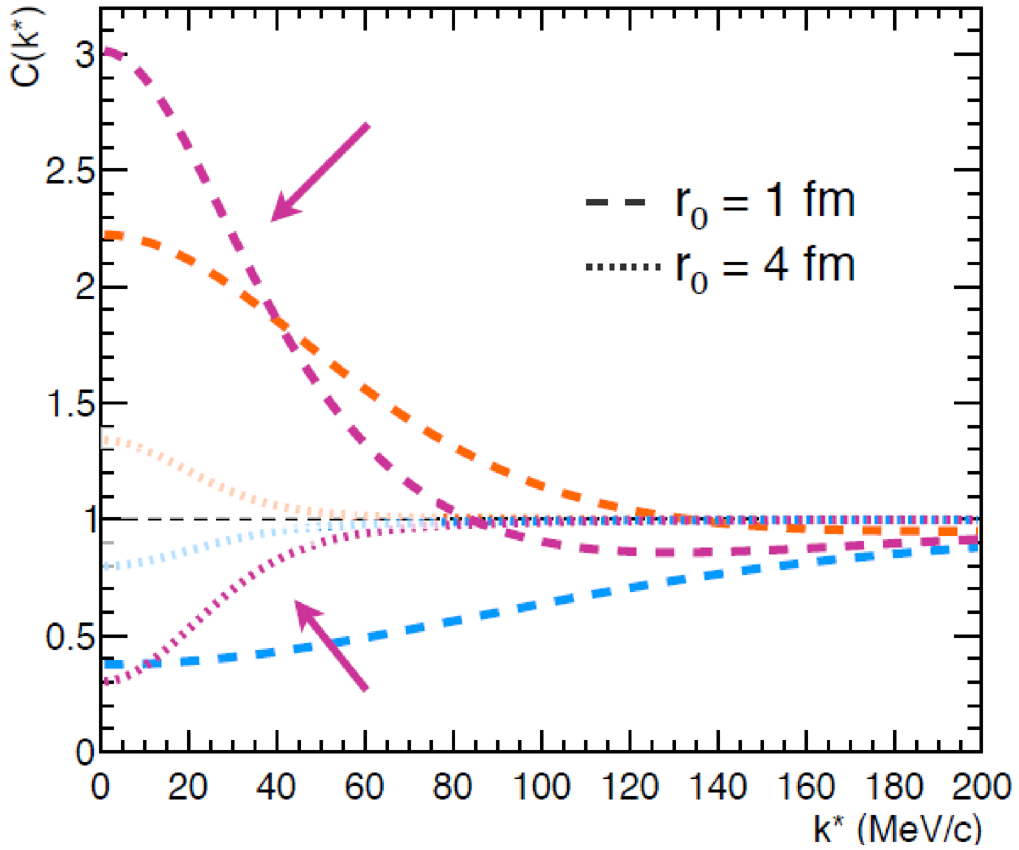

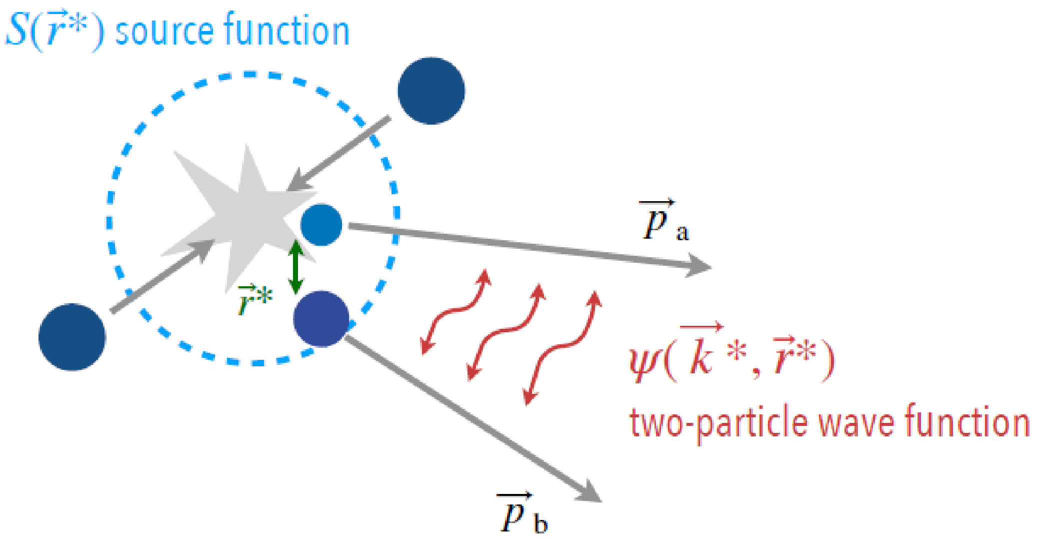

- ➡ Absence of interaction $C(k^*) = 1$
- ➡ Attractive potential $C(k^*) > 1$
- ➡ Repulsive potential $C(k^*) < 1$
- ➡ Bound-state formation $C(k^*) <> 1$

Two particle correlation analysis

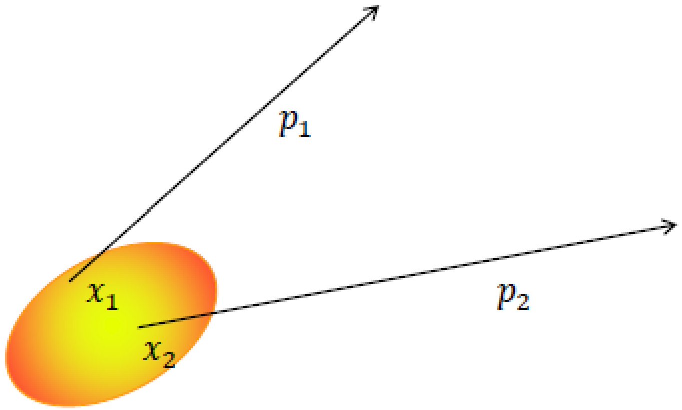

$$P_1(p) = E\frac{dN}{d^3p} = \int d^4x S(x,p)$$

S – is the source parameter

General case

$$C(p_1,p_2) = \frac{P_2(p_1,p_2)}{P_1(p_1)P_1(p_2)}$$

$$P_2(p_1,p_2) = E_1E_2\frac{dN}{d^3p_1d^3p_2}$$

for non-point source

$$C(\boldsymbol{p}_1 - \boldsymbol{p}_2) - 1 \sim \int d^3R\,\rho(\boldsymbol{R})\,\cos(\boldsymbol{R}\cdot(\boldsymbol{p}_1 - \boldsymbol{p}_2))$$

For the assumption of Gaussian shaped emittance source the correlation function C(q,K)

$$C(q,K) = 1 \pm \exp\left[-R_s^2q_s^2 - R_o^2q_o^2 - R_l^2q_l^2 - 2R_{ol}^2q_oq_l\right]$$

$$R_s^2 = \langle \tilde{x}_s^2 \rangle\,, \qquad R_o^2 = \langle(\tilde{x}_o - \beta_\perp\tilde{t})^2\rangle\,,$$

$$R_l^2 = \langle(\tilde{x}_l - \beta_l\tilde{t})^2\rangle\,, \qquad R_{ol}^2 = \langle(\tilde{x}_o - \beta_\perp\tilde{t})(\tilde{x}_l - \beta_l\tilde{t})\rangle$$

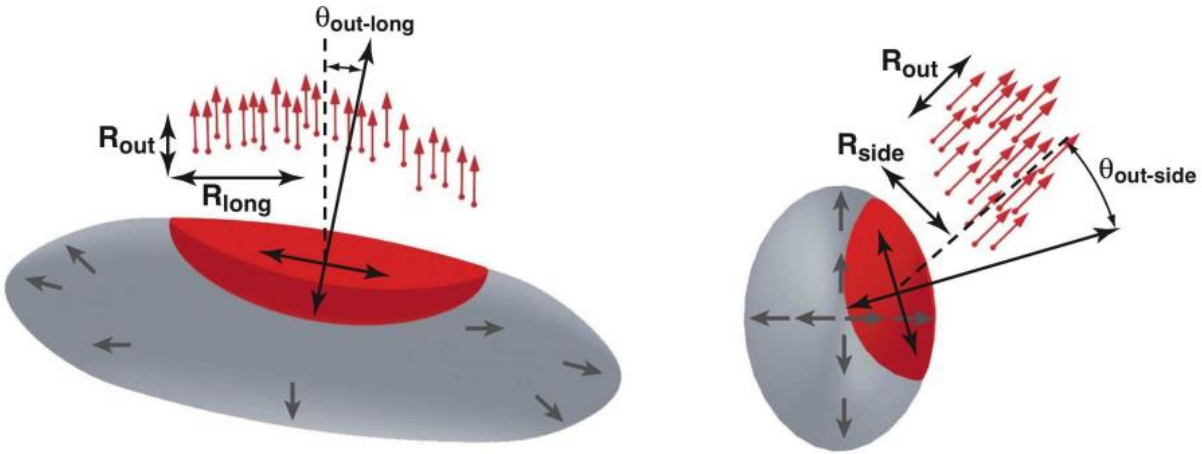

Two particle correlations

proton and anti-proton correlations

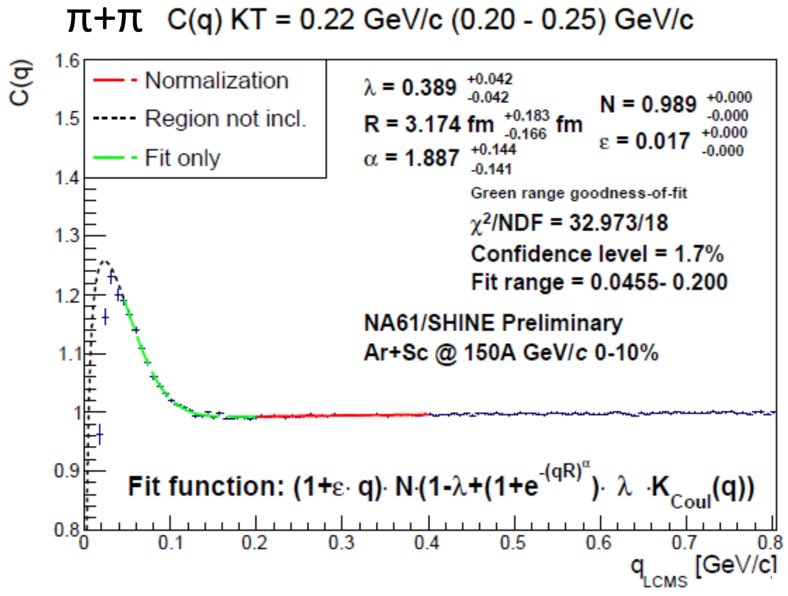

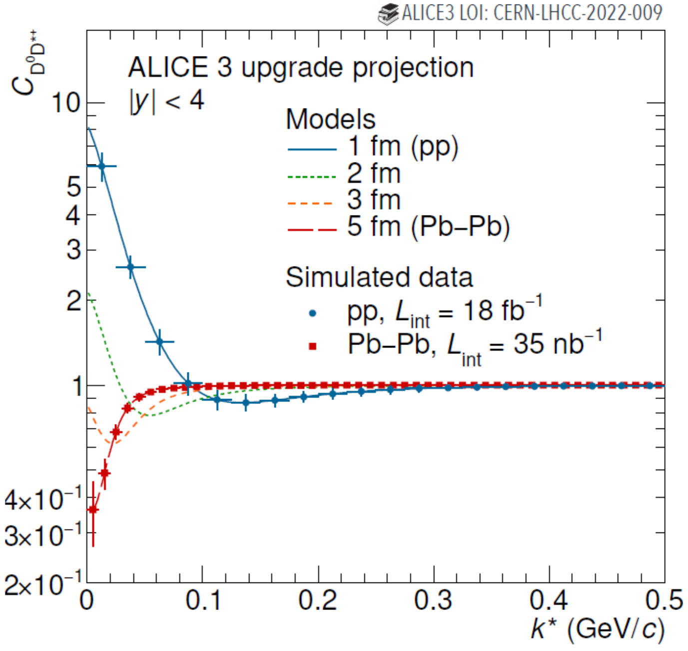

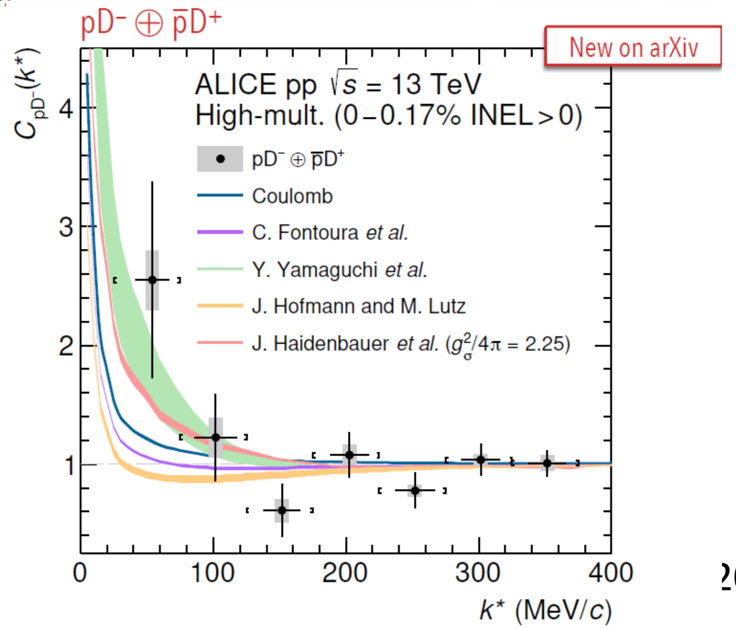

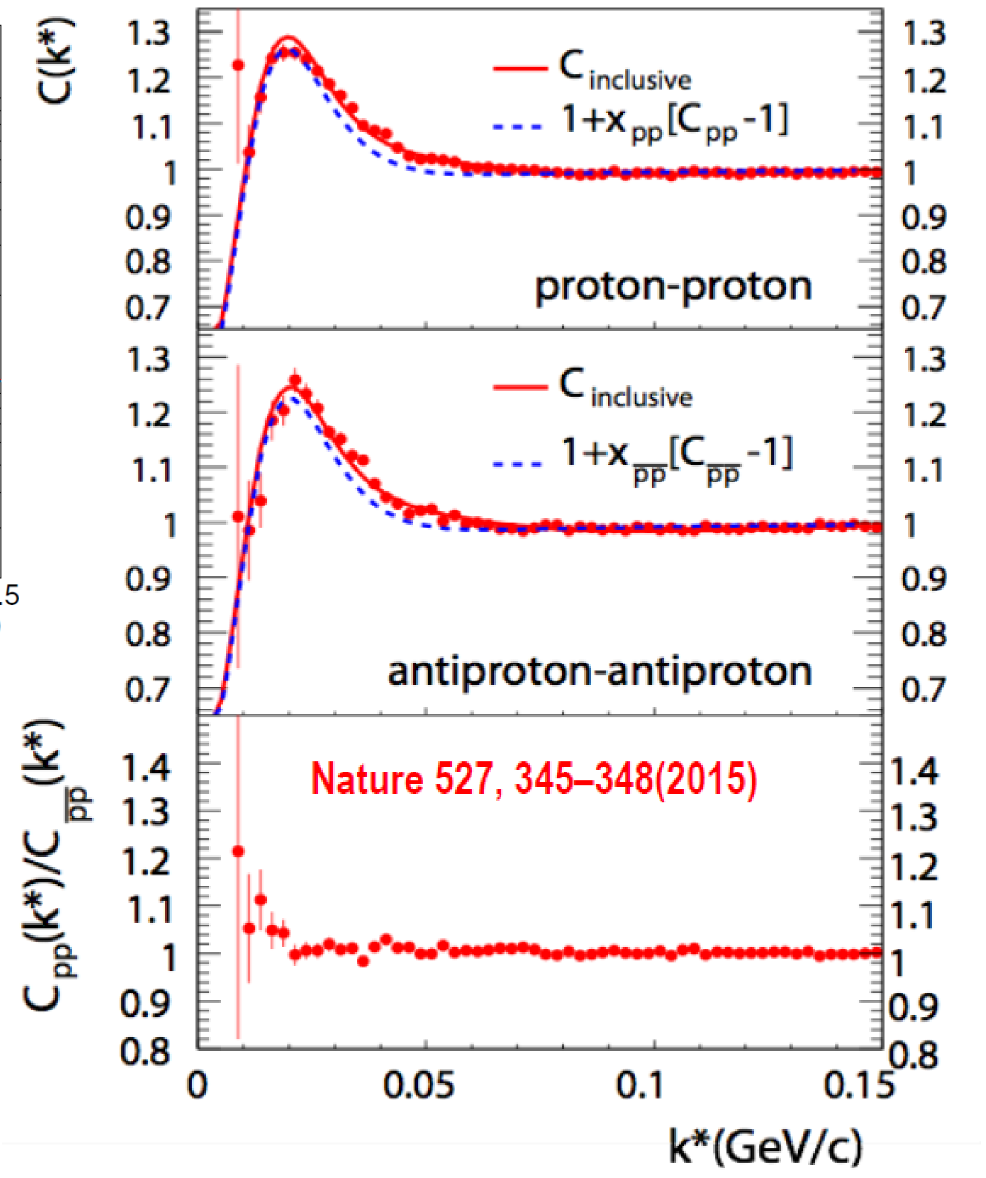

The most vortical fluid

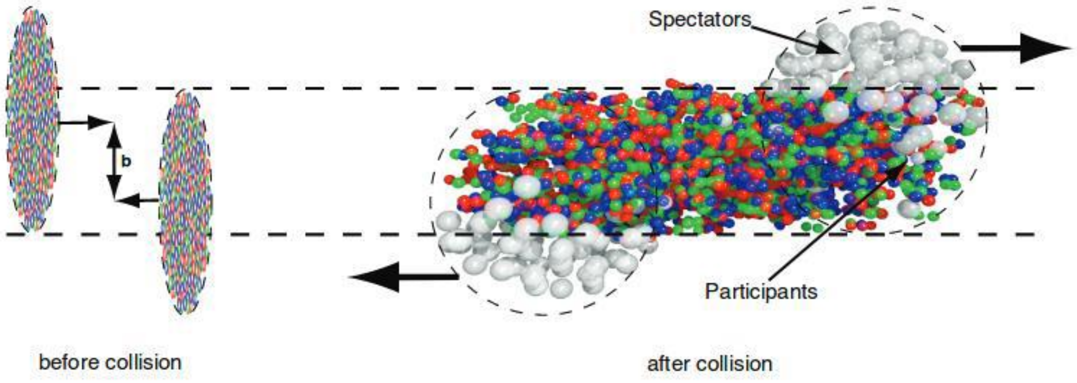

$$\frac{dN}{d\cos\theta^*} = \frac{1}{2}(1 + \alpha_H |\mathcal{P}_H| \cos\theta^*)$$

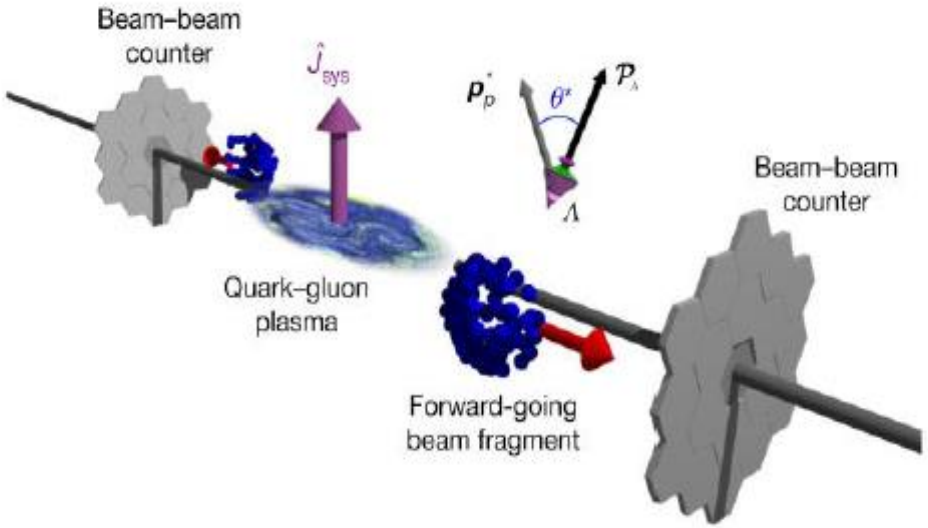

The most vortical fluid

$$\omega = k_B T(\overline{P}_{\Lambda} + \overline{P}_{\overline{\Lambda}})/\hbar = 10^{22} s^{-1}$$

STAR, Nature, 2017, 1701.06657
Phys. Rev. C 98 (2018) 014910

Global polarization of particles

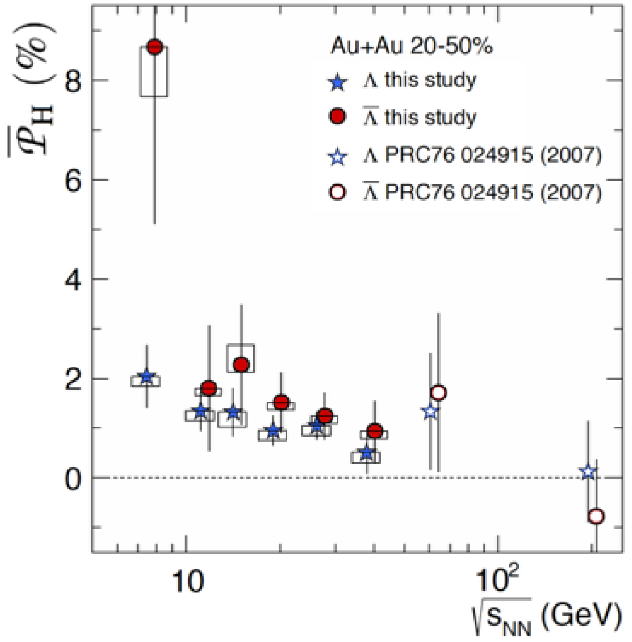

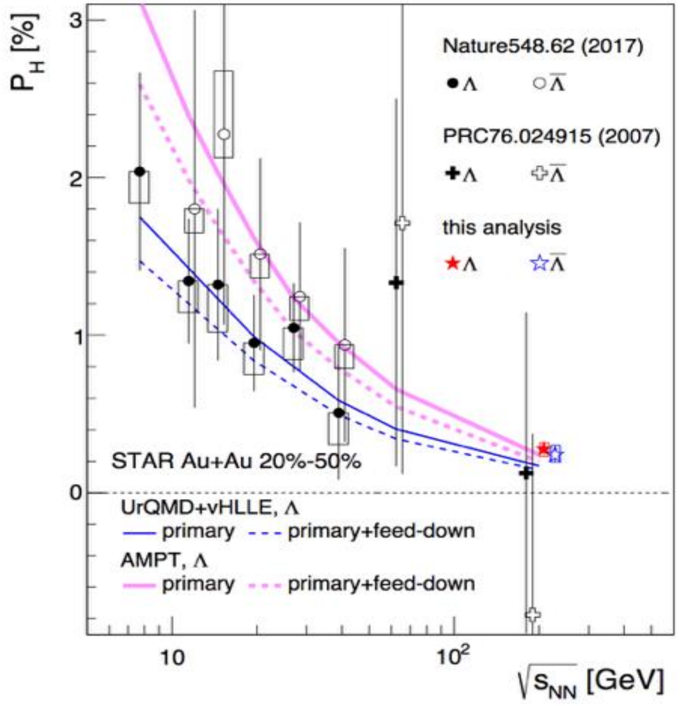

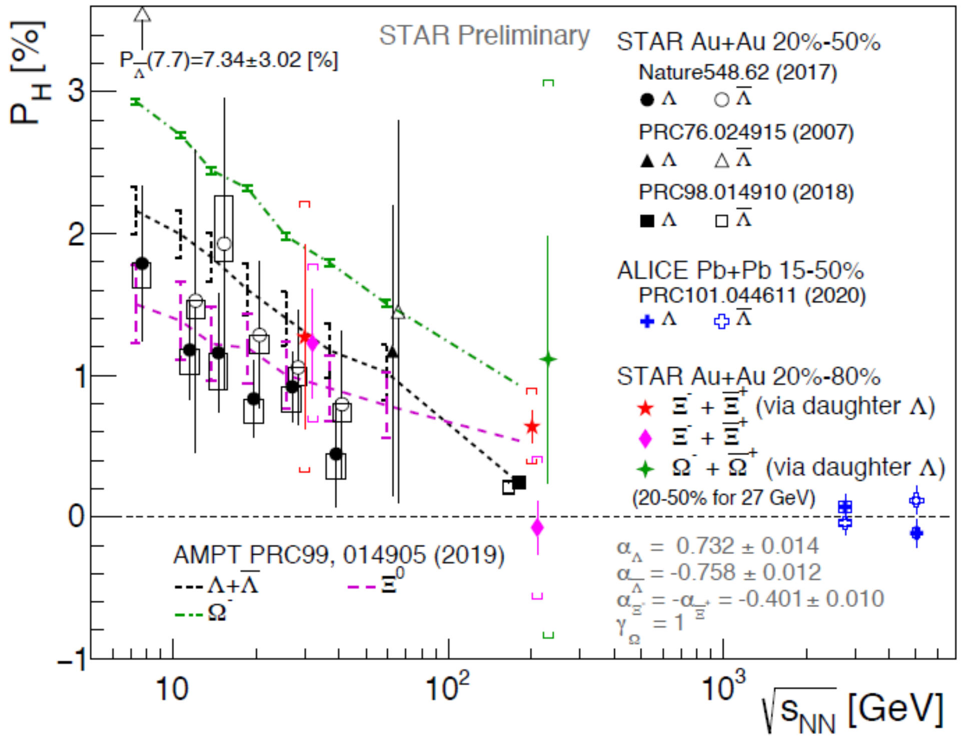

* published results are rescaled by $\alpha_{old}/\alpha_{new}$~0.87

Becattini, Karpenko, Lisa, Upsal, and Voloshin, PRC95.054902 (2017)

$$P_\Lambda \simeq \frac{1}{2}\frac{\omega}{T} + \frac{\mu_\Lambda B}{T}$$

$$P_{\bar{\Lambda}} \simeq \frac{1}{2}\frac{\omega}{T} - \frac{\mu_\Lambda B}{T}$$

μ_Λ: Λ magnetic moment
T: temperature at thermal equilibrium

$$\omega = (P_\Lambda + P_{\bar{\Lambda}})k_B T/\hbar$$
$$\sim 0.02\text{-}0.09\ \text{fm}^{-1}$$
$$\sim 0.6\text{-}2.7 \times 10^{22}\text{s}^{-1}$$

(T=160 MeV)

Nuclear modification of produced particles

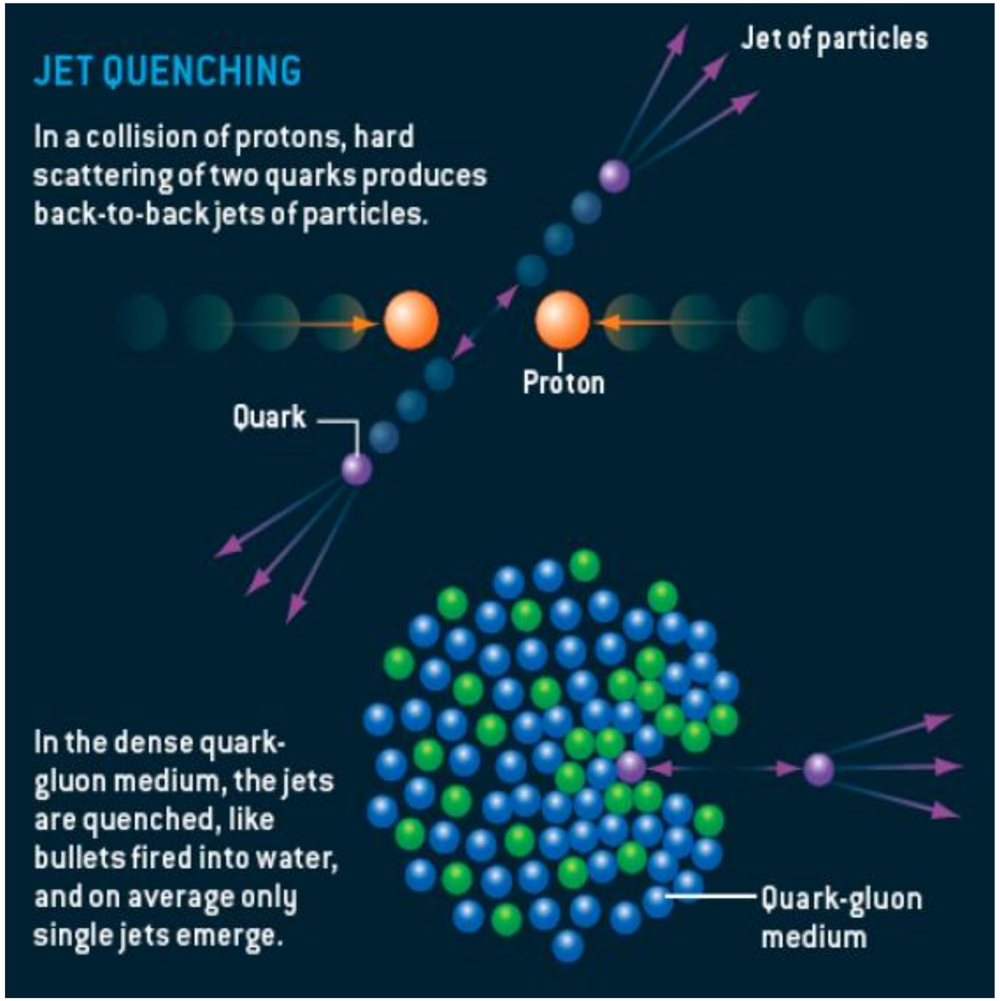

$$R_{AA}(p_t) = \frac{\sigma_{in}^{pp}}{< N_{coll}^{AA} >} \cdot \frac{d^2 N_{AA}/dp_t d\eta}{d^2 \sigma_{pp}/dp_t d\eta}$$

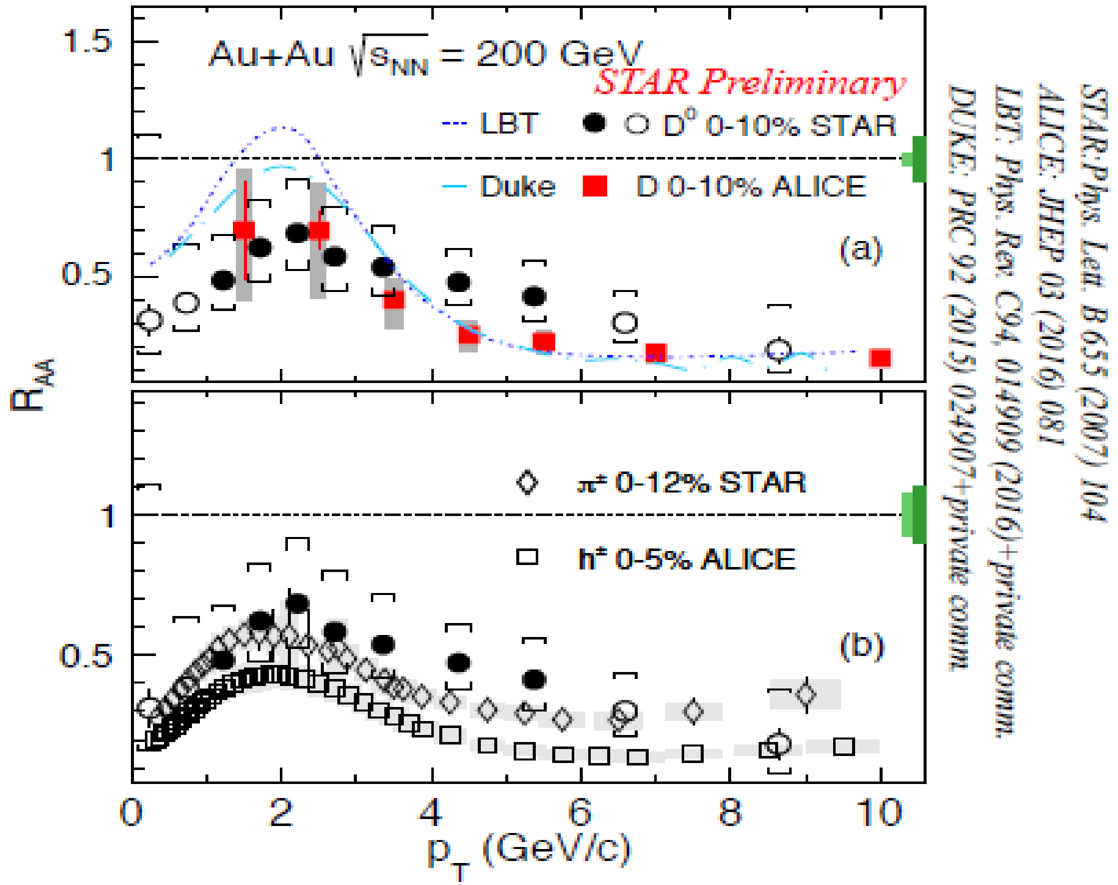

Nuclear modification factor

$$R_{cp} = \frac{d^2N/dp_t d\eta/<N_{bin}>(central)}{d^2N/dp_t d\eta/<N_{bin}>(peripheral)}$$

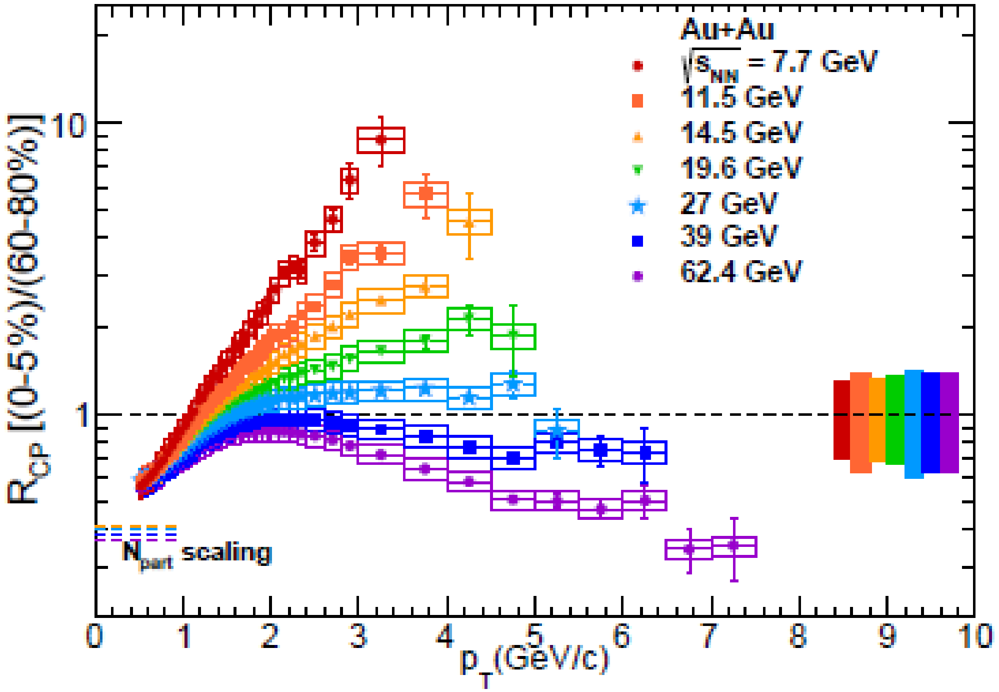

STAR, Phys. Rev. Lett. **121** (2018) 32301

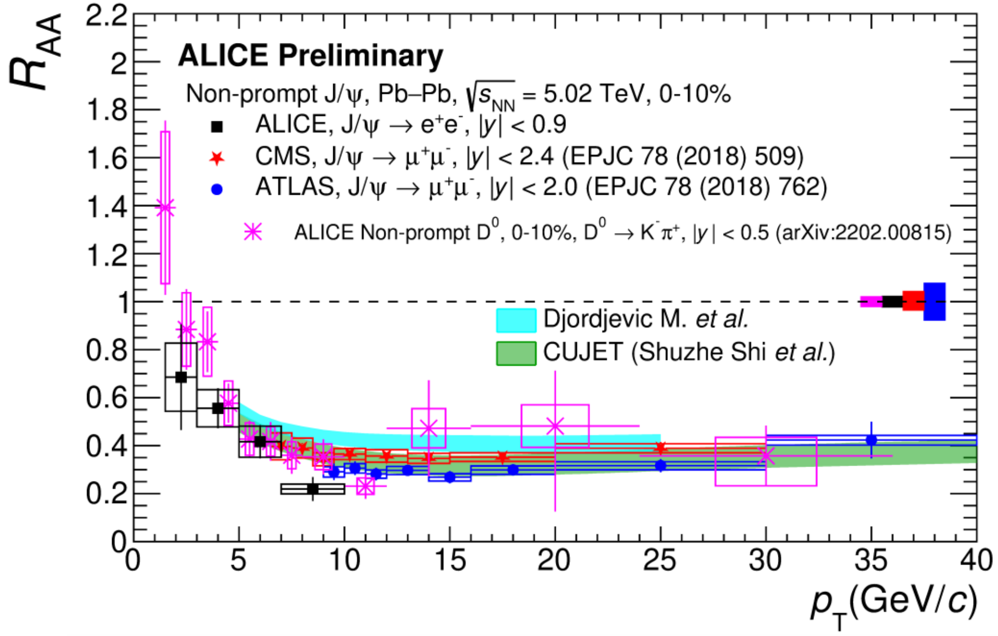

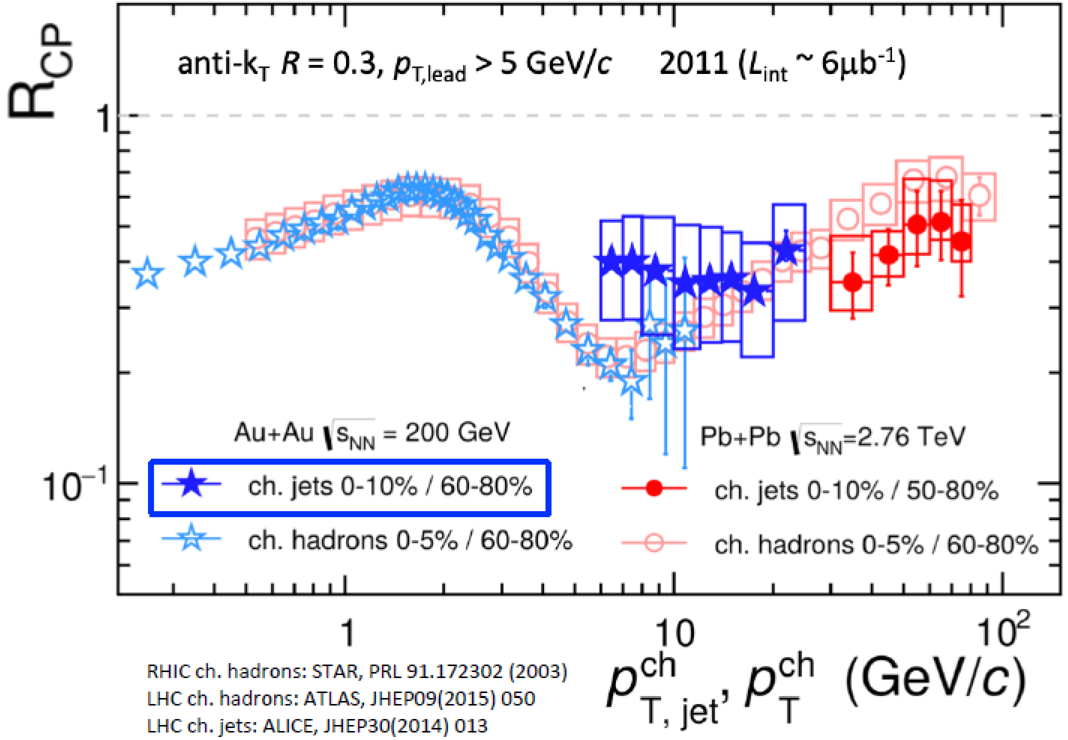

RHIC ch. hadrons: STAR, PRL 91.172302 (2003)
LHC ch. hadrons: ATLAS, JHEP09(2015) 050
LHC ch. jets: ALICE, JHEP30(2014) 013

Light nuclei – snowballs in hell

$_{\Lambda}^{3}H$

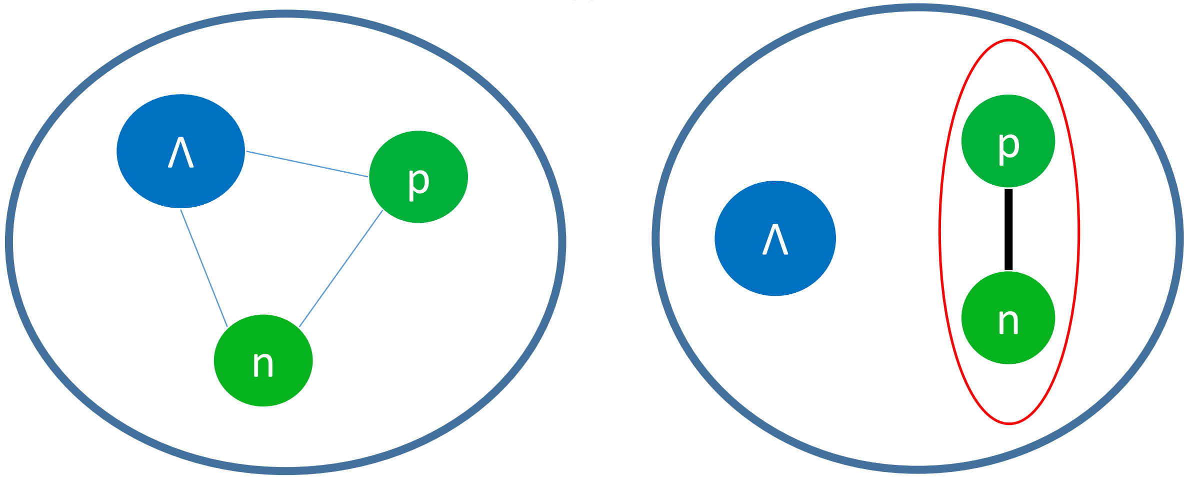

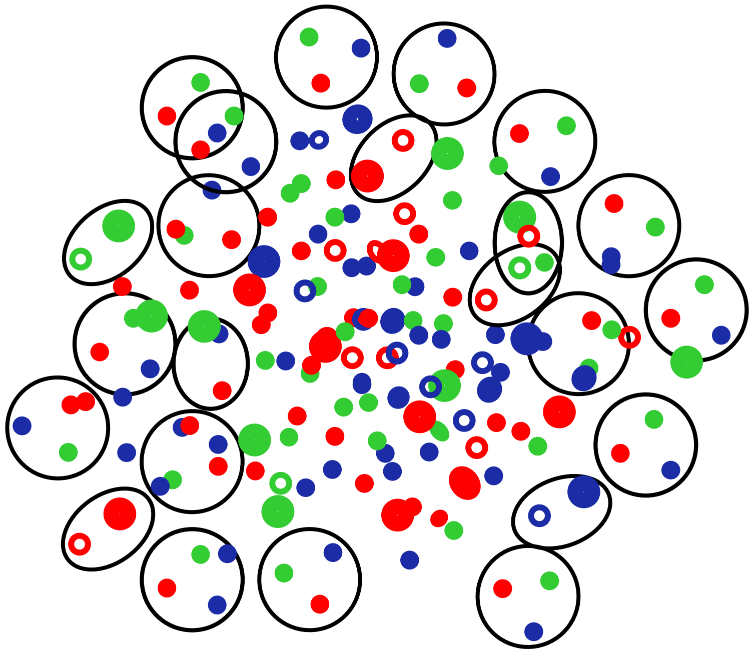

hypertritium r ~ 6 fm

typical size of the fireball of thousands of partons r ~ 10 fm

d

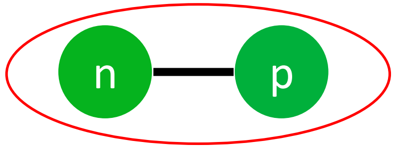

deutron r ~ 2 fm

Fireball T_{kin} 150-160 MeV
Binding energy of deutron 2,22 MeV
Binding energy of lambda in hypertriton 0,41 MeV

Hypertriton and anti-hypertriton

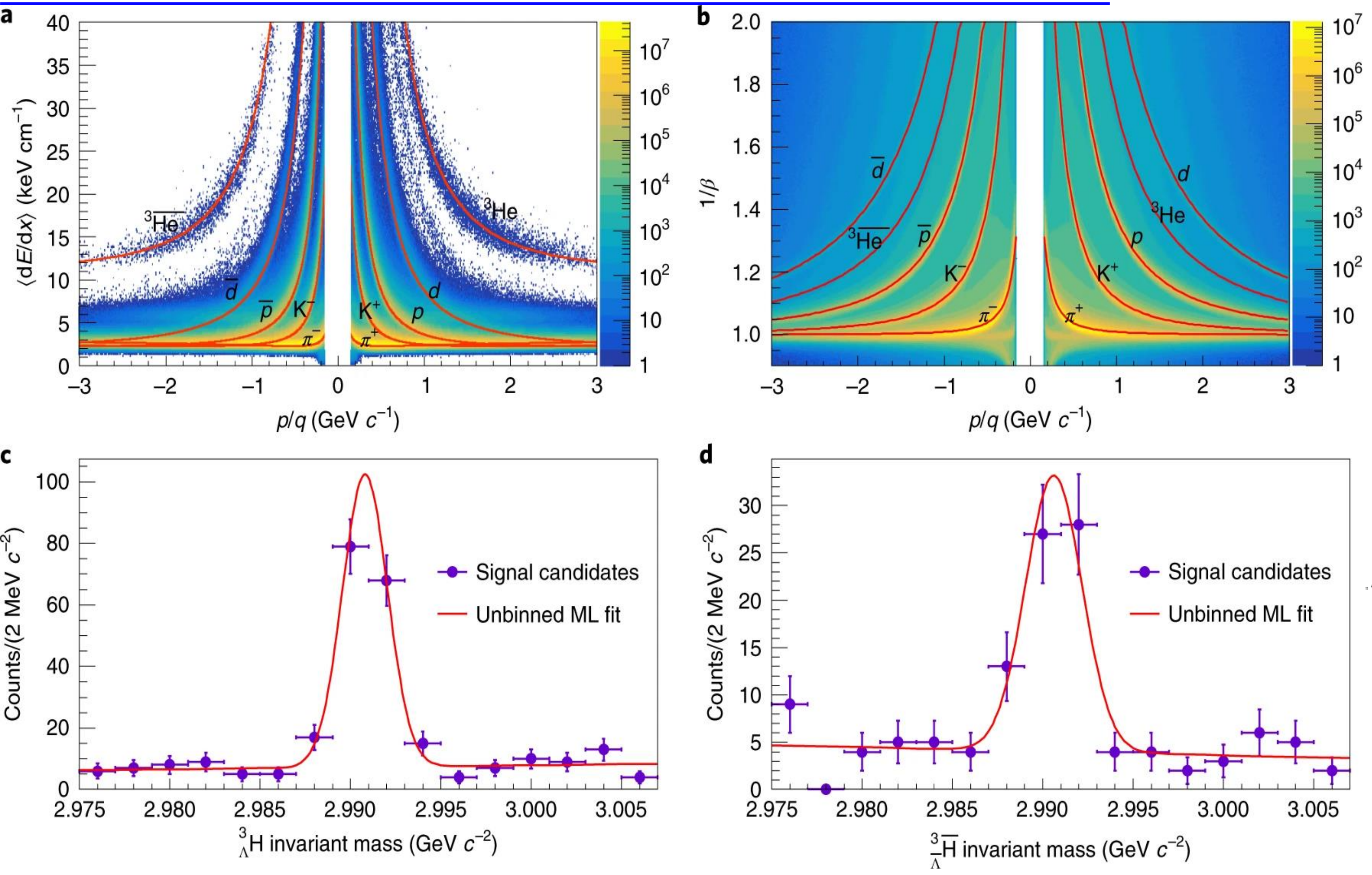

$$ {}^{3}_{\Lambda}\mathrm{H} \rightarrow {}^{3}\mathrm{He} + \pi $$

$$ {}^{3}_{\Lambda}\mathrm{H} \rightarrow \mathrm{d} + \mathrm{p} + \pi $$

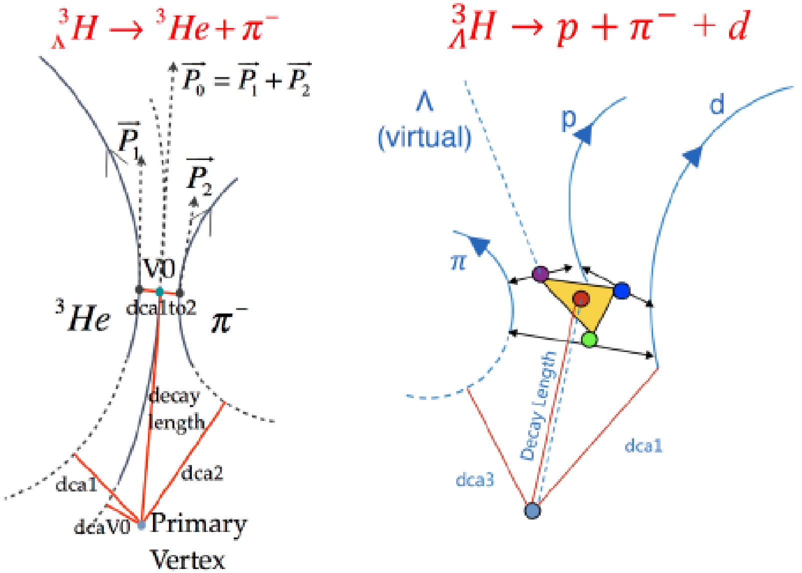

$$ m_{{}^{3}_{\Lambda}H} = 2990.95 \pm 0.13(stat.) \pm 0.11(syst) $$

$$ m_{{}^{3}_{\Lambda}\overline{H}} = 2990.60 \pm 0.28(stat.) \pm 0.11(syst) $$

Nature Physics **16** (2020) 409

Hypertriton and anti-hypertriton

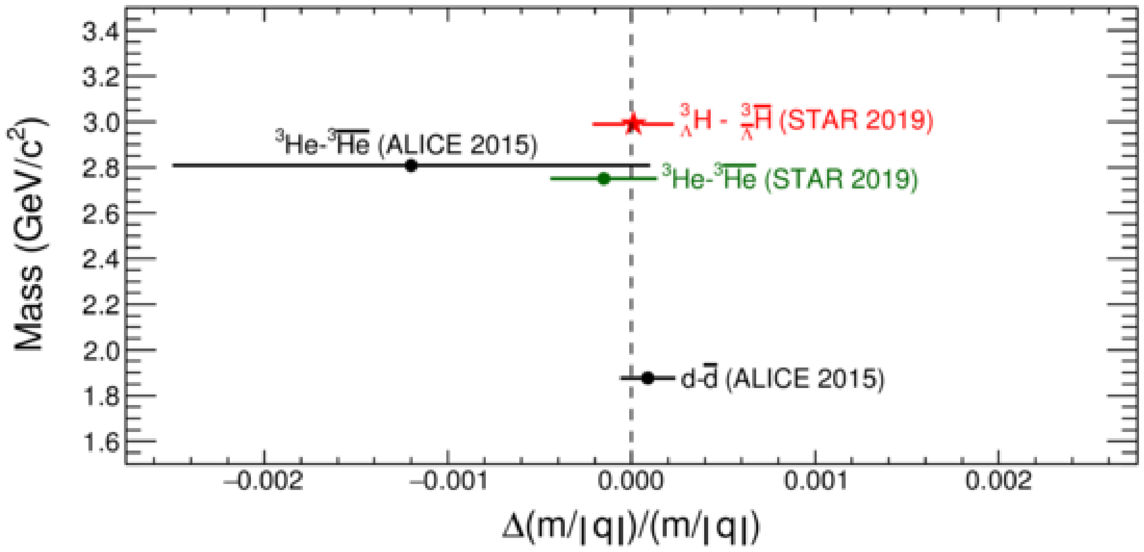

$$\frac{m_{^3_\Lambda H} - m_{^3_\Lambda \overline{H}}}{m} = (0.1 \pm 2.0(\text{stat.}) \pm 1.0(\text{syst.})) \times 10^{-4}$$

This ratio allow to test the CPT symmetry from the perspective of experiment. Mass difference consistent with zero which is supporting the CPT symmetry

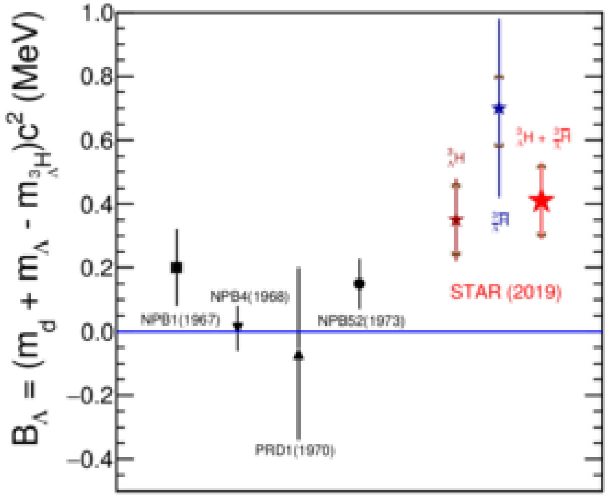

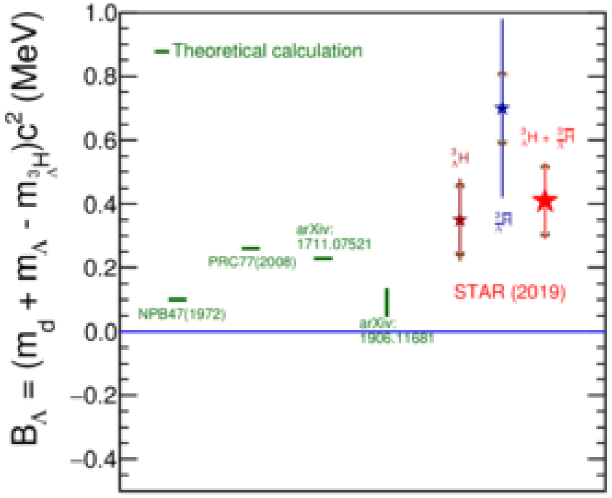

$$B_\Lambda = 0.41 \pm 0.12(stat.) \pm 0.11(syst.) MeV$$

Net-particle cumulants

$$\chi_n^B = \frac{\partial^n (P/T^4)}{\partial(\mu_B/T)^n}\bigg|_T$$

High order cumulants of conserved number distributions are sensitive to critical phenomena, related to the correlation length and susceptibilities.

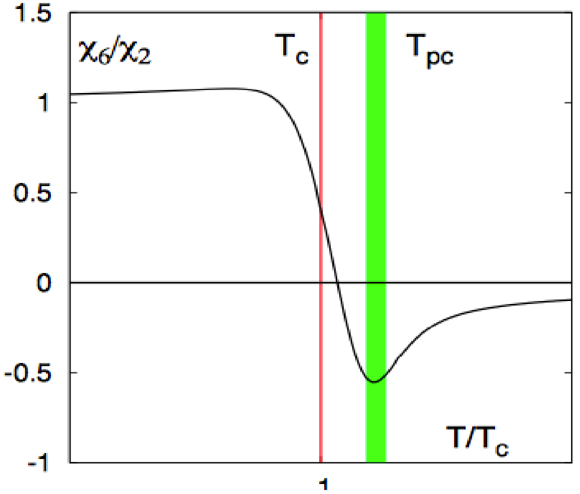

Susceptibility ratios fluctuations near the CP

Phys. Lett. B **785** (2018) 551

Cumulants

$$C_1 = \langle N \rangle$$

$$C_2 = \langle (\delta N)^2 \rangle$$

$$C_3 = \langle (\delta N)^3 \rangle$$

$$C_4 = \langle (\delta N)^4 \rangle - 3\langle (\delta N)^2 \rangle^2$$

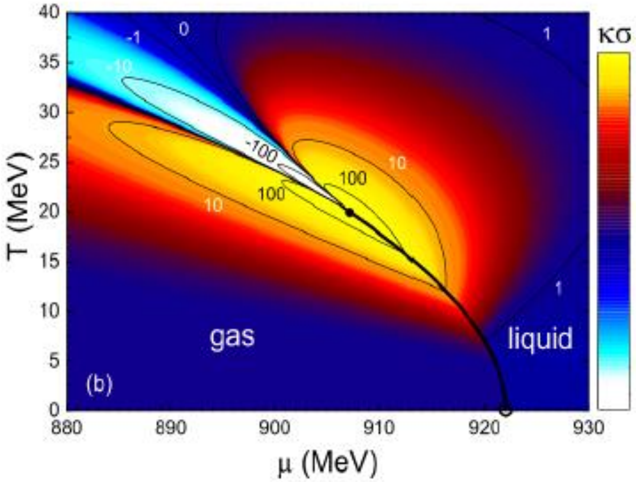

Moments

$$M = C_1, \sigma^2 = C_2, S = \frac{C_3}{(C_2)^{\frac{3}{2}}}, \kappa = \frac{C_4}{(C_2)^2}$$

$$\frac{C_2}{C_1} = \frac{\sigma^2}{M} \qquad \frac{C_3}{C_2} = S\sigma \qquad \frac{C_4}{C_2} = \kappa\sigma^2$$

$$\frac{\chi_2^i}{\chi_1^i} = (\sigma^2/M)^i = \frac{c_2^i}{c_1^i}$$

$$\frac{\chi_3^i}{\chi_2^i} = (S\sigma)^i = \frac{c_3^i}{c_2^i}$$

$$\frac{\chi_4^i}{\chi_2^i} = (\kappa\sigma^2)^i = \frac{c_4^i}{c_2^i}$$

$$i = B, Q, S$$

Energy dependence of net-proton cumulants

Non-monotonic behavior for higher order cumulants.

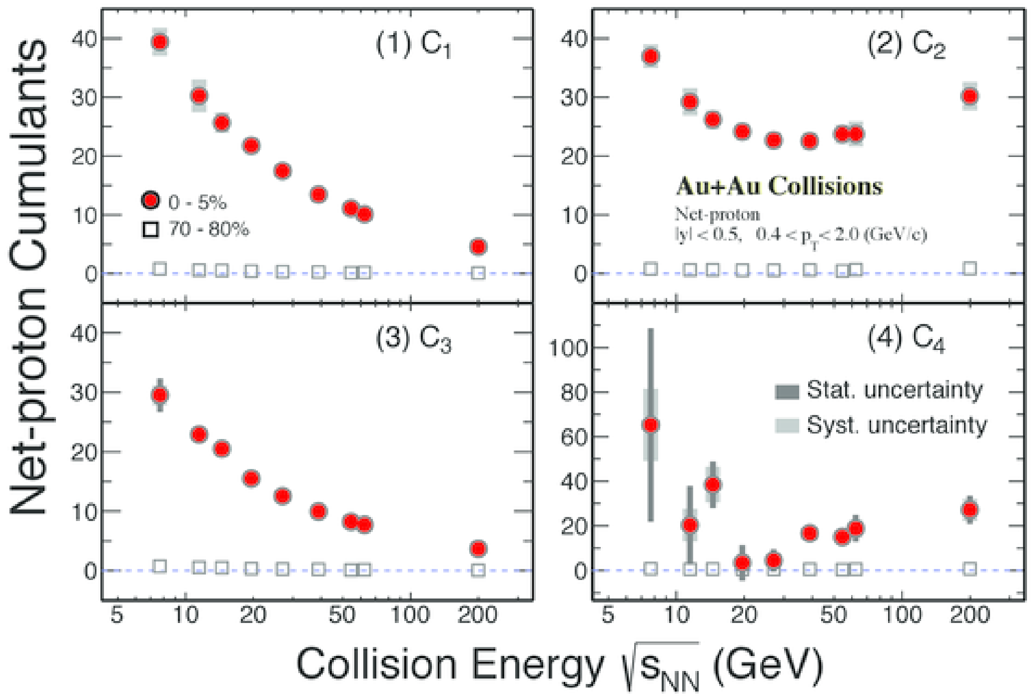

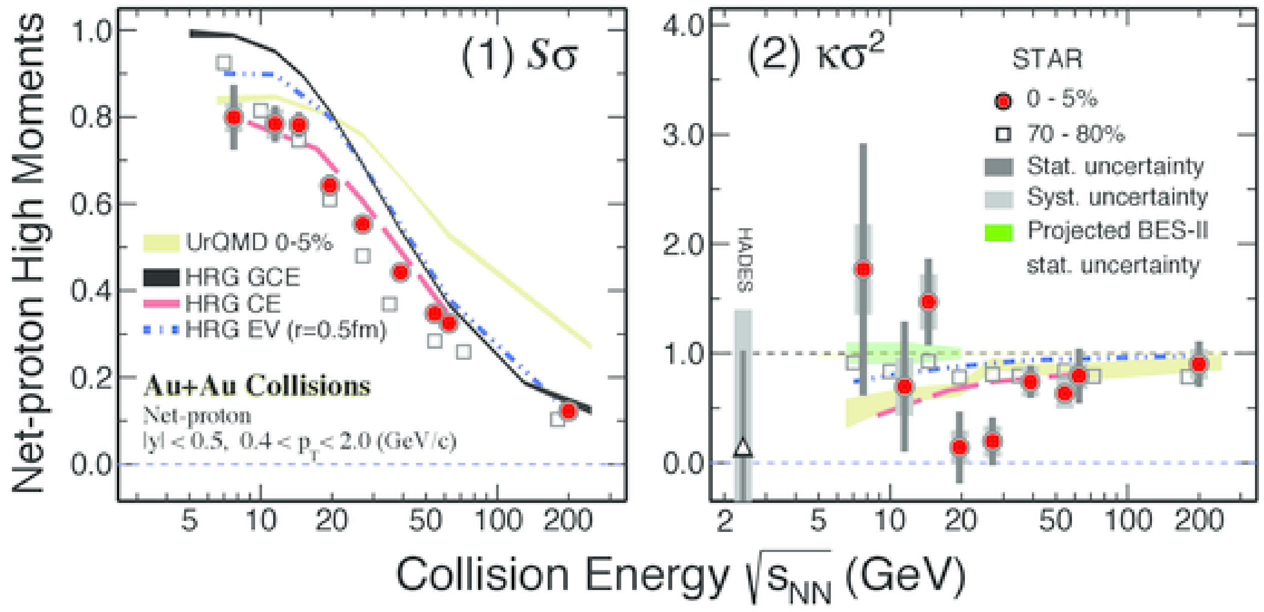

Large values of C_3 and C_4 for central events show that distributions have non-Gaussian shape. It may suggest for the enhanced fluctuations arising from a possible critical point.

arXiv:2001.02852v2

Part 3 What's next on the agenda

Exotic probes
Future facilities

Chiral magnetic effect

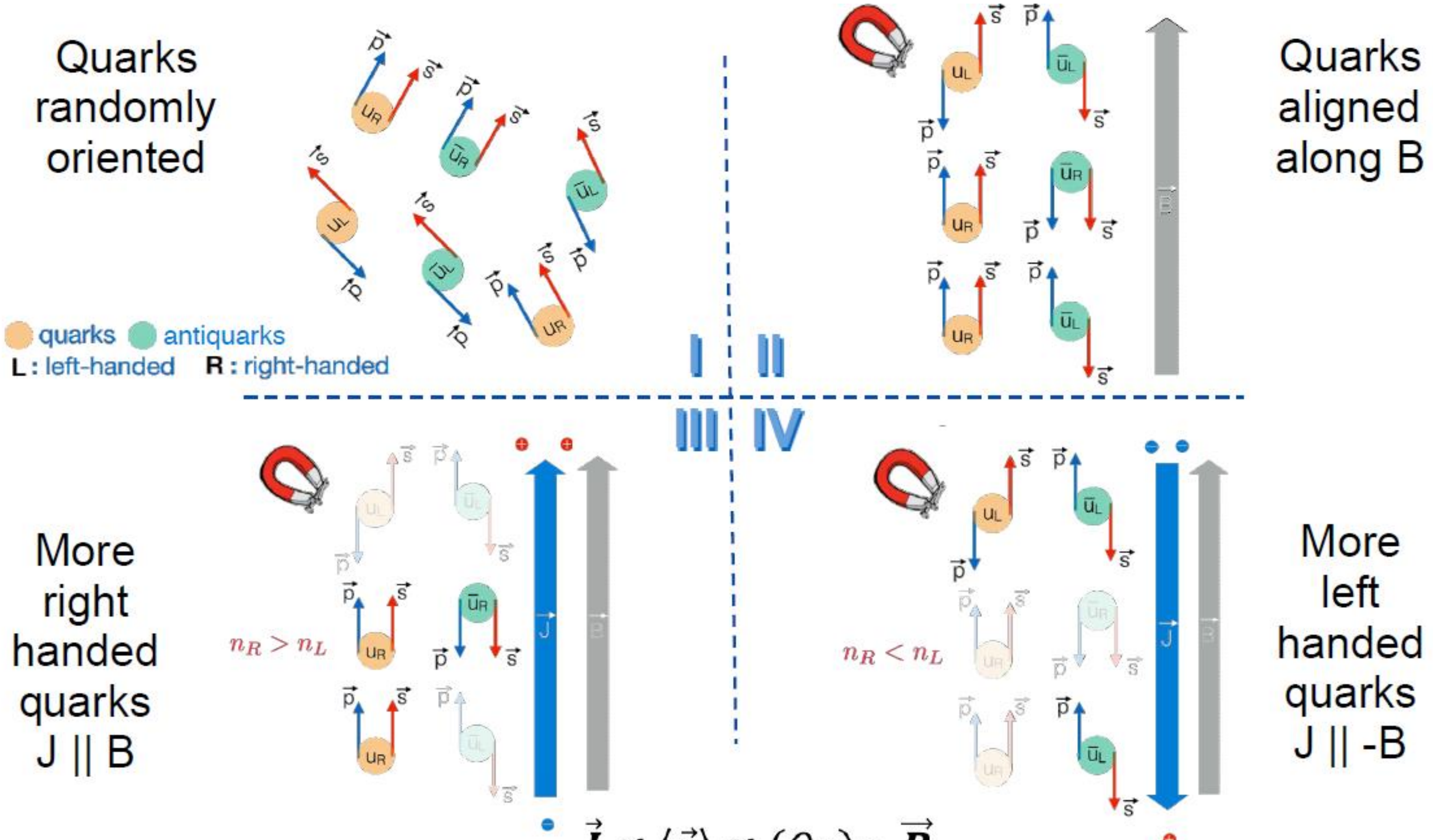

$$\vec{J} \propto \langle \vec{p} \rangle \propto (Qe)\mu_5 \vec{B}$$

Procedure for blind analysis

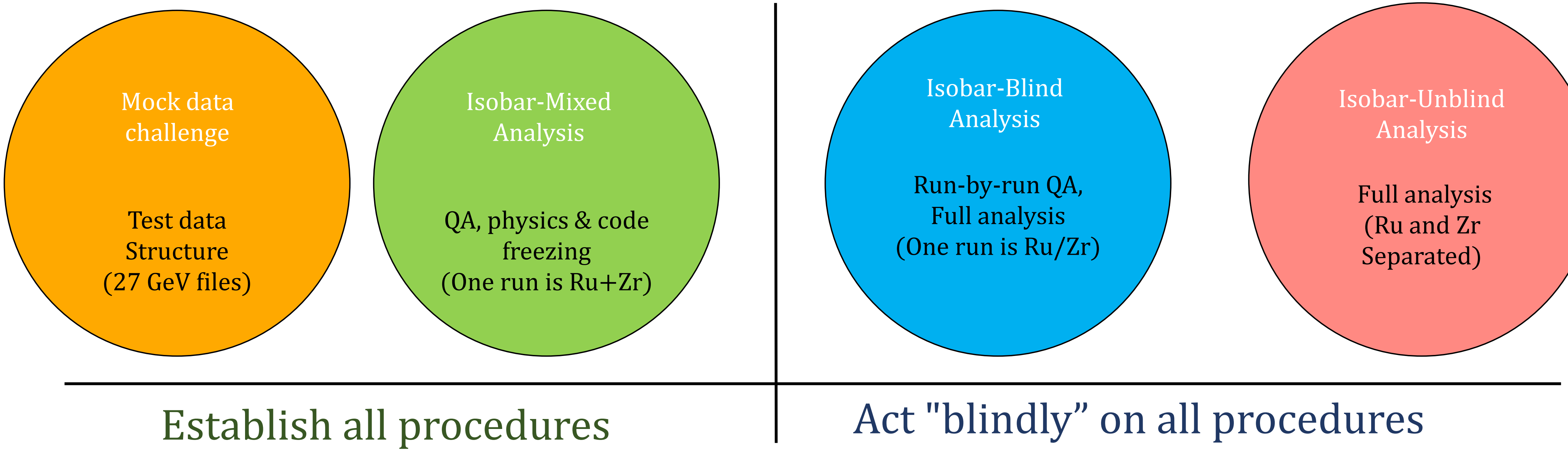

STAR, arXiv:1911.00596 (2019)

CME measurements

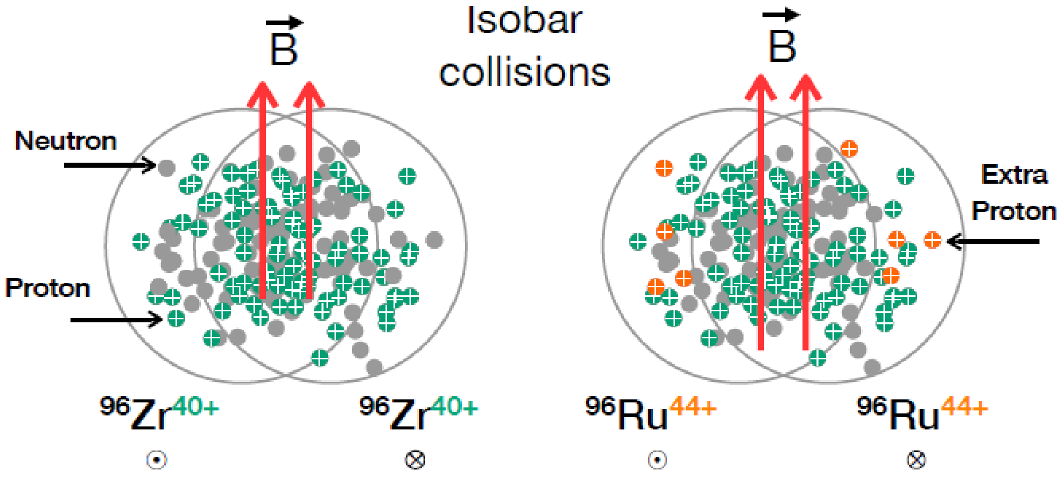

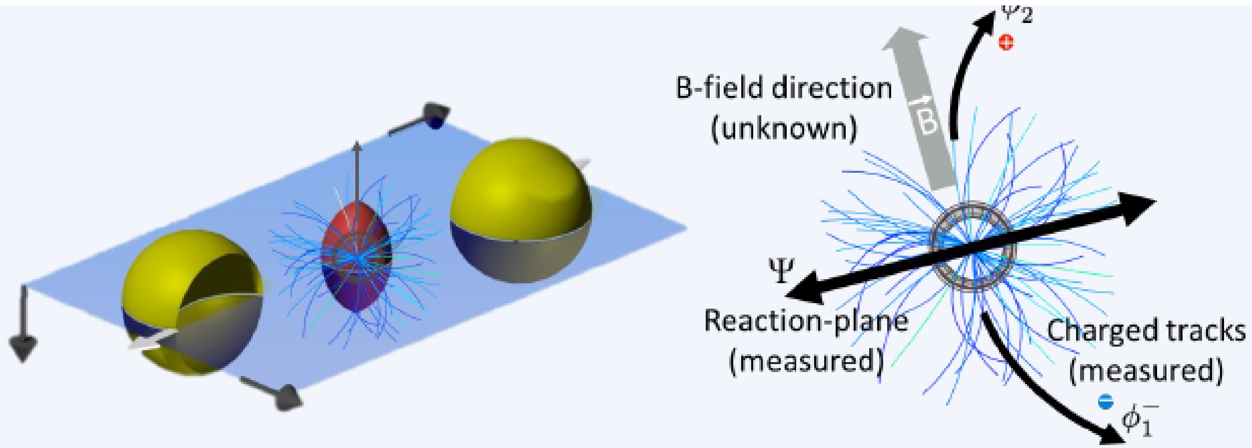

Use $\Delta\gamma$ as an example:

$$\gamma^{\alpha,\beta} \equiv \langle cos(\phi^\alpha + \phi^\beta - 2\psi_2)\rangle \qquad \Delta\gamma = \gamma^{OS} - \gamma^{SS}$$

$$\Delta\gamma = \Delta\gamma^{CME} + k\frac{v_2}{N} + \Delta\gamma^{non-flow}$$

Measurement — Signal — Background 1 — Background 2

$$\Delta\gamma^{Ru+Ru} = \Delta\gamma^{CME} + k\frac{v_2}{N} + \Delta\gamma^{non-flow}$$

$\neq \quad \approx \quad =$

$$\Delta\gamma^{Zr+Zr} = \Delta\gamma^{CME} + k\frac{v_2}{N} + \Delta\gamma^{non-flow}$$

B^2 are ~15% different

Within 4%

STAR results on un-blind CME analysis

Chiral Separation Effect $\mathbf{J}_5 \propto e\mu_V \mathbf{B}$

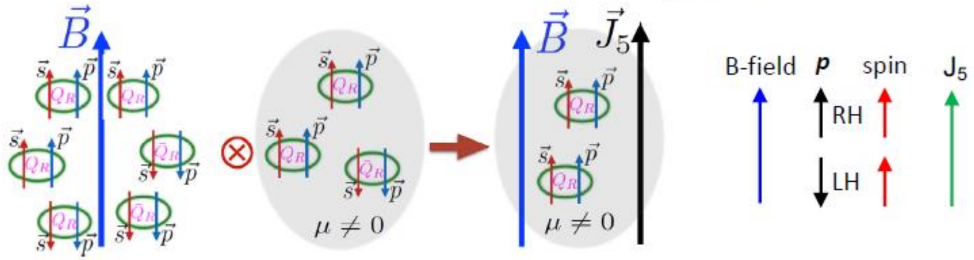

B-field + massless quarks + non-zero μ_V → axial current J_5

Chiral magnetic effect (CME)

$$\mathbf{J}_{\mathbf{cme}} = \sigma_5 \mathbf{B} = \left(\frac{(Qe)^2}{2\pi^2} \mu_5 \right) \mathbf{B},$$

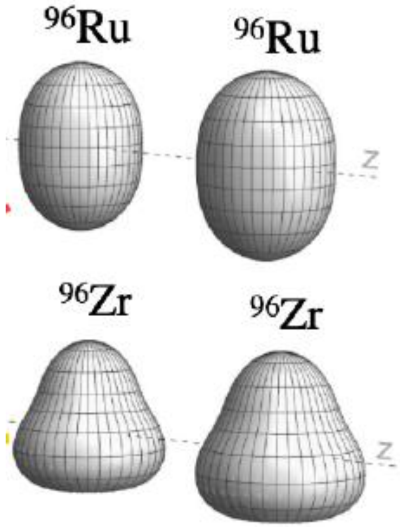

D. Kharzeev, PPNP88, 1 (2016)
STAR, PRC105, 014901 (2022)

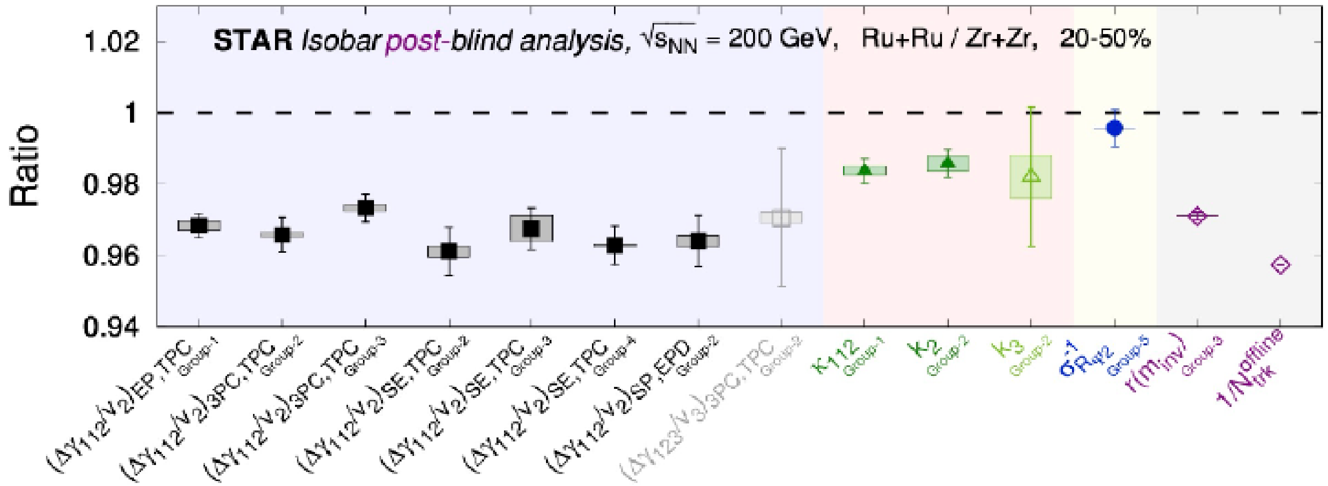

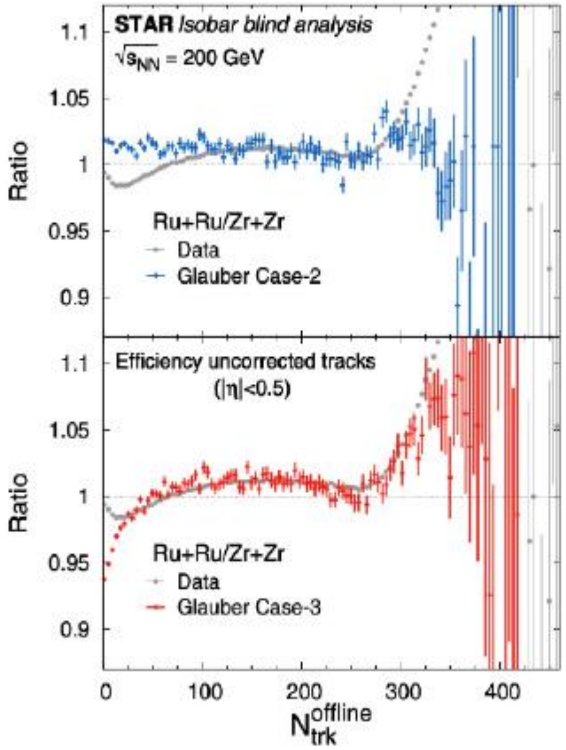

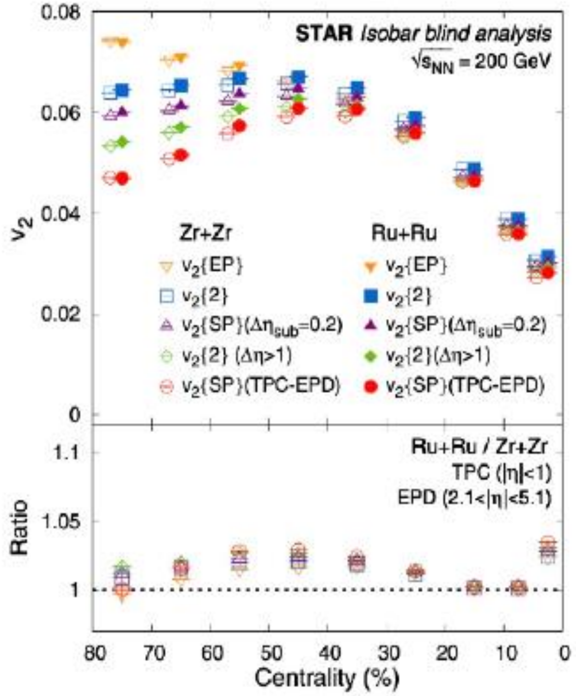

Neutron skin effects

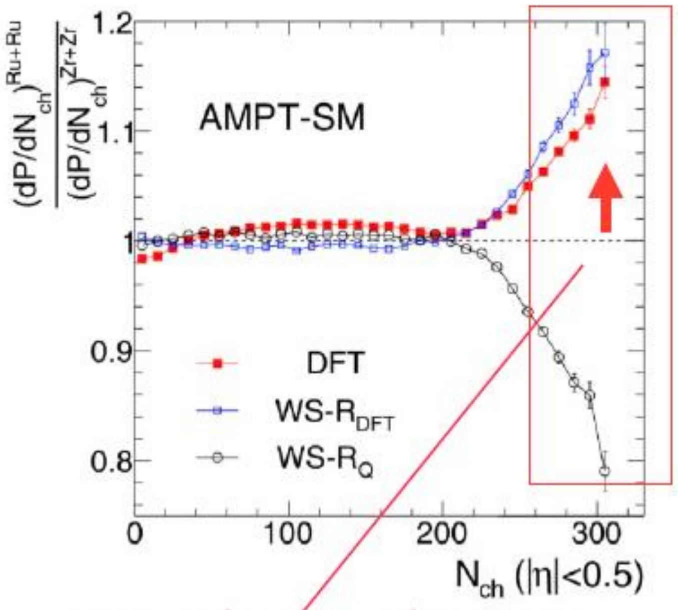

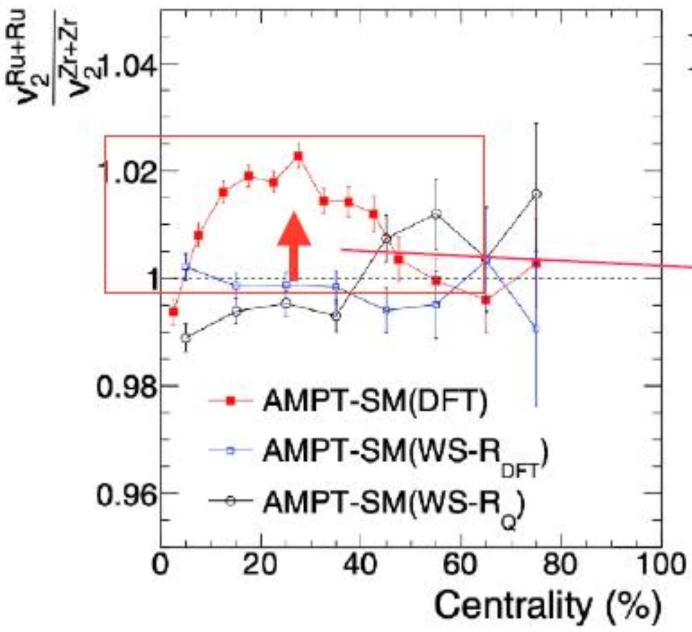

Neutron skin thickness $\Delta r_{np} \equiv \sqrt{\langle r_n^2 \rangle} - \sqrt{\langle r_p^2 \rangle}$

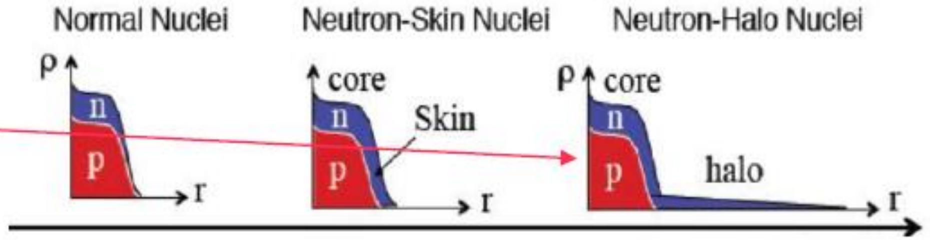

Normal Nuclei	Neutron-Skin Nuclei	Neutron-Halo Nuclei
$R_n = R_p$	$R_n > R_p$	$R_n = R_p$
$a_n = a_p$	$a_n = a_p$	$a_n > a_p$

$$\rho = \frac{\rho_0}{1 + \exp\left[\frac{r - R}{a}\right]}$$

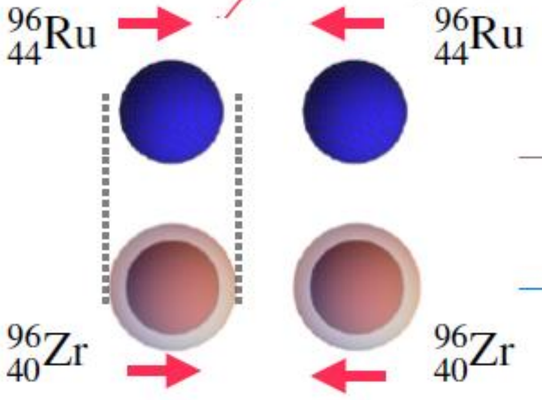

→ Smaller r, larger density → Larger N_{ch} and $\langle p_T \rangle$

→ Larger r, smaller density → Smaller N_{ch} and $\langle p_T \rangle$

HJX, et.al., PRL121, 022301 (2018)
H. Li, HJX, et.al., PRC98, 054907 (2018)
HJX, et.al., PLB819, 136453 (2021)

Nuclear shape matters

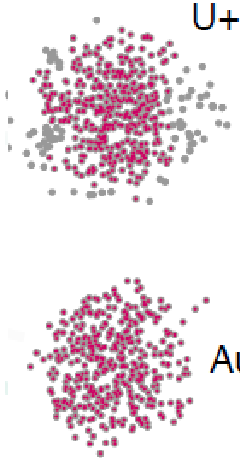

U+U (N_{part}=394)

Au+Au (N_{part}=394)

B-field is different
in Au+Au and U+U

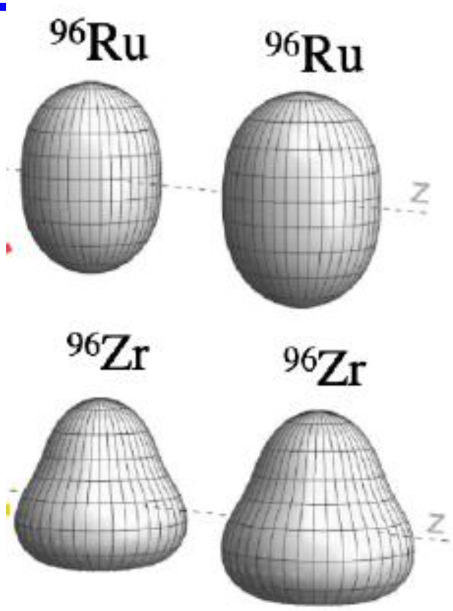

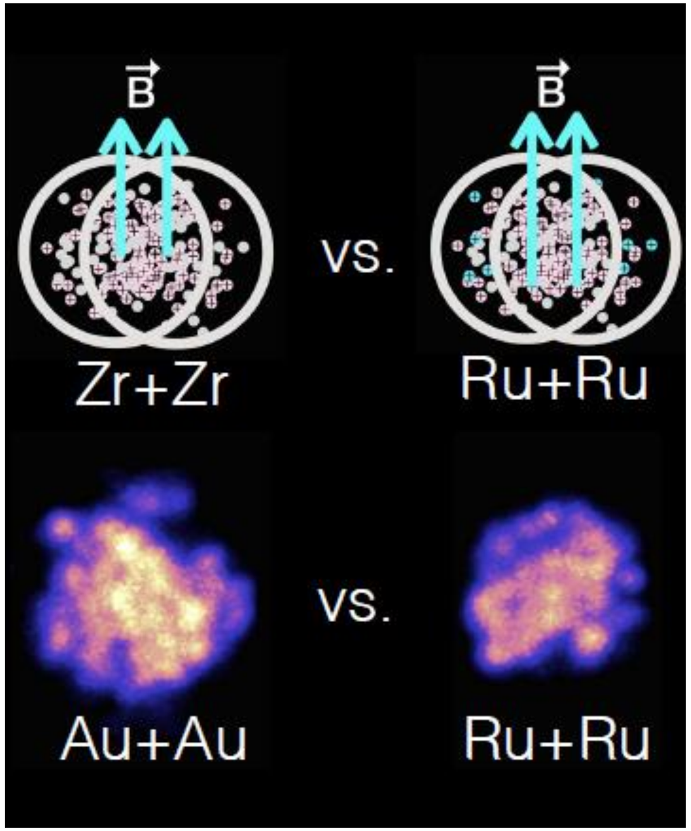

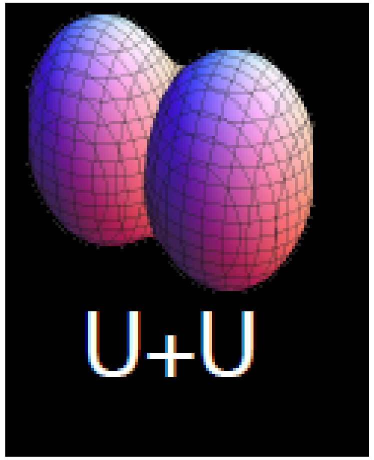

Gold nuclei is almost well shaped almost an ideal sphere, so is lead nuclei

Other nuclei has much more variable shapes, thus we need to carefully take into account trivial effects of interaction region geometry due to the shapes and exact conditions of the collision

NICA (Nuclotron-based Ion Colliding fAcility)

Can accelerate p+p, p+A, A+A

Maximal beam collision energy:
11 GeV for Au+Au
27 GeV for p+p

Energy region is well suited for precise study of the onset of deconfinement and QCD phase transitionin a variety of colliding systems (Bi+Bi, Au+Au, Cu+Cu, Ar+Ar, C+C)
Spin measurements on polarized proton and deuteron beams at SPD

Ring circumference, m	**503,04**
Number of bunches	**22**
r.m.s. bunch length, m	**0,6**
β, m	**0,35**
Energy in c.m., Gev/u	**4-11**
r.m.s. $\Delta p/p$, 10^{-3}	**1,6**
IBS growth time, s	**1800**
Luminosity, $cm^{-2}\ s^{-1}$	**1×10^{27}**

SHINE and AMBER

AMBER plans

Program	Physics Goals	Beam Energy [GeV]	Beam Intensity [s^{-1}]	Trigger Rate [kHz]	Beam Type	Target	Earliest start time, duration	Hardware additions
muon-proton elastic scattering	Precision proton-radius measurement	100	$4 \cdot 10^6$	100	$\mu^\pm$	high-pressure H2	2022 1 year	active TPC, SciFi trigger, silicon veto,
Hard exclusive reactions	GPD E	160	$2 \cdot 10^7$	10	$\mu^\pm$	$NH_3^\uparrow$	2022 2 years	recoil silicon, modified polarised target magnet
Input for Dark Matter Search	$\overline{p}$ production cross section	20-280	$5 \cdot 10^5$	25	p	LH2, LHe	2022 1 month	liquid helium target
$\overline{p}$-induced spectroscopy	Heavy quark exotics	12, 20	$5 \cdot 10^7$	25	$\overline{p}$	LH2	2022 2 years	target spectrometer: tracking, calorimetry
Drell-Yan	Pion PDFs	190	$7 \cdot 10^7$	25	$\pi^\pm$	C/W	2022 1-2 years	
Drell-Yan (RF)	Kaon PDFs & Nucleon TMDs	~100	10^8	25-50	$K^\pm, \overline{p}$	$NH_3^\uparrow$, C/W	2026 2-3 years	"active absorber", vertex detector
Primakoff (RF)	Kaon polarisa-bility & pion life time	~100	$5 \cdot 10^6$	> 10	K^-	Ni	non-exclusive 2026 1 year	
Prompt Photons (RF)	Meson gluon PDFs	≥ 100	$5 \cdot 10^6$	10-100	$K^\pm$ $\pi^\pm$	LH2, Ni	non-exclusive 2026 1-2 years	hodoscope
K-induced Spectroscopy (RF)	High-precision strange-meson spectrum	50-100	$5 \cdot 10^6$	25	K^-	LH2	2026 1 year	recoil TOF, forward PID
Vector mesons (RF)	Spin Density Matrix Elements	50-100	$5 \cdot 10^6$	10-100	$K^\pm, \pi^\pm$	from H to Pb	2026 1 year	

SHINE has collected

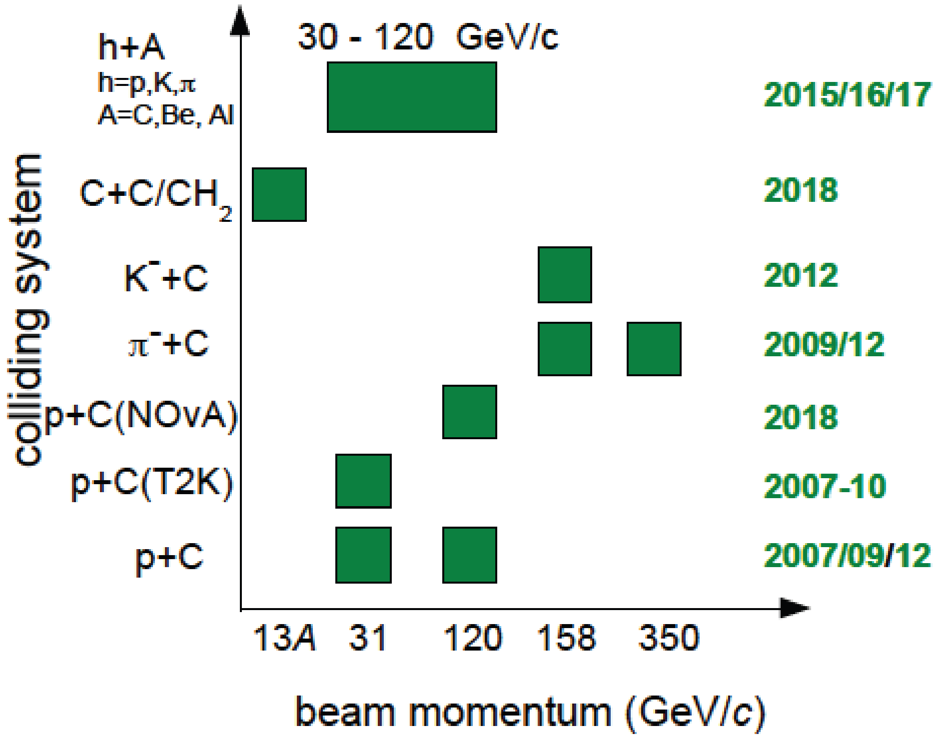

Electron Ion Collider

• Center of Mass Energies	20 GeV – 140 GeV
• Maximum Luminosity	10^{34} cm^{-2}s^{-1}
• Hadron Beam Polarization	80%
• Electron Beam Polarization	80%
• Ion Species Range	p to Uranium
• Number of interaction regions	up to two

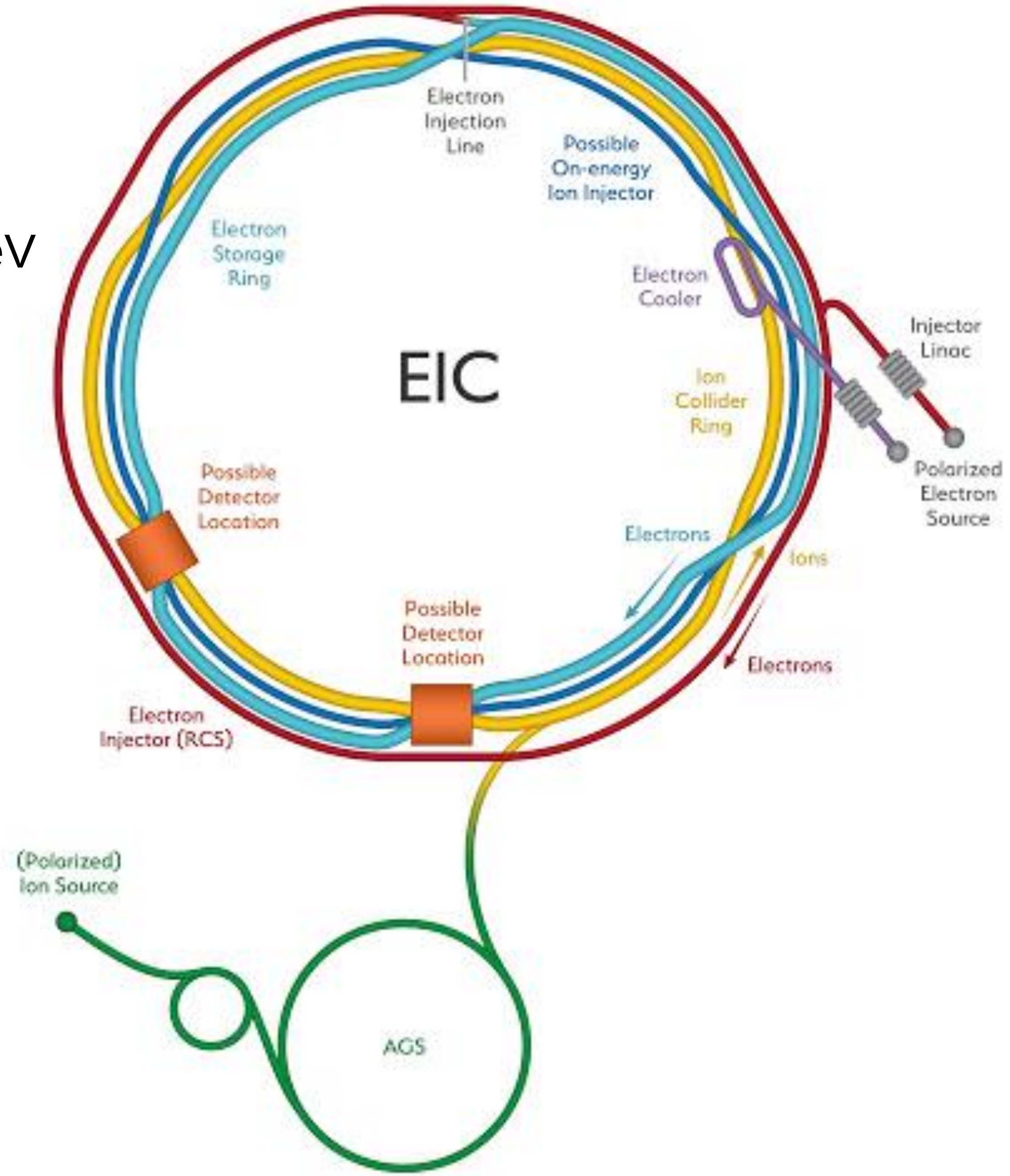

Kinematic coverage

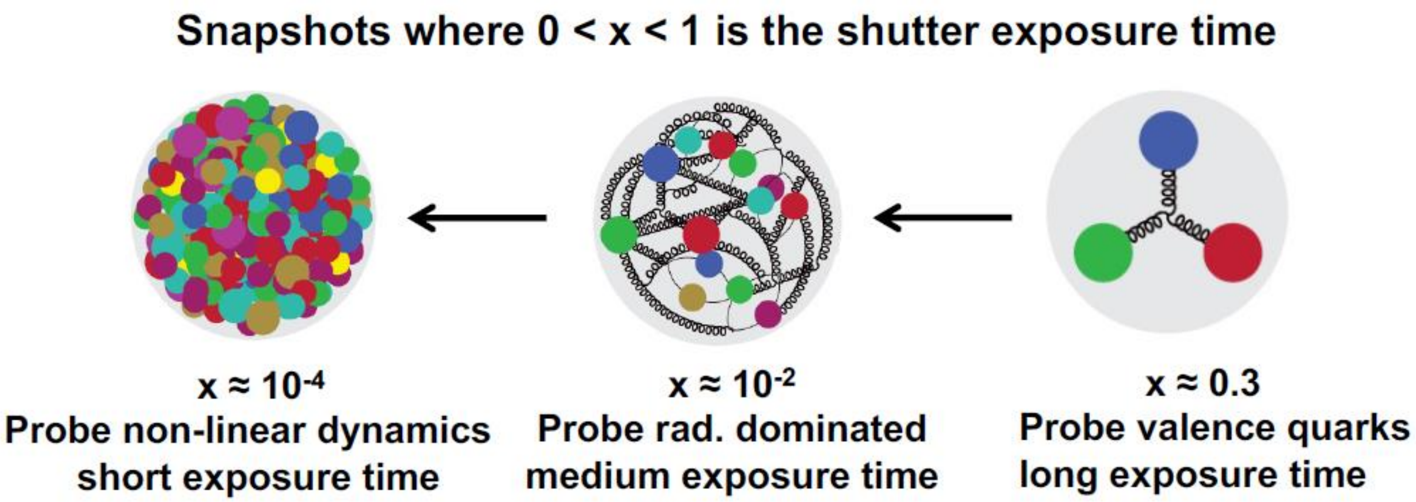

Q^2 is the Lorentz invariant four-momentum transfer and
$x = Q^2/(2m(E-E'))$

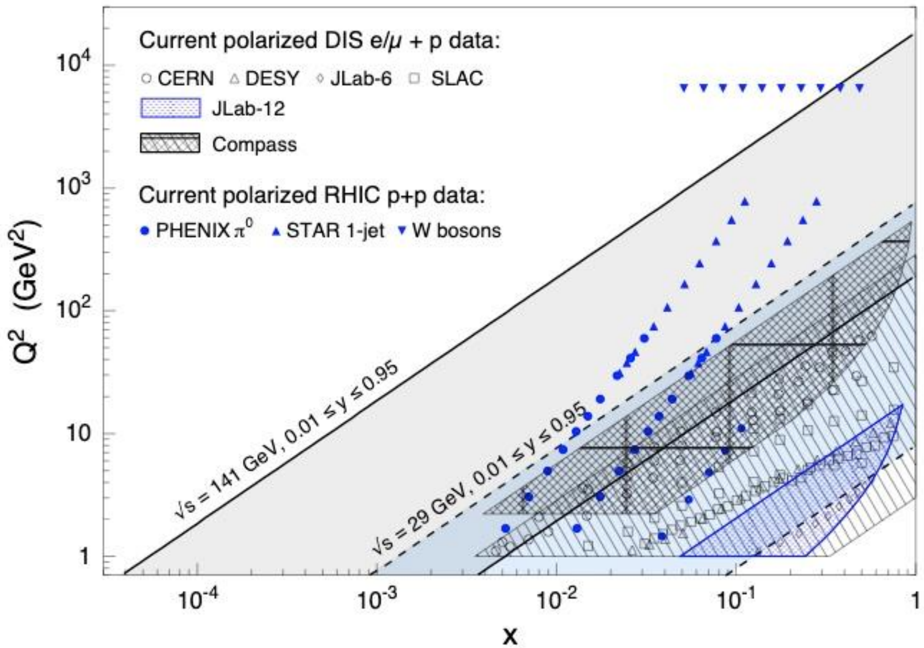

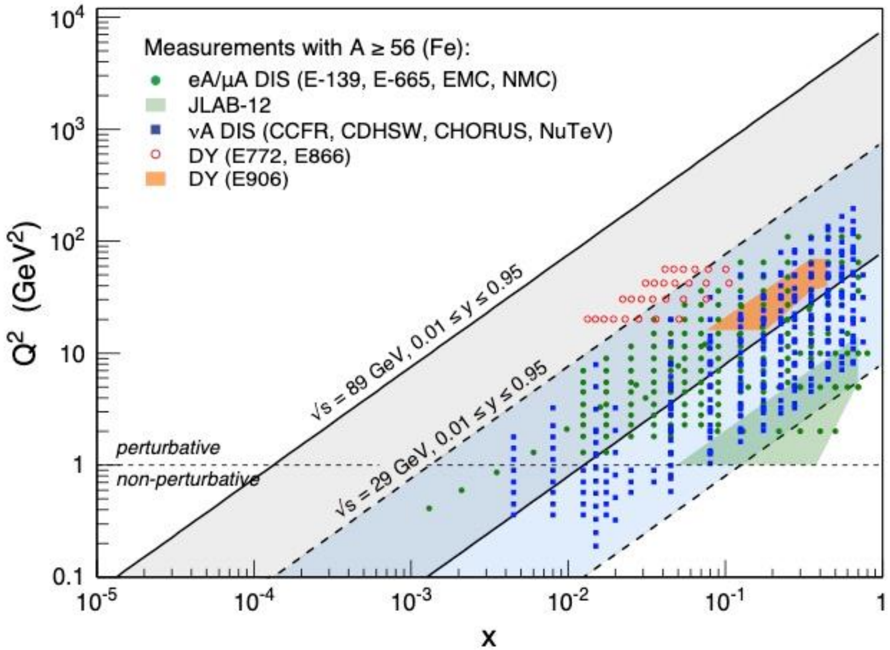

EIC vs HERA

- Center of mass energy: 20 – **140** **(318)** GeV
  - Electrons: 2.5 – 18 (27.5) GeV
  - Protons: 40 – 275 (920) GeV
  (ions: Z/A x E_{proton})

- Luminosity: **10^{34}** **(10^{31})** /cm^2/sec

- Polarization: <70% (both electron and ion) **(only electron)**

- Ion Species: proton – Uranium **(A>1 only in fixed target)**

- Detectors: 2 interaction regions \w complete coverage (almost)
  (4 interaction regions; 2 collider 2 fixed-target;
  limited far-forward coverage)

Thank you!
&
Ready for the questions

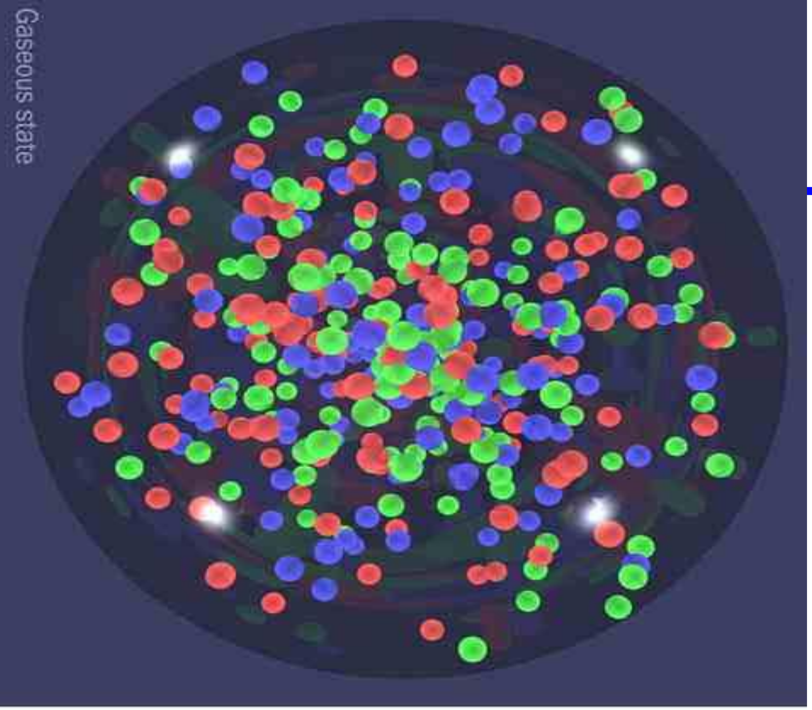
Gaseous state

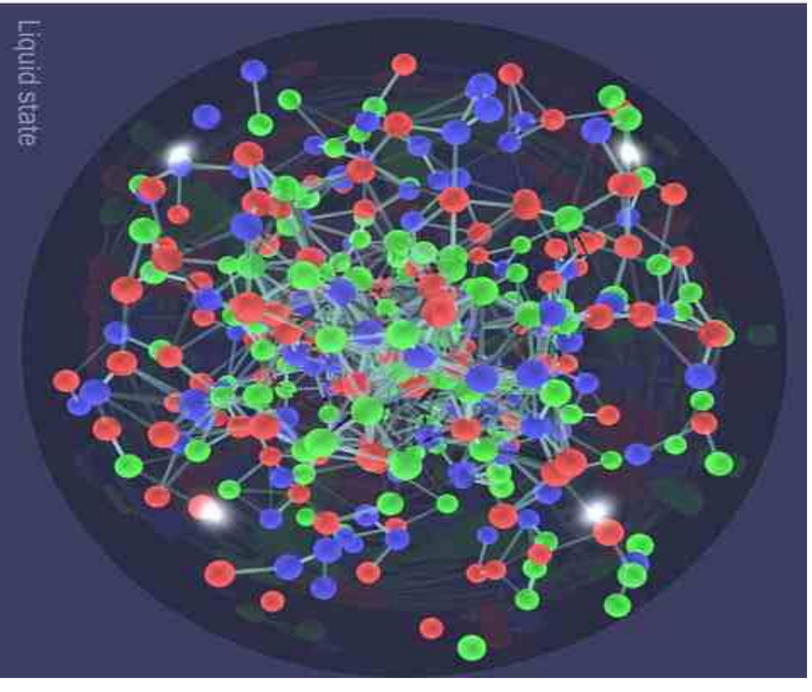
Liquid state

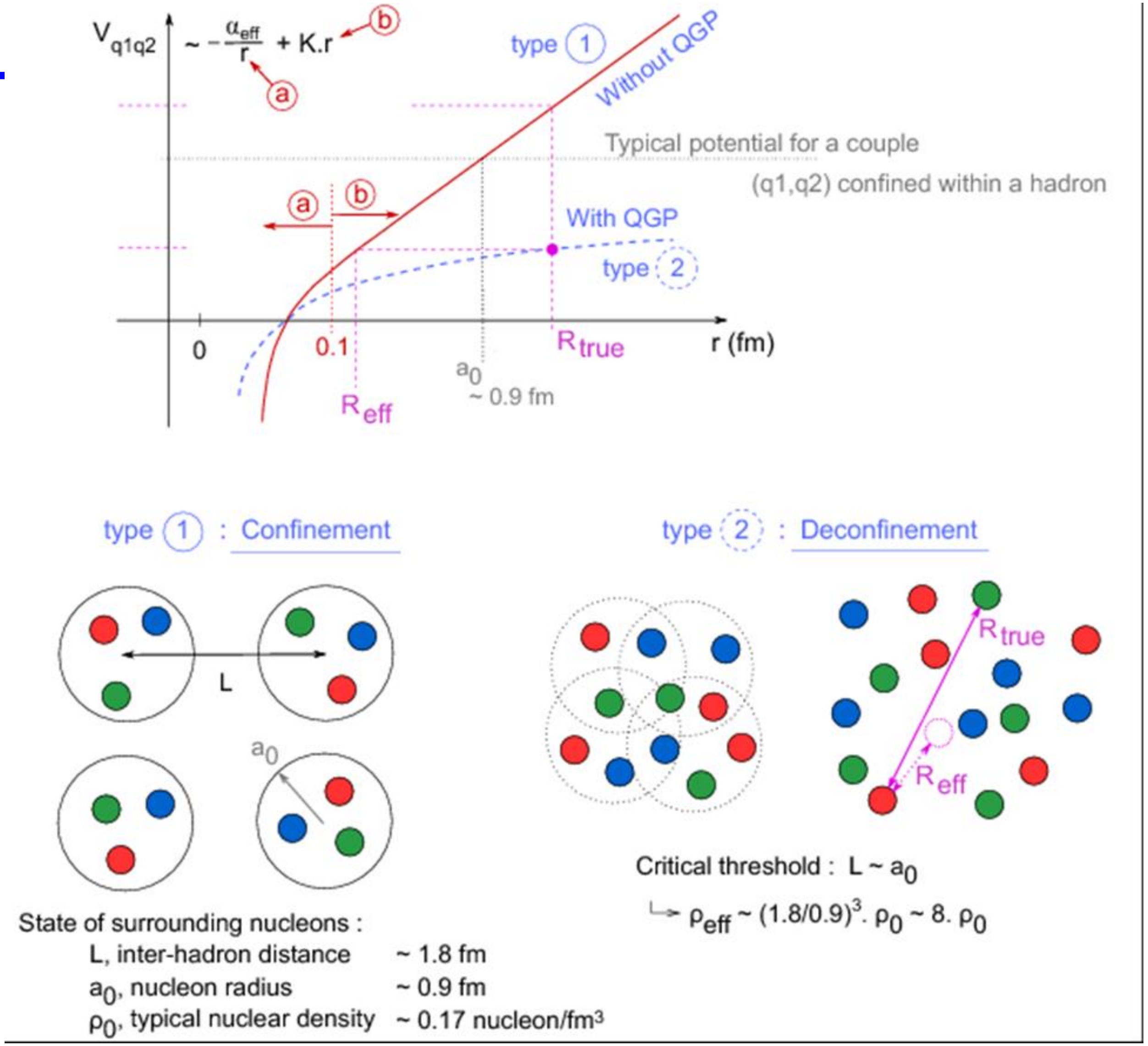
$V_{q1q2} \sim -\frac{\alpha_{eff}}{r} + K.r$
a
b
type 1
Without QGP
Typical potential for a couple
(q1,q2) confined within a hadron
With QGP
type 2
0
0.1
R_{eff}
a_0
~ 0.9 fm
R_{true}
r (fm)
type 1 : Confinement
type 2 : Deconfinement
L
a_0
R_{true}
R_{eff}
Critical threshold : $L \sim a_0$
$\rho_{eff} \sim (1.8/0.9)^3 . \rho_0 \sim 8. \rho_0$
State of surrounding nucleons :
L, inter-hadron distance ~ 1.8 fm
a_0, nucleon radius ~ 0.9 fm
ρ_0, typical nuclear density ~ 0.17 nucleon/fm³

Энергетическая область MPD

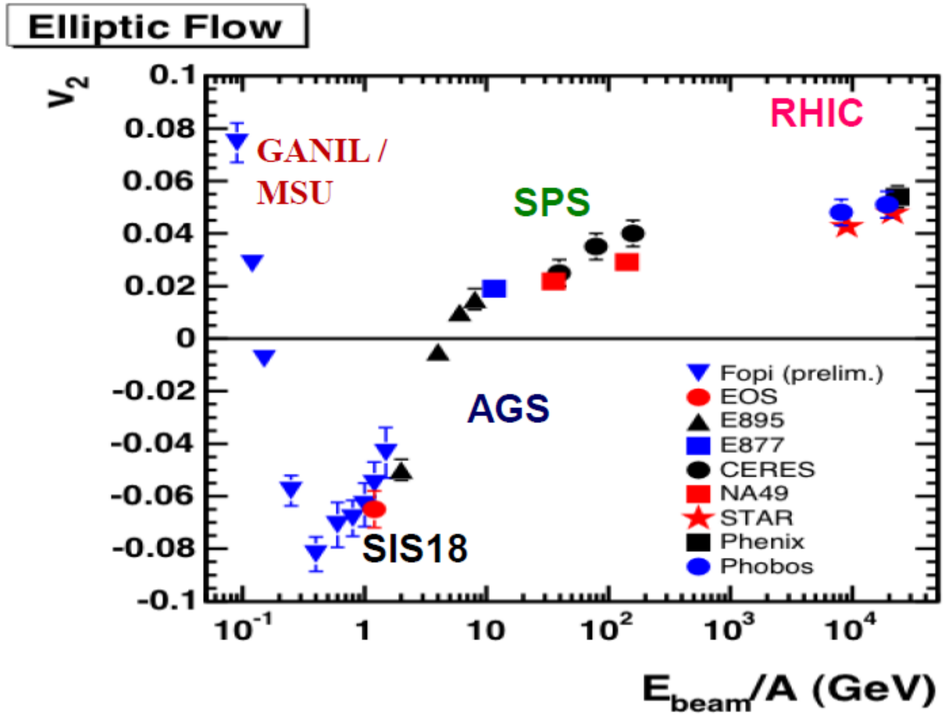

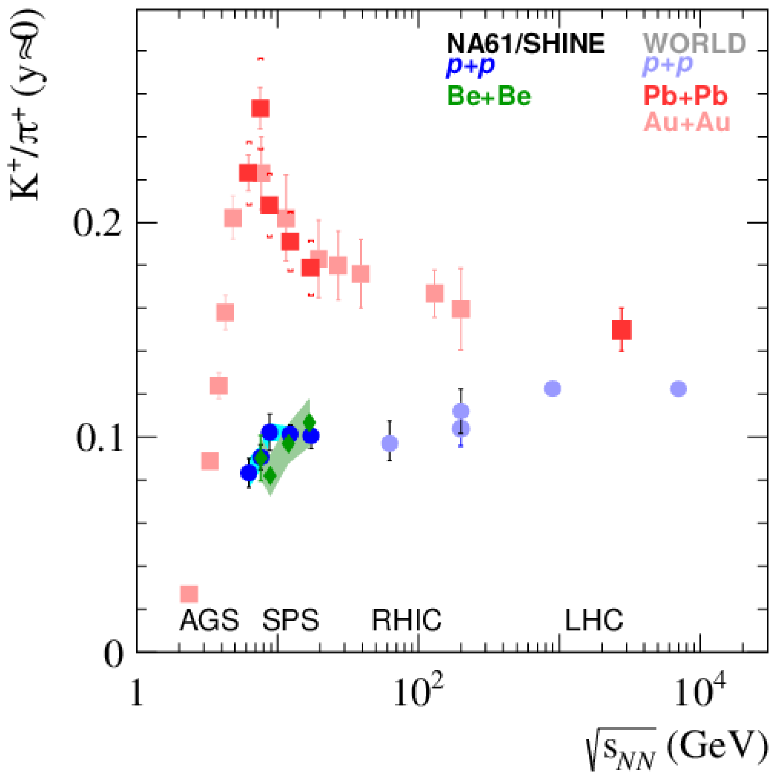

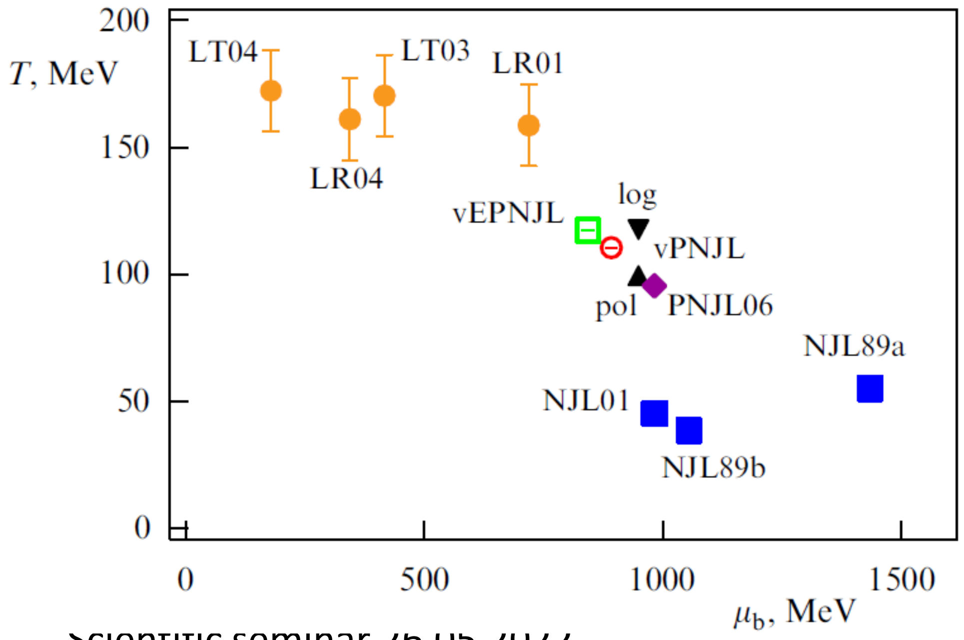

Сравнение объемов файербола

energy	R_{inv} $p-p$ [fm]	R_{inv} $p-\bar{p}$ [fm]
7.7 GeV	$\mathbf{3.59} \pm 0.16 \pm 0.19$	
11.5 GeV	$\mathbf{3.66} \pm 0.08 \pm 0.05$	$\mathbf{3.30} \pm 0.42 \pm 0.28$
19.6 GeV	$\mathbf{3.82} \pm 0.15 \pm 0.06$	$\mathbf{3.32} \pm 0.25 \pm 0.13$
27 GeV	$\mathbf{3.80} \pm 0.12 \pm 0.08$	$\mathbf{3.49} \pm 0.25 \pm 0.16$
39 GeV	$\mathbf{4.00} \pm 0.15 \pm 0.02$	$\mathbf{3.39} \pm 0.12 \pm 0.14$

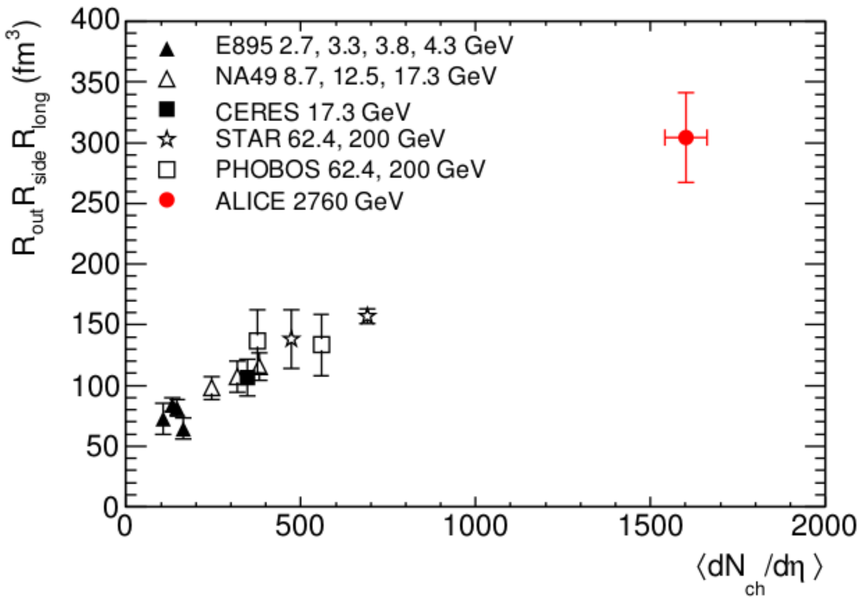

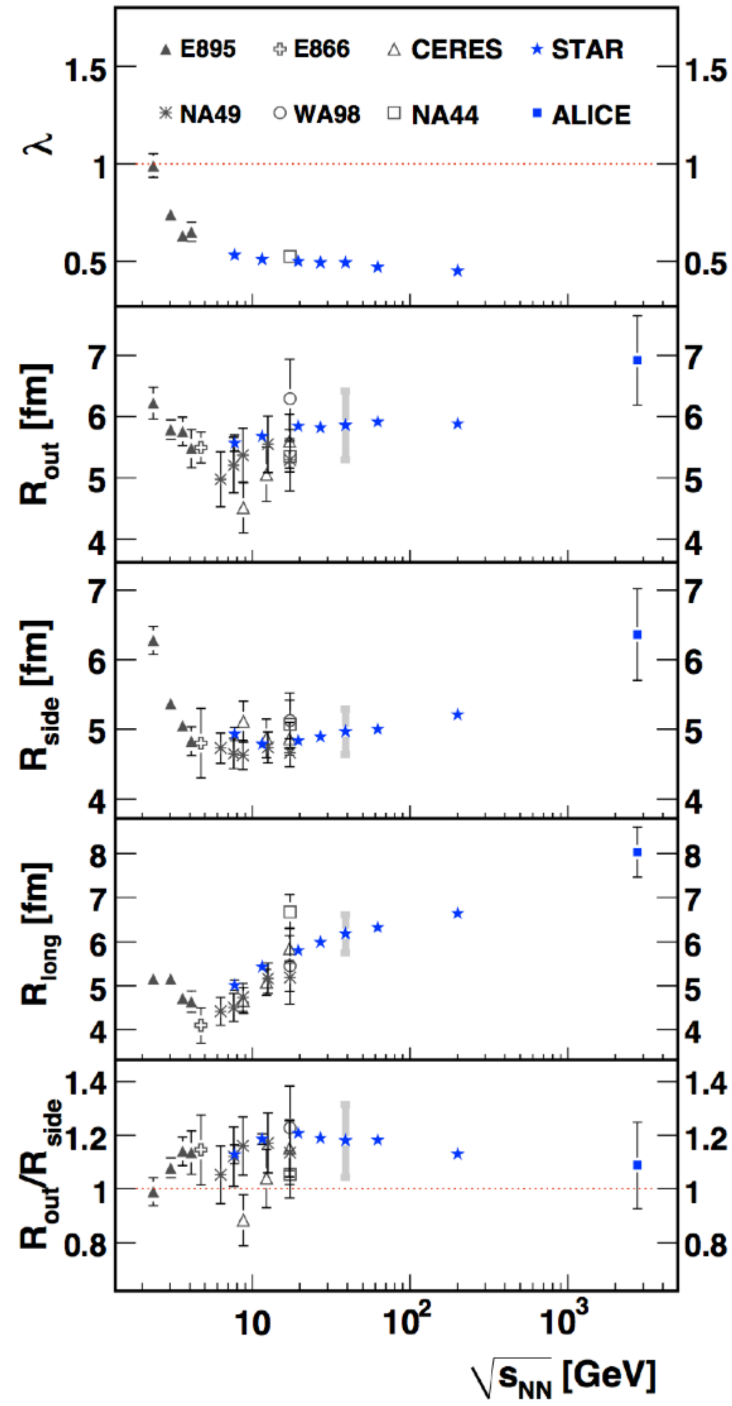

HIC experiments

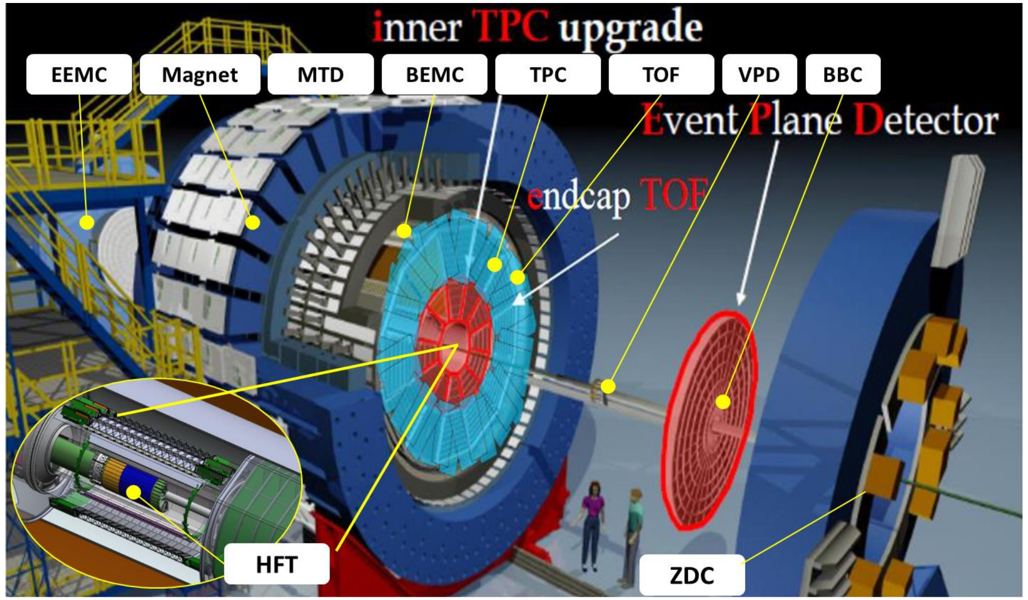

STAR

NA61

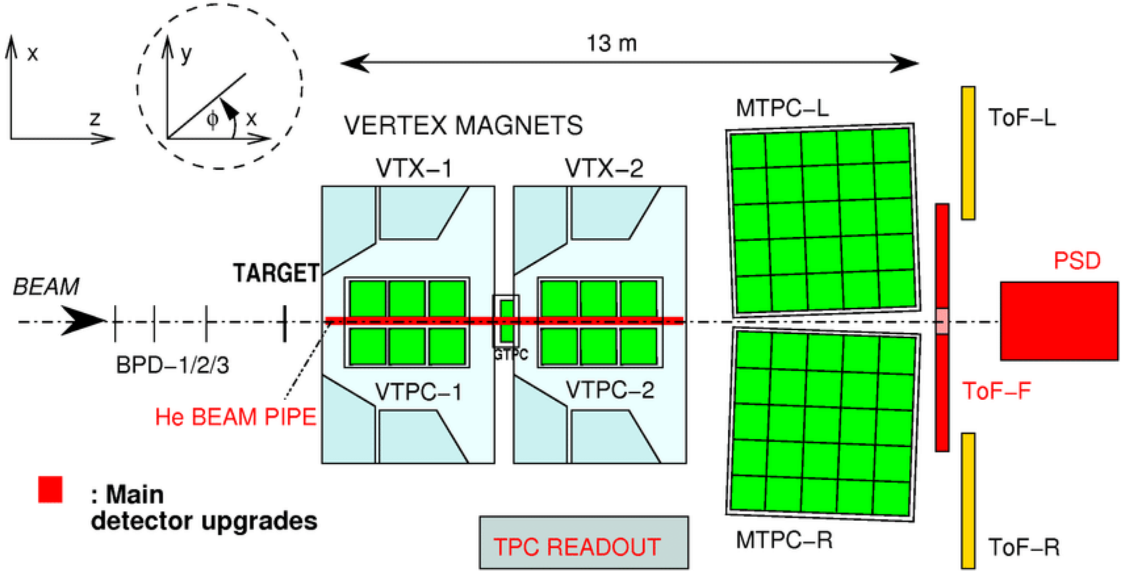

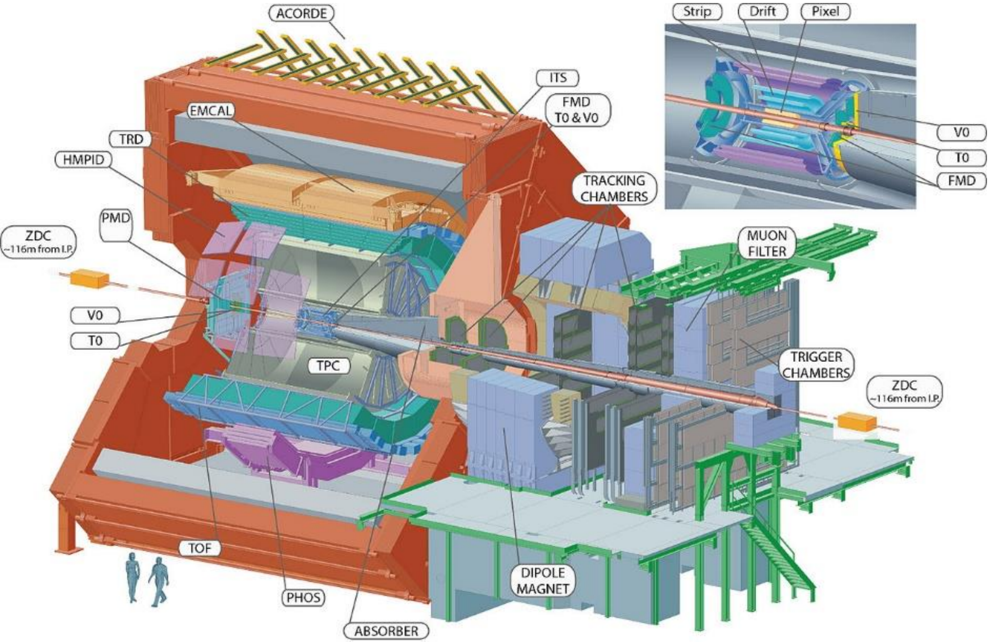

ALICE

CBM

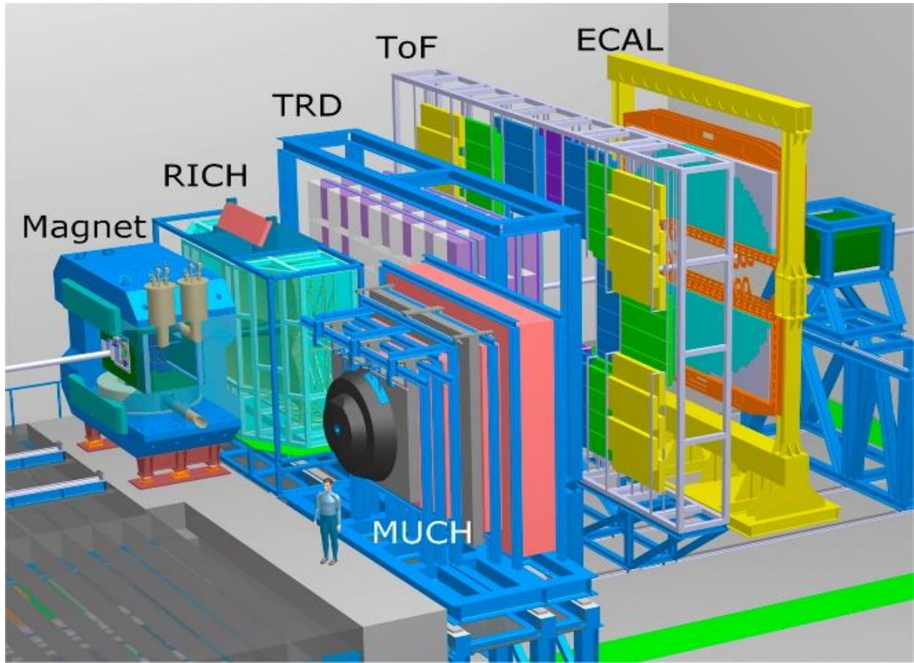

Scientific seminar 26.05.2022

MPD detector

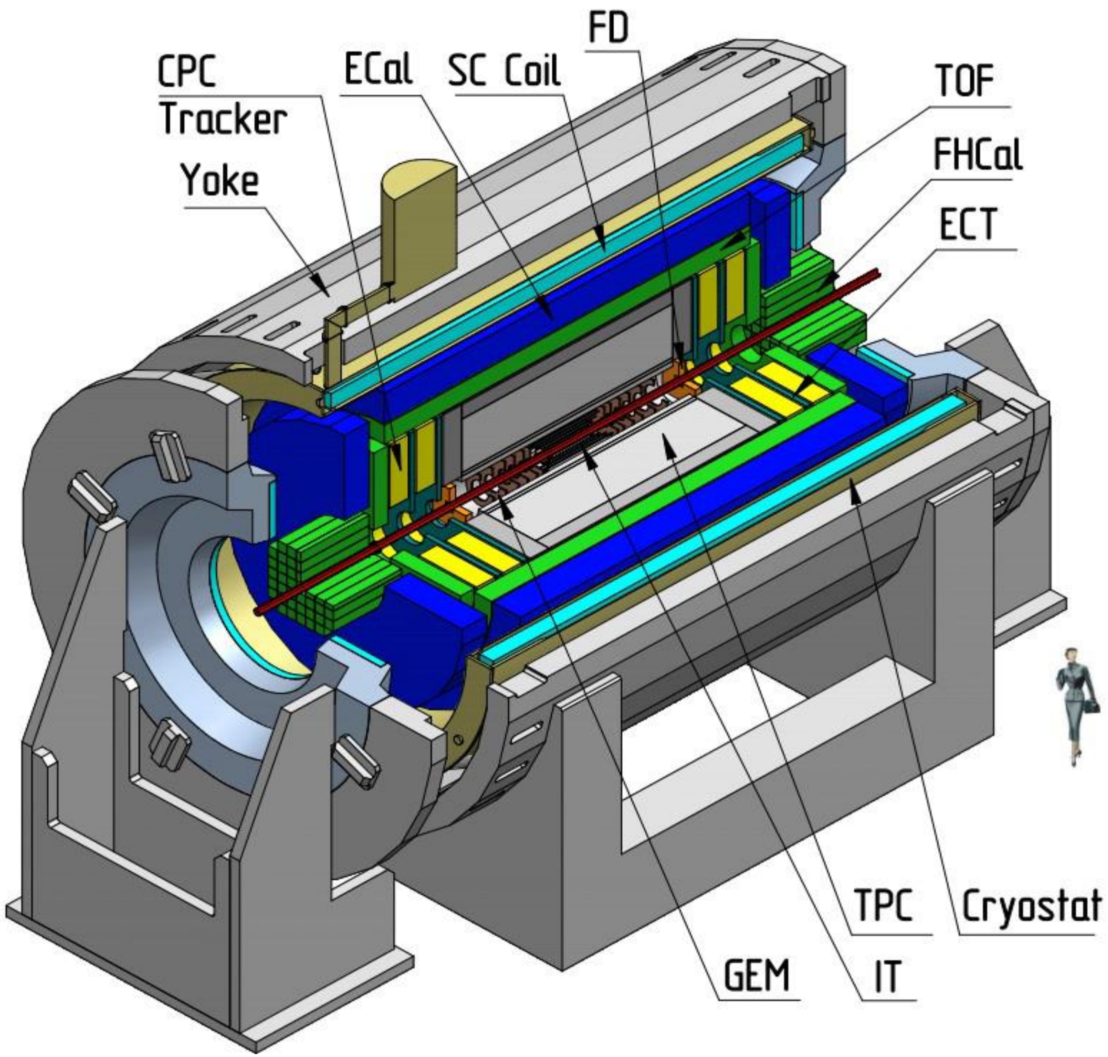

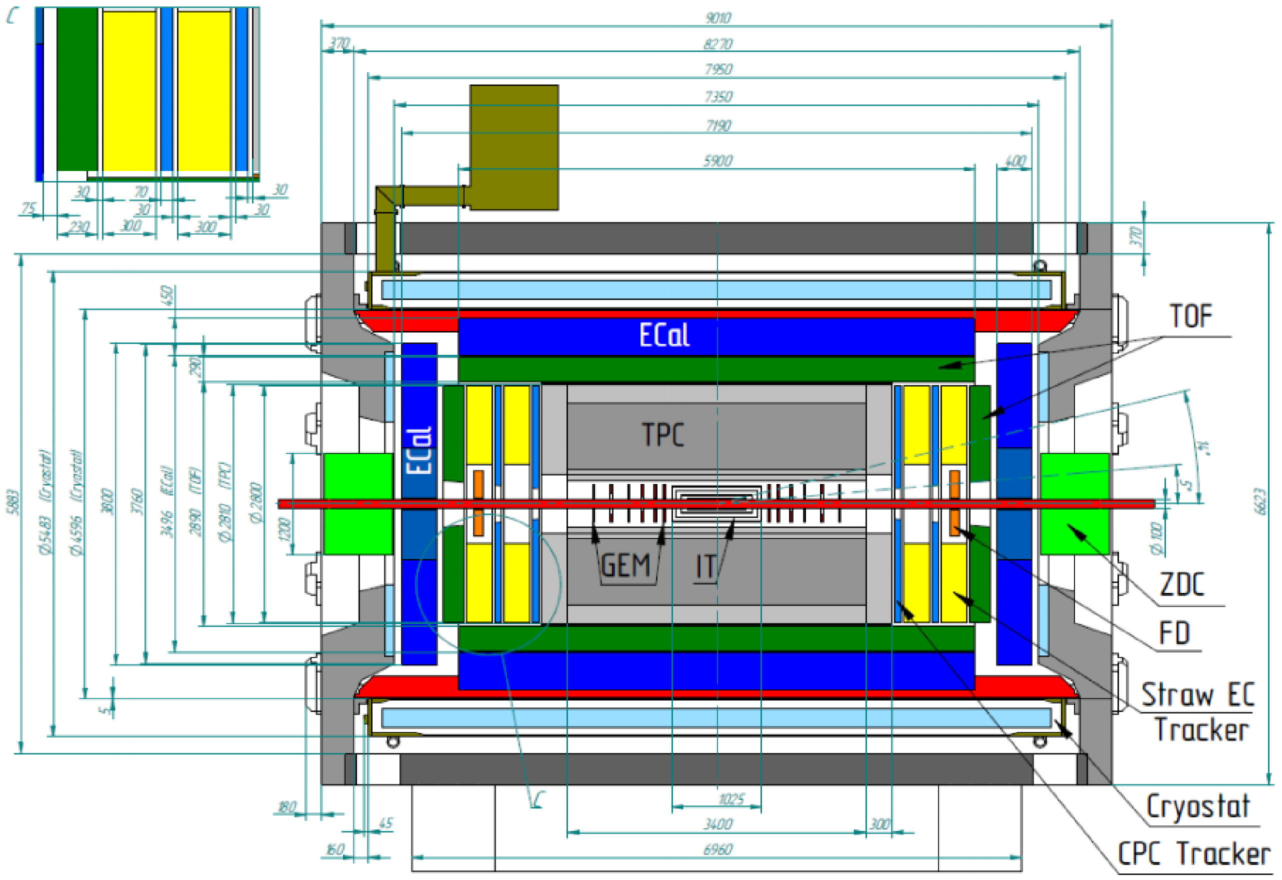

Пособытийные распределения множественности

«чистые» распределения множественности